DECLARATION UNDER 37 C.F.R. §1.132

As a below named inventor of the subject matter for which a United States Letters Patent is currently sought on the inventions entitled:

a) "Transition Metal Dielectric Alloy Materials for MEMS", application serial number 09/910,537 filed June 20, 2001;

b) "MEMS With Flexible Portions of Novel Materials", application serial number 10/176,478 filed June 21, 2002;

c) "MEMS Device Made of Transition Metal Dielectric Alloy Materials", application serial number 10/198,389 filed July 17, 2002; I declare that:

I, Jason S. Reid, have studied and worked for almost 20 years in materials science and related fields. I have a BS in Applied Physics from the University of California, Davis, and a Ph.D. in Applied Physics from California Institute of Technology. My Curriculum Vitae is attached hereto. One of the two references relied upon by the Examiner, Linder et al., has a co-inventor M. -A. Nicolet, who was my research advisor at the California Institute of Technology.

In my opinion, the claims in patent applications 09/901,537 filed July 20, 2001, 10/176,478 filed June 21, 2002, and 10/198,389 filed July 17, 2002, should not be rejected by the Examiner based on an equivalency of early and late transition metals. In particular, in my opinion, it is improper to state that early transition metals and late transition metals are equivalent, whether for all situations, or specifically for the invention of my patent applications, for the reasons below.

Attached are some references that help to make the point that early and late transition metals are not equivalent. For example, in the field of catalysts, it is well known that there is a distinction between early and late transition metals. As set forth in the introduction in Exhibit A ("Very Active Neutral P, O-Chelated Nickel Catalysts for Ethylene Polymerization" Macromolecules 2001, 34, 2438-2442) attached hereto, "For more than 40 years, early transition metal type catalysts have generated considerable scientific interest in industry and in academia. Despite all their advantages (high activity and regio- and stereospecificity), their strongly oxophilic nature limits them to polymerization of nonpolar monomers, with Lewis bases being a poison. Consequently, less oxophilic (softer) catalytic systems based on late transition metals have emerged....." As can be seen in Exhibit A, even in the field of catalysts, early and late transition metals are viewed differently.

Outside the field of catalysts, early and late transition metals are also known to have different properties. Exhibit B ("Chapter 6 Chemistry of Transition Metals" from

(http://www.t.soka.ac.jp/chem/iwanami/inorg/INO_ch6.pdf) as attached hereto talks about early and late transition metals generally, and states (in the 3rd paragraph on page 111) "The Group 3 to 5 metals are now often referred to as early transition metals and they are generally oxophilic and halophilic. Smaller numbers of d electrons and the hardness of these elements explain their affinity toward oxygen and halogens. In the absence of bridging ligands, the formation of metal-metal bonds is difficult for these elements. Organometallic compounds of these metals are known strongly to activate C-H bonds in hydrocarbons. Late transition metals in the groups to the right of the periodic table are soft and have a high affinity toward sulfur or selenium."

Other references talk about the differences as well. Exhibit C states that "Although this approach to NLA materials has been extended to include complexes that contain metal-metal multiple bonds, the use of the early-transition metals has been entirely avoided. There are a number of reasons for this, the most notable of which is that the early transition metals in low oxidation states are more air and moisture sensitive than the late transition metals; the use of low-valent early transition metal (LVETM) complexes, they could prove to be excellent electron donors in NLO active molecules is a significant synthetic challenge.....Compared to the complexes of the late transition metals, the lower effective nuclear charge experienced by the d electrons in low-valent complexes of the early transition metals should render them more polarizable and strongly reducing."

Exhibit D attached hereto in reference to Fig. 6.11 therein, states that "This double humped pattern is very frequent when properties are plotted for transition metals across a transition series. The straight line (full black circles) is obtained by subtracting the CFSE for the given electron count. The linear increase in stability on going through a transition series is caused primarily by increasing acidity (largely due to a decreasing size of the metal cation and electrostatic effects). This forms the basis of the Irving-Williams series. The Irving-Williams series states that for a given ligand, the stability of the complexes increases from Ba to Cu (and then drops for Zn). It should be noted however that as one moves towards the right, the late transition metals prefer softer ligands."

Exhibit E attached hereto states that "We can see clearly that the 13-atom clusters of early transition metals (Y13, Zr13, Nb13, Mo13) prefer the icosahedral structure, while those of late transition metals (Tc13, Ru13, Rh13, Pd13, Ag13, and Cd13) may prefer the BBP structure. Therefore, the BBP structure seems to be favored only when the d shell is more than half filled."

Exhibit F states that "The SONmax, representing the loss of all available (nd) electrons, can be reached in all Transition Element Groups from 3B to 7B. Since this includes all Transition elements up to the "half filled" (nd) shell, they are classified together as the "Early Transition

Elements". In contrast, in the "Late Transition Elements" from Group 8B to 2B which represent the filling of the (nd) shell, the improving penetration of the core by the (nd) electrons causes a rapid decreasing in available SONmax values with increasing Atomic Number. Between these SON limiting values of + II and SONmax, several intermediate SON values may be possible. In the Early Transition Elements, the poor penetration of the core by the (nd) electrons means that these SONs represent thermodynamically unstable oxidizing agents. These Structures can only be captured chemically if they are made kinetically inert by Pauli pair formation, thus the only SONs of practical importance are found in compounds with all of the (nd) electrons paired into MOs. In contrast, the improved penetration by the (nd) electrons through the core in the Late Transition Elements means that intermediate SONs are thermodynamically stable and do not require the kinetic inertia provided by Pauli pairing. Indeed, these SONs are so stable that many (nd) configurations of odd-electron or unpaired even-electrons exist in air-stable compounds, in spite of formally being Free Radicals."

As can be seen from the above, there are real differences between the early and late transition metals. Early transition metals have a greater affinity for, among others, oxygen – as mentioned above. Early transition metals also have a greater affinity for nitrogen. Owing to the decreased stability of late transition metal nitrides over early transition metal nitrides, late transition metal nitrides should have far lower crystallization temperatures. Nitrogen evolution at low temperatures in the late transition metal nitrides is the reason for the difference.

In addition, late transition metal films can be very difficult to etch in plasmas, generally necessitating heavy ion bombardment to induce removal by sputtering. The SF6/O2 discharge mentioned in the Linder et al. reference did not etch a (late transition metal)-Si-N film when we tried this. It is likely that SF6/O2 discharge would also not etch a (late transition metal)-Si-O film either.

The references used for rejecting the claims do not propose that early and late transition metals are equivalent for all uses. Much less, do the applied references propose that early and late transition metals are equivalent for flexible elements in micro-electromechanical systems. Micro-electromechanical systems (MEMS) are often defined as the integration of mechanical structures having dimensions typically on the order of microns or tens of microns, with microelectronics. In one example of the many types of MEMS devices, in the field of spatial light modulators for displays, micromirrors are digitally operated and have dimensions typically (but not always) from 10 to 20 micrometers. I believe that the late transition metals used in the flexible portion of the MEMS device as set forth in the claims of my patent applications have a lower affinity for forming particular compounds (e.g. compounds with nitrogen and/or oxygen)

which can result in different mechanical and electrical properties of the flexible part of the device.

As can be seen from the above, the early and late transition metals are different, and are neither equivalent nor interchangeable as recognized in the art. In my opinion, the early and late transition metals are neither equivalent nor interchangeable, especially for the subject matter set forth in my applications.

I hereby declare that all statements made herein of my own knowledge are true and that all statements made on information and belief are believed to be true; and further that these statements were made with the knowledge that willful false statements and the like so made are punishable by fine or imprisonment, or by both, under Section 1001 of Title 18 of the United States Code and that such willful false statements may jeopardize the validity of the applications or any patent issued thereon.

Jason S Reid

JASON S. REID

Date: 10/21/04

Citizenship: USA

1315 ASHCROFT LN

SAN JOSE, CA 95118

Residence and P.O. Address

Macromolecules **2001**, *34*, 2438−2442

Very Active Neutral P,O-Chelated Nickel Catalysts for Ethylene Polymerization

R. Soula,[†] J. P. Broyer,[†] M. F. Llauro,[†] A. Tomov,[†] R. Spitz,[†] J. Claverie,*[,†] X. Drujon,[‡] J. Malinge,[‡] and T. Saudemont[‡]

LCPP-CPE/CNRS, BP 2077, 43 Bd du 11 Nov 1918, 69616 Villeurbanne Cedex, France; and Ato-Fina, 4/8 Cours Michelet, 92800 Puteaux, France

Received October 3, 2000; Revised Manuscript Received January 22, 2001

ABSTRACT: A series of highly active nickel-based neutral catalysts for ethylene polymerization is presented. These catalysts are obtained by direct complexation of simple fluorinated ketoylides onto bis-(1,5-cyclooctadiene)nickel. Catalyst formation readily occurs in the presence of an olefin, but due to the electron deficiency of the ligand, it hardly happens in the absence of an olefin or another Lewis base. Activities greater than 2×10^6 (g_{PE}/g_{Ni})/h and productivities higher than 15×10^6 g_{PE}/mol_{Ni} are typically observed. These catalysts are also active for the polymerization of α-olefins such as 1-hexene and 1-propene. Polymer characterization indicates that highly linear, low molecular weight PEHD is formed by these complexes.

Introduction

For more than 40 years, early transition metal type catalysts have generated considerable scientific interest in industry and in academia.[1−3] Despite all their advantages (high activity and regio- and stereospecificity), their strongly oxophilic nature limits them to the polymerization of nonpolar monomers, with Lewis bases being a poison. Consequently, less oxophilic (softer) catalytic systems based on late transition metals have emerged,[4−6] so as to find new ways of preparing polymers or copolymers containing polar units or tolerating functionalities. To our knowledge, the very first late transition metal catalysts for ethylene polymerization are an iodorhodium complex generated from Rh-$(C_2H_4)_2$(acac) and I_2 reported by Kealy[7] and a dihydride tetrakistriphenylphosphine ruthenium complex disclosed by Markham in 1972.[8] Since 1965, Yamamoto has developed a diethyl bis(2,2′-bipyridyl)iron complex for the polymerization of butadiene[9] and functionalized vinyl monomers,[10] but no activity was reported in ethylene. Considerable work has been achieved by Keim, eventually leading to the industrialization of the SHOP process.[11] Among the numerous catalysts prepared by Keim,[12−15] the nickel(II) complexes containing a phospho keto−ylide chelate proved to be the best candidates. In 1987, Klabunde[16] showed that, using the same kind of nickel complexes, it was possible to prepare high molecular weight polymers by removing a phosphine with a phosphine sponge, thus opening a vacant coordination site. In addition, the co-polymerization of ethylene with an olefin bearing a polar functionality was achievable if the polar substituent was separated by a spacer of two or more methylene units.[17] Although these catalytic complexes showed a unique tolerance to polar groups, water was still described as a poison of the catalytic systems.[18] By using a phosphorus ylide as ancillary ligand, Ostoja-Starzewski was able to polymerize ethylene without adding a phosphine sponge to the reaction medium.[19−21] These bis(ylide)nickel and palladium catalysts are very active and lead to a wide range of polyethylene molecular weight through change in the ligand.[22] After these pioneering works were disclosed,[23−25] a major contribution was achieved by Brookhart and co-workers[26,27] with the use of bulky substituted α-diimine ligands for the preparation of nickel and palladium cationic complexes. These systems proved to be very active and able to copolymerize ethylene and α-olefins with methyl acrylate.[28] Recently, neutral nickel(II) complexes based on salicylaldimine ligands were developed by Grubbs.[29,30] These complexes allow the synthesis of high molecular weight polyolefins with excellent activity. Finally, Gibson[31,32] and Bennett[33] reported promising work in ethylene polymerization through the use of very low cost and/or low toxicity metals, such as iron and cobalt stabilized with 2,6-bis(imino)pyridyl ligands. These catalysts display excellent activities when activated with MAO. Yet, the use of MAO precludes polymerization of polar olefins or olefins in the presence of water.

In a previous work, we have disclosed preliminary results about catalytic polymerization of ethylene in aqueous emulsion using binuclear phosphorus−oxygen chelating catalysts.[34] To our knowledge, for the very first time, a latex of HDPE was prepared by direct catalytic polymerization in water.[35,36] To continue our studies, we quickly realized that we needed to prepare extremely active catalysts, as we usually observed a loss of activity of 20−100 times when going from an organic medium to an aqueous dispersed medium. We chose to still work with neutral nickel catalysts as we expected MAO activation for cationic complexes to be close to impossible under such conditions. Moreover, we expected cationic complexes formed by borane activation, or an equivalent route, to react with hydroxide ions. Among the ligands that confer a very high activity to the catalysts, we have also decided to select those which are reasonably easy to synthesize. As it is usually accepted that activity is strongly related to the electrophilicity (acidity) of the metal, highly electrowithdrawing fluorinated groups were incorporated onto the ligand. Here, we present first results about the synthesis of these

* Corresponding author. E-mail: claverie@flamel.com. Telephone: (33) 4 72 78 3434. Fax: (33) 4 72 78 3435.
† LCPP-CPE/CNRS.
‡ Ato-Fina.

10.1021/ma001714x CCC: $20.00
Published on Web 03/16/2001

ligands, their use in the preparation of the catalytic complexes, as well as the results obtained with these catalysts in organic phase. In a subsequent paper, results about emulsion polymerization of ethylene and α-olefins will be presented.

Experimental Section

Ligand **1a** and $Ni(COD)_2$ were purchased from a commercial supplier. All solvents and reagents were dried and degassed, according to standard Schlenk techniques. THF was distilled on sodium benzophenone prior to use. NMR analysis was effected on a 400 MHz Bruker instrument. Polymer analyses were made in a mixture of d_3-trichloroethane and d_6-benzene at 90 °C. GPC was determined in 1,3,4-trichlorobenzene at 145 °C, using a Waters AIC instrument. ^{31}P and ^{19}F NMR resonances, recorded on a 200 MHz AMX Bruker instrument, are reported relative to external standards (H_3PO_4, 85% in water, and CF_3Cl).

Synthesis of 6,6,6,5,5,4,4-Heptafluoro-3-oxo-2-(triphenylphosphoranylidene)hexanoic Acid, Ethyl Ester (1b). A slurry of carbethoxymethyltriphenylphosphonium bromide (3.4 g, 7.9 mmol) in 25 mL of anhydrous THF is cooled in an ice water bath and treated with triethylamine (2.4 mL, 17.2 mmol). After 15 min stirring, the mixture is treated dropwise with heptafluorobutyryl chloride (1.28 mL, 8.6 mmol). The mixture is allowed to reach room temperature and left for 1 h. The reaction medium is filtered, the precipitate is washed three times with cold THF, and the filtrate is dried in vacuo, resulting in a powder which is recrystallized in MeOH. Isolated yield: 63%. NMR ^1H (ppm, in $CDCl_3$): C_6H_5 7.4−7.8, 15H, m; OCH_2, 3.78, 2H, q; CH_3, 0.9, 2H, t ($^3J_{H-H}$ = 7 Hz). ^{13}C (ppm, in $CDCl_3$): 13.6, 60.3, 72.6 ($^1J_{C-P}$ = 115 Hz), 124 ($^1J_{C-P}$ = 100 Hz), 129.9 ($^2J_{C-P}$ = 13 Hz), 132.6 ($^4J_{C-P}$ = 3 Hz), 133.4 ($^3J_{C-P}$ = 10 Hz), 165.7 ($^2J_{C-P}$ = 13.5 Hz), 175.2 ($^2J_{C-F}$ = 27 Hz, $^2J_{C-P}$ = 6 Hz). ^{19}F (ppm, in $CDCl_3$) $COCF_2$ −124.9, s; CF_2 −113.7, q ($^3J_{F-F}$ = 1.5 Hz); CF_3 −80.7, t ($^3J_{F-F}$ = 1.5 Hz). ^{31}P (ppm, in $CDCl_3$), 20, s. IR (10% KBr pellet): 3062, 2981, 1709, 1682, 1579, 1571, 1486, 1437, 1330, 1251, 1234, 1200, 1157, 1105, 968, 935, 757, 692, 556, 516 cm^{-1}. Anal. Calcd: C, 57.36; H, 3.70. Found: C, 57.61; H. 3.87.

Synthesis of Pentafluorobenzyl-3-oxo-2-(triphenylphosphoranylidene)propanoic Acid, Ethyl Ester (1c). Same experimental setup as for **1b**, with (ethoxycarbonylmethyl)-triphenyl phosphonium bromide (0.8 g, 2.0 mmol), triethylamine (0.6 mL, 4.2 mmol), and pentafluorobenzoyl chloride (0.3 mL, 2.1 mmol). Isolated yield: 52%. NMR ^1H (ppm, in $CDCl_3$): C_6H_5 7.5−7.6 and 7.7−7.8, 15H, m; OCH_2, 3.65, 2H, q; CH_3, 0.58, 2H, t ($^3J_{H-H}$ = 7 Hz). ^{13}C (ppm, in $CDCl_3$): 13.5, 58.9, 74.2 ($^1J_{C-P}$ = 110 Hz), 124.7 ($^1J_{C-P}$ = 94 Hz), 128.8 ($^2J_{C-P}$ = 13 Hz), 132.4 ($^4J_{C-P}$ = 3 Hz), 133.5 ($^3J_{C-P}$ = 10 Hz), 166.7 ($^2J_{C-P}$ = 13 Hz), 178.7 ($^2J_{C-P}$ = 7 Hz). ^{19}F (ppm, in $CDCl_3$) C_6F_5 −145.2, dd ($^3J_{F-F}$ = 22 Hz, $^4J_{F-F}$ = 6.7 Hz),-157.8, t ($^3J_{F-F}$ = 22 Hz), −163.7, td ($^3J_{F-F}$ = 22 Hz, $^4J_{F-F}$ = 6.7 Hz). ^{31}P (ppm, in $CDCl_3$), 18.3, s. IR: 1661, 1562, 1517, 1496, 1437, 1369, 1341, 1293, 1244, 1103, 1087, 983, 940, 692, 542 cm^{-1}. Anal. Calcd: C, 64.21; H, 3.72. Found: C, 64.49; H, 3.84.

Synthesis of Pentafluorobenzyl-3-oxo-2-(triphenylphosphoranylidene)propanoic Acid, *tert*-Butyl Ester (1d). Same experimental setup as for **1b**, with (*tert*-butoxycarbonylmethyl)triphenylphosphonium bromide (1.65 g, 4.0 mmol), triethylamine (1.3 mL, 8.2 mmol), and pentafluorobenzoyl chloride (0.6 mL, 4 mmol). Isolated yield: 62%. NMR ^1H (ppm, in $CDCl_3$): C_6H_5 7.4−7.9, 15H, m; CH_3, 0.96, 9H, s. ^{13}C (ppm, in $CDCl_3$): 28.8, 76.3, 74.2 ($^1J_{C-P}$ = 110 Hz), 124.7 ($^1J_{C-P}$ = 94 Hz), 128.8 ($^2J_{C-P}$ = 13 Hz), 132.4 ($^4J_{C-P}$ = 3 Hz), 133.5 ($^3J_{C-P}$ = 10 Hz), 166.7 ($^2J_{C-P}$ = 13 Hz), 178.7 ($^2J_{C-P}$ = 7 Hz). ^{19}F (ppm, in $CDCl_3$): C_6F_5 −145.2, dd ($^3J_{F-F}$ = 22 Hz, $^4J_{F-F}$ = 7.4 Hz),-158.0, t ($^3J_{F-F}$ = 22 Hz), −163.8, td ($^3J_{F-F}$ = 22 Hz, $^4J_{F-F}$ = 7.4 Hz). ^{31}P (ppm, in $CDCl_3$): 18.1, s. IR: 1666, 1552, 1516, 1495, 1437, 1359, 1303, 1247, 1167, 1108, 988, 941, 692, 543, 521 cm^{-1}. Anal. Calcd: C, 65.27; H, 4.24. Found: C, 65.28; H, 4.31.

Synthesis of pentafluorobenzyl-3-oxo-2-(triphenylphosphoranylidene)propanoic acid, benzyl ester (1e). Same experimental setup as for **1b**, with (benzyloxycarbonylmethyl)-triphenylphosphonium bromide (0.98 g, 2.0 mmol), triethylamine (0.58 mL, 4.2 mmol), and pentafluorobenzoyl chloride (0.3 mL, 2.1 mmol). Isolated yield: 32%. NMR ^1H (ppm, in $CDCl_3$): C_6H_5, 7.2−7.4, 20H, m; CH_2, 5.1, 2H, s. ^{13}C (ppm, in $CDCl_3$): 65.7, 74.4 ($^1J_{C-P}$ = 112 Hz), 124.5 ($^1J_{C-P}$ = 94 Hz), 128.0, 128.2, 128.5, 128.8 ($^2J_{C-P}$ = 13 Hz), 132.4 ($^4J_{C-P}$ = 3 Hz), 133.5 ($^3J_{C-P}$ = 10 Hz), 135.6, 166.3 ($^2J_{C-P}$ = 13 Hz), 178.7 ($^2J_{C-P}$ = 7 Hz). ^{19}F (ppm, in $CDCl_3$): C_6F_5 −145.7, dd ($^3J_{F-F}$ = 23 Hz, $^4J_{F-F}$ = 7 Hz), −157.4, t ($^3J_{F-F}$ = 23 Hz), −163.8, td ($^3J_{F-F}$ = 23 Hz, $^4J_{F-F}$ = 7 Hz). ^{31}P (ppm, in $CDCl_3$): 18.6, s. IR: 1648, 1554, 1519, 1487, 1440, 1341, 1288, 1274, 1066, 986, 754, 690, 545, 510, 501 cm^{-1}. Anal. Calcd: C, 67.55; H, 3.67. Found: C, 67.32; H, 3.95.

Typical Polymerization Procedure. In a Schlenk tube, 23.5 mg of $Ni(COD)_2$ is dissolved in 8.5 mL of toluene. Then, 4 mL of this solution is added to 8.9 mg of ligand **1a**. The solution is left stirring for 15 min, and 0.6 mL of this solution is added to 400 mL of toluene in a thick glass reactor. The solution is then cannula transferred into a 1 L stainless steel reactor, equipped with a mechanical stirrer (magnetic induction), a thermocouple, a sampling valve, and an external jacket heated at 70 °C. Ethylene is immediately introduced at 3 bar. Ethylene is continuously fed into the reactor at 3 bar from a high-pressure 1 L reservoir. The pressure drop in the reservoir is recorded, to assess activity and productivity measurements. The reaction medium (400 mL) is added to methanol (600 mL), and the polymer (70 g) collected through filtration.

Synthesis of *cis*-Bis{ethyl-1,1,1-trifluoro(3-diphenylphosphanyl)acetoenolato|*O,P*|}nickel(II) (5). In a Schlenk tube, 113 mg (410 μmol) of $Ni(COD)_2$ and 178 mg (400 μmol) of ligand **1a** are solubilized in 4 mL of benzene. This solution is stirred during 2 h at room temperature and 0.4 mL are taken and introduced in a pressure NMR tube fitted with a Teflon adapter for vacuum lines.

NMR confirms that no COD has been displaced from the nickel center and that the resonances of the ligand are unchanged. NMR: $Ni(COD)_2$, 2.07 ppm, s, 16H; 4.29 ppm, s, 8H (coordinated COD protons); ester protons of ligand **1a**, 0.83 ppm, t, 3H; 3.90 ppm, q, 2H.

A 1 mL aliquot of the starting reaction medium is transferred to another Schlenk tube which is heated 30 min at 60 °C. NMR: 60% $Ni(COD)_2$, 2.07 ppm, s, 16H; 4.29 ppm, s, 8H; 40% free COD, 2.20 ppm, s, 5H; 5.57 ppm, s, 2.5H; 90% free ligand **1a**, 0.83 ppm, t, 3H; 3.90 ppm, q, 2H; 10% coordinated ligand **1a**, 0.65 ppm, t, 0.3H; 3.78 ppm, q, 0.2H.

To another 1 mL of the starting reaction medium is added 656 mg (250 μmol) of triphenylphosphine. The solution turns immediately to orange, and after 2 h stirring at room temperature, 0.4 mL of the brown solution is introduced in a NMR tube and the spectrum is run. NMR: 10% $Ni(COD)_2$, 2.07 ppm, s, 1.6H; 4.29 ppm, s, 0.8H; 90% free COD, 2.20 ppm, s, 16H; 5.57 ppm, s, 8H; 50% free ligand **1a**, 0.83 ppm, t, 1.5H; 3.90 ppm, q, 1H; 50% coordinated ligand **1a**, 0.65 ppm, t, 1.5H; 3.78 ppm, q, 1H.

To another 2 mL of the starting reaction medium is added 126 μL (1 mmol) of hexene. The solution turns immediately to yellow. The solution is stirred for 2 h at 60 °C. The solution is dark brown. NMR: 100% free COD, 2.20 ppm, s, 16H; 5.57 ppm, s, 8H (free COD protons); hexene, no more peaks between 4.5 and 5.0 ppm (allylic protons) and also between 5.7 and 6.0 ppm (vinylic protons), but many broad peaks appeared in the region between 0.6 and 2.0 ppm (polyhexene).

To a solution of $Ni(COD)_2$ (206 mg) in toluene is added the ligand **1a** (667 mg). The solution is stirred 2 h at 60 °C and overnight at room temperature. The solution is filtered to remove the nickel metal and dried under vacuum. The yellow solid is recrystallized in a solution of toluene/heptane to yield 60% (485 mg) of complex **5**. RMN ^1H: 0.65 ppm, t, 3H; 3.65 ppm, q, 2H; 6.56 ppm, t, 4H; 6.80 ppm, t, 2H; 7.30 ppm, d, 4H. RMN ^{19}F: −68.1 ppm, s. RMN ^{31}P: 37.3 ppm, s.

Results and Discussion

1. Synthesis of Fluorine-Containing Keto−Ylide Ligands. The rationale for our choice of ligand lies in

Scheme 1. Synthesis of the Polymerization Catalyst 2 Starting from the Ligand 1

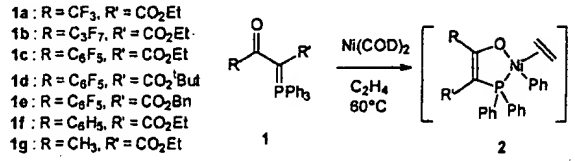

Scheme 2. One-Pot Synthesis of the Ligand 1 Starting from Commercially Available Phosphonium Salt 3

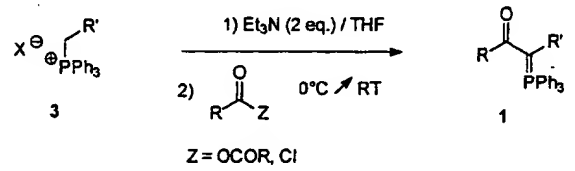

the fact that their synthesis is particularly easy and well-known,[37] since these molecules are also used in the field of organic chemistry, as precursors for vicinal tricarbonyl molecules, for example.[38] In addition, it is well-known that the oxidative addition of such a ligand to zerovalent nickel compounds (most preferably Ni(COD)$_2$) leads to an alkylated metal due to transfer of a phenyl group from the phosphorus atom to the nickel atom (Scheme 1).[39] Therefore, in the same step, ligand displacement and metal alkylation are effected, ruling out the use of an alkylating agent such as MAO. Finally, no additional Lewis base (such as triphenylphosphine or pyridine) is added to stabilize the metal center into a 16-electron conformation. Note that in our hands, ligand complexation occurs only after ethylene addition (vide infra). This route presents the additional advantage that no phosphine sponge is necessary to prepare high molecular weight polymers.[40] The general method used to synthesize our ligands is outlined in Scheme 2. This reaction is described by Hamper[41] as a one-pot synthesis when the phosphonium salt is bearing an ester group, because the acidity of the proton is high enough to be removed by a weak base such as triethylamine. The synthesis of ligand **1a** is described by Hamper through the reaction of trifluoroacetic anhydride with the corresponding phosphonium salt **3**. We have extended the reaction to the synthesis of ligands **1b–e** using heptafluorobutanoyl chloride and pentafluorobenzoyl chloride. The yield of the reaction ranges from 60% to 80%, and the final product is easily recrystallized from methanol. The ligands are characterized by ^{1}H, ^{13}C, ^{19}F, and ^{31}P NMR, IR, and microanalysis (see Experimental Section).

2. Synthesis of the Catalytic System. Catalysts can be prepared by reacting the ylide with a suitable source of nickel(0) such as bis(1,5-cyclooctadiene)nickel (Ni(COD)$_2$). Isolated catalysts are most usually prepared by adding a strongly nucleophilic ligand such as phosphine[42] or a less nucleophilic one (for example pyridine),[18] to fill the vacancy. In our case, complex synthesis is readily followed by ^{1}H NMR, since the resonances of the COD protons of the ligated and free forms are shifted from 4.29 to 5.56 ppm for the vinylic protons and from 2.07 to 2.20 for the allylic ones. Similarly, free and bound ligands display notably different resonances for the ester group (see Experimental Section). When Ni(COD)$_2$ is contacted with the ligand in a stoichiometric amount (or more) at room temperature (at a concentration of 0.1 mol/L or less), no observed reaction occurs within hours (Scheme 3). Upon heating at 60 °C, ligand insertion and rearrangement occurs, to form dimer **4** in 10% yield. The rest of Ni(COD)$_2$ decomposes when exposed to heat. In the case of a ratio of Ni(COD)$_2$ to ligand **1a** smaller than 0.5, we observe the formation of complex **5**, which has been crystallized and analyzed by X-ray (Figure 1). Water present in the reaction medium has been trapped in the crystal.

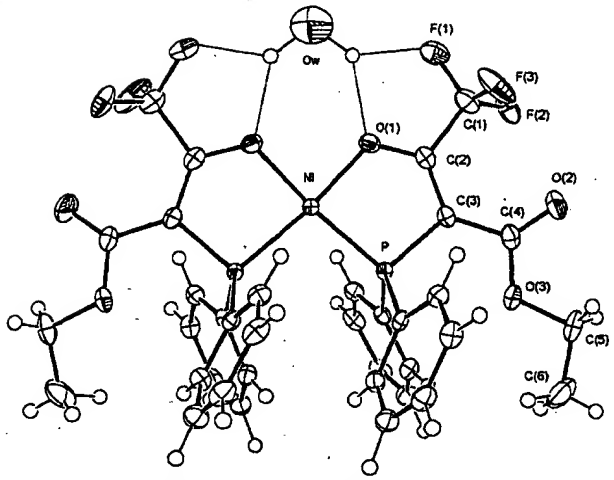

Figure 1. Crystal structure of **5** (ORTEP diagram).

Complexes analogous to **4** and **5** have already been described by Klabunde.[16] For example, starting from complex PhNi(Ph$_2$PCH=C(Ph)O)(PEt$_3$), the addition of a phosphine sponge (Rh(acac)(C$_2$H$_4$)$_2$) leads to the complex **4**. In our case, we believe that, due to the very low electron-donating character of our ligands, the displacement of COD by the ylide is difficult, and needs to be assisted by an additional Lewis base.

This Lewis base can be either an olefin, such as ethylene or 1-hexene, or a phosphine (Scheme 4). With ethylene, at a pressure of 1 atm and at room temperature, COD is partially displaced, and 22% of the nickel centers are transformed into nickel(II) enolato–phosphine. When 5 equiv (0.5 mol/L) of 1-hexene are reacted at room temperature with Ni(COD)$_2$ (0.1 mol/L) and the ylide (0.1 mol/L), less than 20% of the complex is formed. However, after 15 min heating at 60 °C, not only is all the COD uncoordinated but also all the 1-hexene is polymerized. As shown below, our complexes are active not only for the polymerization of ethylene but also for the homo- and co-polymerization of other α-olefins.

When the solution of Ni(COD)$_2$ and ylide is reacted with 20 equiv of PPh$_3$, the solution turns from light yellow to deep purple at room temperature. NMR analysis indicates that 50% of the ylide is bound to the nickel, forming complex **6**, and 50% is left unreacted because part of the nickel is engaged under the form of Ni(PPh$_3$)$_4$. Nevertheless, with less than 20 equiv of phosphine (10 equiv, e.g.), yields of complex **6** are lower, and some Ni(COD)$_2$ remains unreacted.

6 is only active in polymerization (and not in oligomerization) if the phosphine is removed by contact with a phosphine sponge such as Ni(COD)$_2$.[43] Up to date, we have not been able to crystallize the phosphine bound complexes, so polymerization results with **6** will not be presented in this paper.

This set of observations prompted us to prepare in situ our complexes by reacting 1 equiv of ylide dissolved in toluene to 1 or 2 equiv of Ni(COD)$_2$ in toluene at room

Scheme 3. Possible Reactions of a Solution of $Ni(COD)_2$ and Ligand 1a under Different Conditions of Ratio and of Temperature

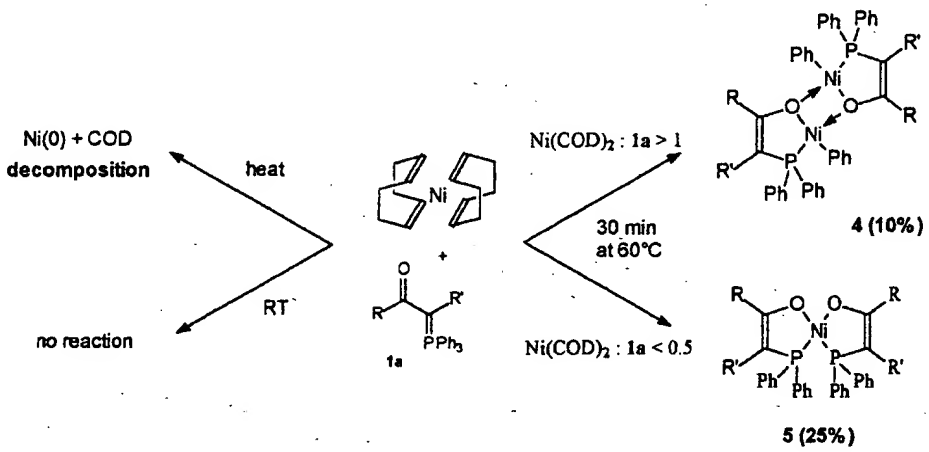

Scheme 4. Reactions of Complexation of a Solution of $Ni(COD)_2$ and Ligand 1a Exposed to Different Lewis Bases

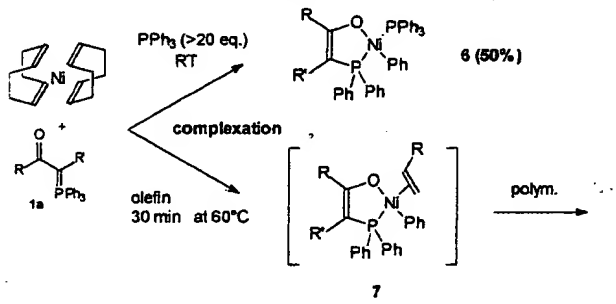

temperature for 30 min, in the presence of an olefin. We found the catalyst activity to be little dependent on the ratio of ylide: $Ni(COD)_2$, unless a large excess of $Ni(COD)_2$ is used (>4 equiv), where a slight deactivation is observed.

3. Results in Ethylene Homopolymerization. The different ligands used are represented in Scheme 1. The results of some representative ethylene polymerizations with catalysts **1a–g** are presented in Table 1. We believe that these catalysts are more active nickel catalysts than those reported in open literature, when compared under similar conditions.[44,45] Very small amounts of catalyst are used in order to avoid important exotherms and complete loss of temperature control. The catalytic solution is added to the diluent of the reaction (toluene or heptane), and the combined solutions are injected into the reactor. As soon as the temperature reaches its set point, ethylene is added and an immediate ethylene uptake is observed. Two main points emerge from these results. First, the activities obtained are very high for late transition metal catalyst[31,46] and comparable to homogeneous metallocenes under the same conditions.[1,3] Second, the low molecular weight polyethylene thus produced is virtually devoid of branching (Table 1).

The influence of the ligand fluorine atoms on the activity is remarkable, as seen by comparison of entries 1 and 2 to entries 11 and 12 (nonfluorinated analogues). The CF_3 is the most active so that the polymerizations are hardly temperature controlled (exotherms of more than 40 °C are observed for catalyst amount of more than 12 μmol/L). The heptafluoropropyl ligand **1b** (entry 3) gives almost the same activities as the trifluoro one

Table 1. Polymerization Data for Catalysts 1a–g

entry no.[a]	n (μmol/L)	catal no.	prod (kg/g_{Ni})	act. ($kg/g_{Ni}/h$)	M_w[b] (g/mol)	M_w/M_n	br/ 1000 C
1	6	**1a**	272	>2000	3500	2.7	0.9
2[c]	9	**1a**	102	970	4800	3.1	0.8
3	12	**1b**	154	1400	3700	3.2	1.0
4	13.5	**1c**	58	610	3800	3.7	0.8
5[c]	9	**1c**	58	420	5000	3.2	0.6
6	9	**1d**	112	1180	3700	3.0	0.7
7[c]	9	**1d**	126	500	4700	3.7	0.8
8	9	**1e**	100	1080	3700	3.5	0.8
9[c]	9	**1e**	64	560	4600	3.4	0.7
10[d]	15	**1b**	51	140	4400	3.6	0.9
11	135	**1f**	8	35	8000	2.9	1.0
12[e]	60	**1g**	0.5	10	10 000	3.1	1.1
13[f]	30	**1a**	1	15	1500	2.0	na
14[g]	30	**1a**	0.5		1700[h]	1.4	na

[a] Polymerizations were carried out with the active catalyst in 400 mL of toluene at 3 bar of ethylene and 70 °C. [b] Determined by GPC at high temperature vs polyethylene standards uncorrected. [c] Reactions in 400 mL of heptane. [d] Solvent: toluene/water (300/100 mL). [e] Literature value. [f] Propylene polymerization. [g] Hexene polymerization. [h] Determined by SEC in THF vs polystyrene standards uncorrected.

1a (entries 1 and 3). The pentafluoro catalysts **1c–e** are less active (entries 4–9), probably because of the decreased electrophilicity. The presence of the ester in α of the ketone was thought to be important as it stabilizes by resonance the enolate bond formed during the complexation step of the metal. Indeed, there is a slight difference in activity between ligands **1a** and the ligand in which R′ is a proton under the same conditions (entry 1 for **1a** and a measured activity of 1000 (kg/g_{Ni})/h for the other ligand).[47] We also naively thought that, by increasing the bulk of the ester alkoxy group, it was possible to exert a control over the selectivity toward higher molecular weights. However, as this group is not directed to the metal center where the coordination, insertion, isomerization, and transfer steps take place, it is unable to impart such a property to the catalyst. Accordingly, no molecular weight difference can be observed by increasing bulk on the alkoxide substituent (entries 4, 6, and 8); yet a small increase in activity, which could be nonsignificant, is observed. As proposed by Brookhart,[28] control over molecular weight distribution can be obtained by blocking the axial faces of the metal, thus inhibiting the associative displacement of the coordinated growing chain through β-H elimination.

In our case, the square planar geometry of the catalyst implies that both axial faces of the nickel center are readily accessible, thus leading to low molecular weight distribution. Notably, the polydispersity indices are characteristic of single site homogeneous catalysts. Molecular weights determined by GPC and NMR tend to prove that low molecular weight polyethylene is synthesized. The ^{13}C and ^{1}H NMR microstructure studies showed three general features of the polymers obtained: first, there is an equal number of unsaturated and saturated chain ends, second, there is a very low methyl branching content (less than 1 per 1000 C) and third, few internal double bonds due to β-H transfer followed by β-H addition on a more substituted carbon are observed (1 per 1000 C). This hints that the dominant mechanism for the production of this highly linear polymer is initiation by a nickel hydride, propagation, and termination by β-hydride elimination.

The influence of the solvent on the activity has also been studied. As the solubility of ethylene in toluene is 4 times greater than in heptane,[48] the observed activities are superior in toluene than in heptane (entries 6 and 7). However, there is no solvent effect on the molecular weight. Very low activities were observed in THF. Our current work deals with the polymerization of ethylene in very polar solvent such as water.[35]

Conclusion

In this paper, we have presented a family of electron deficient keto−ylide ligands which are particularly active for the polymerization of ethylene. Their synthesis and their use in the preparation of catalytic complexes have been reviewed. Finally, the results in ethylene homopolymerization have been discussed. Our actual work concentrates on the polymerization of ethylene in water and the co-polymerization of ethylene with other nonpolar and polar monomers.

Acknowledgment. We wish to thank Pr. P. Richard for the RX structure. R.S. wishes to thank CNRS for a BDI fellowship.

Supporting Information Available: Tables of crystal and intensity collection data, positional and thermal parameters, and all bond distances and angles and a figure showing the crystal structure for **5**. This material is available free of charge via the Internet at http://pubs.acs.org.

References and Notes

(1) Coates, G. W.; Waymouth, R. M. *Comprehensive Organometallic Chemistry II*; Hegedus, L., Ed.; Pergamon Press: Oxford, England, 1995; Vol. 12, p 1193.
(2) Hlatky, G. G. *Chem. Rev.* **2000**, *100*, 1347.
(3) Soga, K.; Shiono, T. *Prog. Polym. Sci.* **1997**, *22*, 1503.
(4) Britovsek, G. J. P.; Gibson, V. C.; Wass, D. F. *Angew. Chem., Int. Ed.* **1999**, *38*, 428.
(5) Ittel, S. D.; Johnson, L. K.; Brookhart, M. *Chem. Rev.* **2000**, *100*, 1169.
(6) Boffa, L. S.; Novak, B. M. *Chem. Rev.* **2000**, *100*, 1479.
(7) Kealy, T. J. (du Pont de Nemours, E. I.) U. S. Patent 3,474,-082, **10/1969**. We believe that the rhodium complex is not a coordination catalyst for the polymerization because the extremely harsh conditions (125 °C, 3000 atm) and the use of radical sources (HI, EtOH, and KI) suggest that actually this patent deals with radical polymerization.
(8) James, B. R.; Markham, L. D. *J. Catal.* **1972**, *27*, 442.
(9) Yamamoto, A.; Morifuji, K.; Ikeda, S.; Saito, T.; Uchida, Y.; Misono, A. *J. Am. Chem. Soc.* **1965**, *87*, 4652.
(10) Yamamoto, T.; Yamamoto, A.; Ikeda, S. *Bull. Chem. Soc. Jpn.* **1972**, *45*, 1104.
(11) Behr, A.; Keim, W. *Arabian J. Sci. Eng.* **1985**, *10*, 377.
(12) Keim, W.; Appel, R.; Storeck, A.; Krüger, C.; Goddard, R. *Angew. Chem., Int. Ed. Engl.* **1981**, *20*, 116.
(13) Keim, W.; Behr, A.; Limbacker, B.; Kruger, C. *Angew. Chem., Int. Ed.* **1983**, *22*, 503.
(14) Keim, W.; Appel, R.; Gruppe, S.; Knoch, F. *Angew. Chem., Int. Ed. Engl.* **1987**, *26*, 1012.
(15) Müller, U.; Keim, W.; Krüger, C.; Betz, P. *Angew. Chem., Int. Ed. Engl.* **1989**, *28*, 1011.
(16) Klabunde, U.; Mulhaupt, R.; Herskovitch, T.; Janowicz, A. H.; Calabrese, J.; Ittel, S. D. *J. Polym. Sci., A: Polym. Chem.* **1987**, *25*, 1989.
(17) Klabunde, U.; Ittel, S. D. *J. Mol. Catal.* **1987**, *41*, 123.
(18) Klabunde, U. (E. I. du Pont de Nemours) U.S. Patent 4,698,-403, **10/1987**.
(19) Ostaja-Starzewski, K.; Witte, J.; Bartl, H. (Bayer AG) U.S. Patent 4,620,021, **10/1986**.
(20) Ostoja-Starzewski, K. A.; Wittte, J. *Angew. Chem., Int. Ed. Engl.* **1985**, *24*, 599.
(21) Ostoja-Starzewski, K. A.; Wittte, J. In *Transition-Metal Catalyzed Polymerizations*; Quirck, R. P., Ed.; Cambridge University Press: Cambridge, England, 1988; p 472.
(22) Ostoja-Starzewski, K. A.; Wittte, J. *Angew. Chem., Int. Ed. Engl.* **1987**, *26*, 63.
(23) Mason, R. F. (Shell Oil Co.) U.S. Patent 3,676,523, 1972.
(24) Beach, D. L.; Harrison, J. J. (Gulf Research & Development Co.) U.S. Patent 4,529,554, 1985.
(25) Desjardins, S. Y.; Cavell, K. J.; Hoare, J. L.; Skelton, B. W.; Sobolev, A. N.; White, A. H.; Keim, W. *J. Organomet. Catal.* **1997**, *544*, 163.
(26) Johnson, L. K.; Killian, C. M.; Brookhart, M. *J. Am. Chem. Soc.* **1995**, *117*, 6414.
(27) Johnson, L. K.; Mecking, S. M.; Brookhart, M. *J. Am. Chem. Soc.* **1996**, *118*, 267.
(28) Mecking, S.; Johnson, L. K.; Wang, L.; Brookhart, M. *J. Am. Chem. Soc.* **1998**, *120*, 888.
(29) Wang, C.; Friedrich, S.; Younkin, T. R.; Li, R. T.; Grubbs, R. H.; Bansleben, D. A.; Day, M. W. *Organometallics* **1998**, *17*, 3149.
(30) Younkin, T. R.; Connor, E. F.; Henderson, J. I.; Friedrich, S. K.; Grubbs, R. H.; Bansleben, D. A. *Science* **2000**, *287*, 460.
(31) Britovsek, G. J. P.; Gibson, V. C.; Kimberley, B. S.; Maddox, P. J.; McTavish, S. J.; Solan, G. A.; White, A. J. P.; Williams, D. J. *J. Chem. Soc., Chem. Commun.* **1998**, 849.
(32) Britovsek, G. J. P.; Bruce, M.; Gibson, V. C.; Kimberley, B. S.; Maddox, P. J.; Mastroianni, S.; McTavish, S. J.; Redshaw, C.; Solan, G. A.; Strömberg, S.; White, A. J. P.; Williams, D. J. *J. Am. Chem. Soc.* **1999**, *121*, 8728.
(33) Small, B. L.; Brookhart, M.; Bennett, A. M. A. *J. Am. Chem. Soc.* **1998**, *120*, 1049.
(34) Tomov, A.; Broyer, J. P.; Spitz, R. In *Polymers in Dispersed Media I*; Claverie, J., Charreyre, M.-T., Pichot, C., Eds.; Wiley: Weinheim, Germany, 2000; Vol. 150, p 53.
(35) Tomov, A.; Spitz, R.; Saudemont, T.; Drujon, X. (Elf Atochem. S. A.) French Patent 98.12476, 1998.
(36) Held, A.; Bauers, F. M.; Mecking, S. *J. Chem. Soc., Chem. Commun.* **2000**, 301.
(37) Hartley, F. R. *The Chemistry of Organophosphorus Compounds*; John Wiley & Sons: New York, Vol. 3.
(38) Wasserman, H. H.; Baldino, C. M.; Coats, S. J. *J. Org. Chem.* **1995**, *60*, 8231.
(39) Keim, W.; Kowalt, F. H.; Goddard, R.; Krüger, C. *Angew. Chem., Int. Ed. Engl.* **1978**, *17*, 466.
(40) The oligomerization is often due to the presence of a Lewis base. Indeed, the competition in the chelation between ethylene and the Lewis base leads to low molecular weight material.
(41) Hamper, B. C. *J. Org. Chem.* **1988**, *53*, 5558.
(42) Hirose, K.; Keim, W. *J. Mol. Catal.* **1992**, *73*, 271.
(43) Oligomers can be synthesized if no phosphine sponge is used.
(44) Klabunde, U. (E. I. Du Pont de Nemours) U.S. Patent 4,716,-205, **12/1987**.
(45) Bauer, R.; Chung, H.; Barnett, K. W.; Glockner, P. W.; Keim, W. (Shell Oil Co.) U. S. Patent 3,686,159, **8/1972**.
(46) Gibson reported catalytic activity of this order with 2,6-bis-(imino)pyridyliron(II) chloride activated by MAO (100 equiv).
(47) Touchard, V. Master's Thesis, Université Claude Bernard Lyon 1, 2000.
(48) Mattioli, V. Ph.D. Thesis, University Claude Bernard Lyon 1, 2000.

MA001714X

6 Chemistry of Transition Metals

****

Simple substances of transition metals have properties characteristic of metals, *i.e.* they are hard, good conductors of heat and electricity, and melt and evaporate at high temperatures. Although they are used widely as simple substances and alloys, we typically encounter only iron, nickel, copper, silver, gold, platinum, or titanium in everyday life. However, molecular complexes, organometallic compounds, and solid-state compounds such as oxides, sulfides, and halides of transition metals are used in the most active research areas in modern inorganic chemistry.

****

Transition elements are metallic elements that have incomplete *d* or *f* shells in the neutral or cationic states. They are called also transition metals and make up 56 of the 103 elements. These transition metals are classified into the *d*-block metals, which consist of 3*d* elements from Sc to Cu, 4*d* elements from Y to Ag, and 5*d* elements from Hf to Au, and *f*-block metals, which consist of lanthanoid elements from La to Lu and actinoid elements from Ac to Lr. Although Sc and Y belong to the *d*-block, their properties are similar to those of lanthanoids. The chemistry of *d*-block and *f*-block elements differs considerably. This chapter describes the properties and chemistry of mainly *d*-block transition metals.

6.1 Structures of metal complexes

(a) Central metals

Properties of *d*-block transition metals differ considerably between the first (3*d*) and the second series metals (4*d*), although the differences in properties between the second and the third series (5*d*) metals is not pronounced. Metallic radii of elements from scandium, Sc, to copper, Cu, (166 to 128 pm) are significantly smaller than those of yttrium, Y, to silver, Ag, (178 to 144 pm) or those of lanthanum, La, to gold, Au, (188 to 146 pm). Further, metal compounds of the first series transition metals are rarely 7 co-ordinate, whereas transition metals from the second and third series may be 7 to 9 coordinate. Cerium, Ce, (radius 182 pm) ~ lutetium, Lu, (radius 175 pm) fall between La and Hf and, because of the lanthanide contraction, metallic radii of the second and third series transition metals show little variation.

Higher oxidation states in the second and third series transition metals are

considerably more stable than those in the first series transition metals. Examples include tungsten hexachloride, WCl_6, osmium tetroxide, OsO_4, and platinum hexafluoride, PtF_6. Compounds of the first series transition metals in higher oxidation states are strong oxidants and thus are readily reduced. On the other hand, whereas M(II) and M(III) compounds are common among the first series transition metals, these oxidation states are generally uncommon in compounds of second and third series metals. For example, there are relatively few Mo(III) or W(III) compounds compared with many Cr(III) ones. Aqua ions (ions with water ligands) are very common among compounds of first series metals but few are known amongst the second and third metal compounds.

Metal carbonyl cluster compounds of first series transition metals with M-M bonds in low oxidation states exist but halide or sulfide cluster compounds are rare. In general, metal-metal bonds are formed much more easily in the 4*d* and 5*d* metals than in the 3*d* ones. Magnetic moments of the first series transition metal compounds can be explained in terms of spin-only values (*cf.* Chapter 6.2 (d)) but it is difficult to account for the magnetic moments of the second and third series compounds unless complex factors such as spin-orbital interactions are taken into account.

Thus, it is necessary to acknowledge and understand the significant differences in chemical properties that exist between metals of the first and later series metal compounds, even for elements in the same group.

Properties of the *d*-block transition metals are different not only in the upper and lower positions in the periodic table but also in the left and right groups. The Group 3 to 5 metals are now often referred to as **early transition metals** and they are generally oxophilic and halophilic. Smaller numbers of *d* electrons and the hardness of these elements explain their affinity toward hard oxygen and halogens. In the absence of bridging ligands, the formation of metal-metal bonds is difficult for these elements. Organometallic compounds of these metals are known strongly to activate C-H bonds in hydrocarbons. **Late transition metals** in the groups to the right of the periodic table are soft and have a high affinity toward sulfur or selenium.

The *d*-block transition metals have *s*, *p*, and *d* orbitals and those with n electrons in the *d* orbitals are termed **ions with a d^n configuration**. For example, Ti^{3+} is a d^1 ion, and Co^{3+} a d^6 ion. The number of electrons occupying the orbitals split by the ligand field (*cf.* 6.2(a)) is denoted by a superscript on the orbital symbol. For example, an ion with 3 electrons in t_{2g} and 2 electrons in e_g is described as $t_{2g}^3 e_g^1$.

(b) Ligands

Compounds of metal ions coordinated by ligands are referred to as **metal complexes**. Most ligands are neutral or anionic substances but cationic ones, such as the

tropylium cation, are also known. Neutral ligands, such as ammonia, NH_3, or carbon monoxide, CO, are independently stable molecules in their free states, whereas anionic ligands, such as Cl^- or $C_5H_5^-$, are stabilized only when they are coordinated to central metals. Representative ligands are listed in Table 6.1 according to the ligating elements. Common ligands or those with complicated chemical formula are expressed in abbreviated forms.

Those ligands with a single ligating atom are called **monodentate ligands**, and those with more than one ligating atoms referred to as **polydentate ligands**, which are also called **chelate ligands**. The number of atoms bonded to a central metal is the **coordination number**.

Table 6.1 Representative ligands

Name	Abbreviation	Formula
hydrido		H^-
carbonyl		CO
cyano		CN^-
methyl	Me	CH_3^-
cyclopentadienyl	Cp	$C_5H_5^-$
carbonato		CO_3^{2-}
ammine		NH_3
pyridine	py	C_5H_5N
bipyridine	bipy	$C_{10}H_8N_2$
triphenylphosphine	PPh_3	$P(C_6H_5)_3$
aqua	aq	H_2O
acetylacetonato	acac	$CH_3C(O)CH_2C(O)CH_3^-$
thiocyanato		SCN^-
chloro		Cl^-
ethylenediaminetetraacetato	edta	$(OOCCH_2)_2NCH_2CH_2N(CH_2COO)_2^{4-}$

(c) Coordination number and structures

Molecular compounds which consist of *d*-block transition metals and ligands are referred to as complexes or **coordination compounds**. The coordination number is determined by the size of the central metal, the number of *d* electrons, or steric effects arising from the ligands. Complexes with coordination numbers between 2 and 9 are known. In particular 4 to 6 coordination are the most stable electronically and

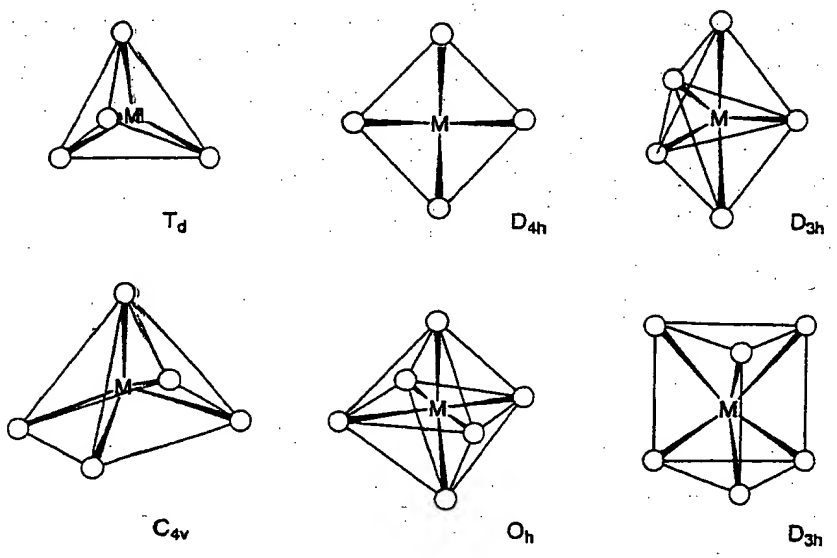

Fig. 6.1 Structure of 4 ~ 6 coordination.

geometrically and complexes with these coordination numbers are the most numerous (Fig. 6.1). Complexes with the respective coordination numbers are described below.

Two co-ordinate complexes

Many electron-rich d^{10} ions, *viz*: Cu^+, Ag^+, and Au^+, form linear complexes such as $[Cl\text{-}Ag\text{-}Cl]^-$ or $[H_3N\text{-}Au\text{-}NH_3]^+$. A zero-valent complex $[Pd(PCy_3)_2]$ with very bulky tricyclohexylphosphine ligands is also known. Generally, stable 2-coordinate complexes are known for the late transition metals.

Three co-ordinate complexes

Although $[Fe\{N(SiMe_3)_3\}_3]$ is one example, very few 3-coordinate complexes are known.

Four co-ordinate complexes

When four ligands coordinate to a metal, tetrahedral (T_d) coordination is the least congested geometry, although a number of square planar (D_{4h}) complexes are known. $[CoBr_4]^{2-}$, $Ni(CO)_4$, $[Cu(py)_4]^+$, $[AuCl_4]^-$ are all examples of tetrahedral complexes. There are a few known examples of square planar complexes with identical ligands, such as $[Ni(CN)_4]^{2-}$, or $[PdCl_4]^{2-}$. In the case of **mixed ligand complexes**, a number of square planar complexes of d^8 ions, Rh^+, Ir^+, Pd^{2+}, Pt^{2+}, and Au^{3+}, have been reported. Examples include $[RhCl(PMe_3)_3]$, $[IrCl(CO)(PMe_3)_2]$, $[NiCl_2(PEt_3)_2]$, and $[PtCl_2(NH_3)_2]$ (Et = C_2H_5).

Cis and trans **geometrical isomers** are possible for complexes with two different kinds of ligands, and were first noted when A. Werner synthesized 4-coordinate $[PtCl_2(NH_3)_2]$. As tetrahedral complexes do not give geometrical isomers, Werner was able to conclude that his 4-coordinate complexes were square planar. Recently *cis*-$[PtCl_2(NH_3)_2]$ (Cisplatin) has been used for the treatment of tumors and it is noteworthy that only the ***cis*** isomer is active.

Exercise 6.1 Write the formal name of *cis*-$[PtCl_2(NH_3)_2]$.
[Answer] *cis*-diamminedichloroplatinum.

Five co-ordinate complexes

Trigonal bipyramidal (D_{3h}) $Fe(CO)_5$ or square pyramid (C_{4v}) $VO(OH_2)_4$ are examples of 5-coordinate complexes. Previously, 5-coordinate complexes were rare but the number of new complexes with this coordination is increasing. The energy difference between the two coordination modes is not large and structural transformation readily occurs. For example, the molecular structure and infrared spectrum of $Fe(CO)_5$ are consistent with a trigonal bipyramid structure, but the ^{13}C NMR spectrum shows only one signal at the possible lowest temperature, which indicates that the axial and equatorial carbonyl ligands are fluxional in the NMR time scale (10^{-1}~10^{-9} s). Structural transformation takes place via a square pyramid structure and the mechanism is well known as **Berry's pseudorotation**.

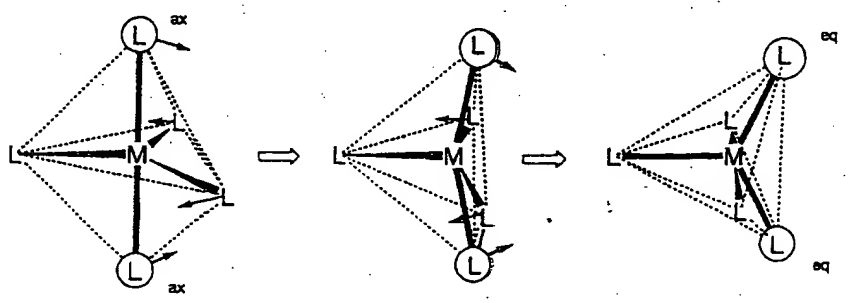

Fig. 6.2 Berry's pseudorotation.

Six co-ordinate complexes

When six ligands coordinate to a central metal, octahedral (O_h) coordination is the most stable geometry and the majority of such complexes assume this structure. In particular, there are a number of Cr^{3+} and Co^{3+} complexes which are inert to ligand exchange reactions, represented by $[Cr(NH_3)_6]^{3+}$ or $[Co(NH_3)_6]^{3+}$. They have been particularly important in the history of the development of coordination chemistry. $[Mo(CO)_6]$, $[RhCl_6]^{3-}$, *etc.* are also octahedral complexes. In the case of mixed ligands, *cis*- and *trans*-$[MA_4B_2]$ and *mer*- and *fac*-$[MA_3B_3]$ geometrical isomers, and for chelate ligands, Δ-$[M(A\text{-}A)_3]$ and Λ-$[M(A\text{-}A)_3]$ **optical isomers** (Fig. 6.3) are possible. The octahedral structure shows tetragonal (D_{4h}), rhombic (D_{2h}), or trigonal (D_{3h}) distortions caused by electronic or steric effects. The tetragonal distortion of $[Cu(NH_3)_6]^{2+}$ by an electronic factor is a typical example of the Jahn-Teller effect (refer to 6.2(a)).

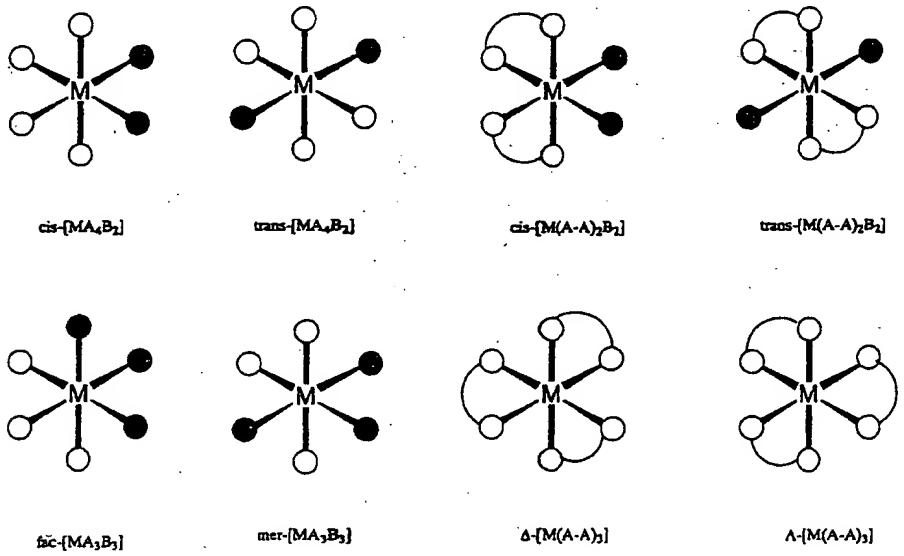

Fig. 6.3 Geometrical isomers of 6-coordination.

Six ligating atoms can assume trigonal prism coordination. Although this coordination is seen in $[Zr(CH_3)_6]^{2-}$ or $[Re\{S_2C_2(CF_3)_2\}_3]$, few metal complexes with this coordination structure are known because octahedral coordination is sterically less strained. This notwithstanding, it has long been known that the bonding mode of sulfur atoms around a metal is trigonal prism in solid-state MoS_2 and WS_2.

Exercise 6.2 Write the chemical formula of potassium diamminetetra(isothiocyanato)chromate(III).

[Answer] $K[Cr(NCS)_4(NH_3)_2]$.

Higher co-ordinate complexes

Metal ions of the second and third transition metal series can sometimes bond with more than seven ligating atoms and examples are $[Mo(CN)_8]^{3-}$ or $[ReH_9]^{2-}$. In these cases, smaller ligands are favorable to reduce steric congestion.

6.2 Electronic structure of complexes

It is necessary to learn a few concepts to understand the structure, spectrum, magnetism, and reactivity of complexes which depend on *d* electron configurations. In particular, the theory of electronic structure is important.

(a) Ligand field theory

Ligand field theory is one of the most useful theories to account for the electronic structure of complexes. It originated in the application of the **crystal field theory** of ionic crystals to metal complex systems.

Six co-ordinate octahedral complexes

The five *d* orbitals of transition metal cations are degenerate and have equal energy.

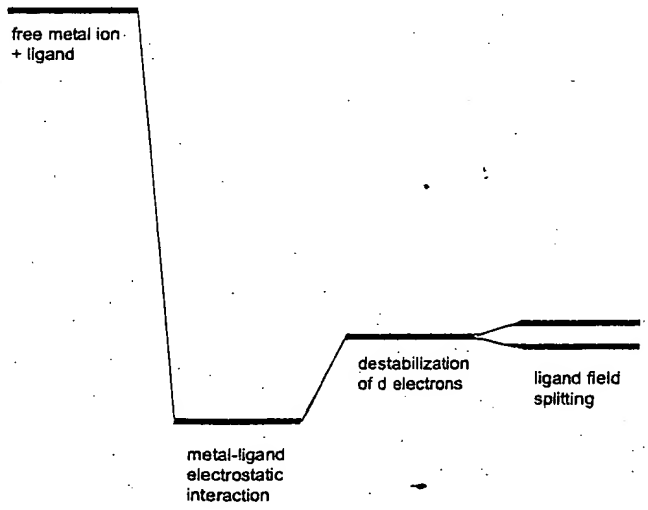

Fig. 6.4 Change of electronic energy upon complex formation.

The spherical negative electric field around a metal cation results in the total energy level being lower than that of a free cation because the electrostatic interactions. The repulsive interaction between the electrons in the metal orbitals and the negative electric field destabilizes the system and compensates for the stabilization to some extent (Fig. 6.4).

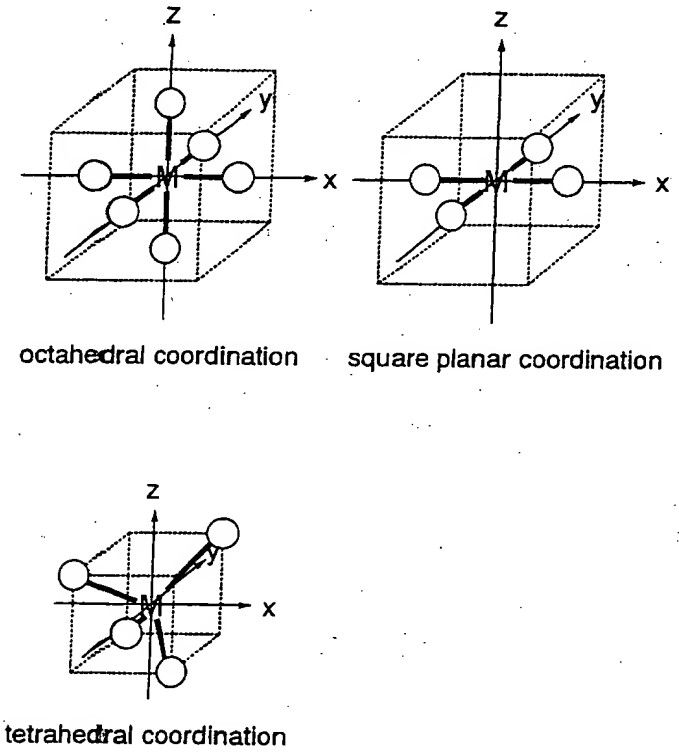

Fig. 6.5 Ligand positions in the Cartesian coordinate with a metal ion at the origin.

Let us assume that instead of a uniform spherical negative field, the field is generated by six ligands coordinating octahedrally to a central metal. The negative field of the ligands is called the **ligand field.** Negative charge, in the case of anionic ligands, or a negative end (lone pair), in the case of neutral ligands, exert a repulsive force on the metal *d* orbitals which is anisotropic depending on the direction of the orbitals. The position of the metal cation is taken as the origin and Cartesian coordinates are constructed (Fig. 6.5). Then, d_{x2-y2} and d_{z2} orbitals are aligned along the directions of the axes and the d_{xy}, d_{yz}, and d_{xz} orbitals are directed between the axes. If ligands are placed on the axes, the repulsive interaction is larger for the e_g orbitals (d_{x2-y2}, d_{z2}) than for the t_{2g}

orbitals (d_{xy}, d_{yz}, d_{xz}), and the e_g orbitals are destabilized and the t_{2g} orbitals are stabilized to an equal extent. In the following discussion, only the energy difference between the t_{2g} and e_g orbitals is essential and the average energy of these orbitals is taken as the zero of energy. If the energy difference between the two e_g and three t_{2g} orbitals is set to Δ_o, the energy level of the e_g orbitals is $+3/5\Delta_o$ and that of the t_{2g} orbitals is $-2/5\Delta_o$ (Fig. 6.6). (Δ_o may also be expressed as 10 Dq. In this case, the energy level of the e_g orbitals is +6 Dq and that of the t_{2g} orbitals -4 Dq.)

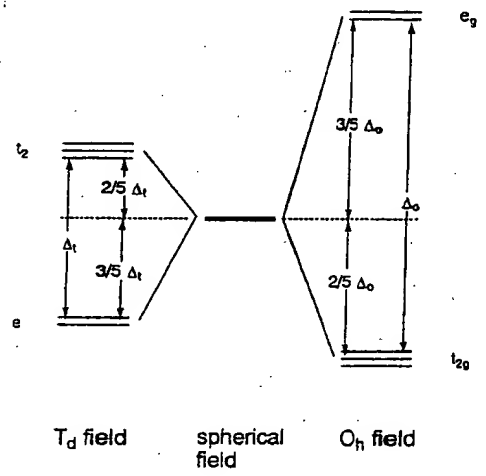

Fig. 6.6 Ligand field splitting in tetrahedral and octahedral complexes.

Transition metal ions have 0 to 10 *d* electrons and when the split *d* orbitals are filled from a lower energy level, the electron configuration $t_{2g}^{x}e_g^{y}$ corresponding to each ion is obtained. With the zero energy level chosen as the average energy level, the energy of the electron configuration relative to zero energy becomes

$$\text{LFSE} = (-0.4x + 0.6y)\,\Delta o$$

This value is called the **ligand field stabilization energy**. The electron configuration with smaller value (taking the minus sign into consideration) is more stable. LFSE is an important parameter to explain some properties of *d*-block transition metal complexes.

A condition other than the orbital energy level is required to explain the filling of electrons being populated into the split t_{2g} and e_g orbitals. Two electrons can occupy an orbital with anti-parallel spins but a strong electrostatic repulsion occurs between two electrons in the same orbital. This repulsive interaction is called **pairing energy**, *P*.

When the number of *d* electrons is less than three, the pairing energy is minimized by loading the electrons in the t_{2g} orbital with parallel spins. Namely, the electron configurations arising are t_{2g}^1, t_{2g}^2, or t_{2g}^3.

Two possibilities arise when the fourth electron occupies either of the t_{2g} or e_g orbitals. The lower energy orbital t_{2g} is favorable but occupation of the same orbital gives rise to pairing energy, *P*. The total energy becomes

$$-0.4\Delta o \times 4 + P = -1.6\Delta o + P$$

If the fourth electron occupies the energetically unfavorable e_g orbital, the total energy becomes

$$-0.4\Delta o \times 3 + 0.6\Delta o = -0.6\Delta o$$

The choice of the electron configuration depends on which of the above values is larger. Therefore if $\Delta o > P$, t_{2g}^4 is favoured and this is called the strong field case or the **low spin electron configuration**. If $\Delta o < P$, $t_{2g}^3 e_g^1$ is favoured and this is called the weak field case or the **high spin electron configuration**. A similar choice is required for d^5, d^6, and d^7 octahedral complexes, and in the strong field case, t_{2g}^5, t_{2g}^6, or $t_{2g}^6 e_g^1$ configurations are favoured, whereas in the weak field case, $t_{2g}^3 e_g^2$, $t_{2g}^4 e_g^2$, or $t_{2g}^5 e_g^2$ configurations are favoured. The ligand field splitting parameter Δo is decided by the nature of the ligands and metal, whereas the pairing energy, *P*, is almost constant and shows only a slight dependence on the identity of the metal.

Square planar complexes

Complexes with four ligands in a plane containing the central metal are termed square planar complexes. It is easier to understand the electronic energy levels of the *d* orbitals in square planar complexes by starting from those for hexacoordinate octahedral complexes. Placing the six ligands along the Cartesian axes, the two ligands on the z axis are gradually removed from the central metal and finally only four ligands are left on the x,y plane. The interaction of the two z coordinate ligands with the d_{z2}, d_{xz}, and d_{yz} orbitals becomes smaller and the energy levels of these ligands lower. On the other hand, the remaining four ligands approach the metal and the d_{x2-y2} and d_{xy} energy levels rise as a result of the removal of the two ligands. This results in the order of the energy levels of five d orbitals being d_{xz}, $d_{yz} < d_{z2} < d_{xy} << d_{x2-y2}$ (Fig. 6.7). Rh^+, Ir^+, Pd^{2+}, Pt^{2+}, and Au^{3+} complexes with a d^8 configuration tend to form square planar structures because eight electrons occupy the lower orbitals leaving the highest d_{x2-y2} orbital empty.

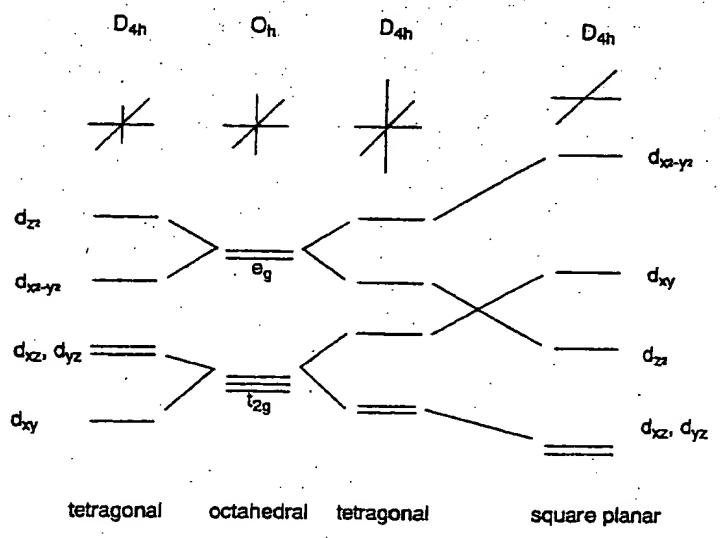

Fig. 6.7 Change of the orbital energy from octahedral to square planar complexes.

Tetrahedral complexes

Tetrahedral complexes have four ligands on the apexes of a tetrahedron around the central metal. $[CoX_4]^{2-}$ (X = Cl, Br, I), $Ni(CO)_4$, *etc.* are all examples of 4-coordination complexes (Fig. 6.5). When a metal is placed on the origin of the Cartesian axes, as in the octahedral complexes, *e* orbitals (d_{x2-y2}, d_{z2}) are distant from ligands and t_2 orbitals (d_{xy}, d_{yz}, d_{xz}) are nearer ligands. Consequently, the electronic repulsion is larger for the t_2 orbitals, which are destabilized relative to the *e* orbitals. The ligand field exerted by four ligands splits the fivefold degenerate orbitals of the central metal into twofold degenerate *e* and threefold degenerate t_2 sets (Fig. 6.6). The t_2 set has energy of $+2/5\ \Delta_t$ and the *e* set $-3/5\ \Delta_t$ with a ligand field splitting of Δ_t. As the number of the ligands is 4/6 = 2/3 of that in hexacoordinate octahedral complexes, and overlap of the ligands with the orbitals is smaller, and the ligand splitting Δt is about a half of Δo. Consequently, only high-spin electron configurations are known in tetrahedral complexes. The ligand field splitting energies calculated by the above method are shown in Table 6.2.

Table 6.2 Ligand field stabilization energy (LFSE)

		Octahedral				Tetrahedral	
		Strong field (LS)		Weak field(HS)			
d^n	Example	n	Δo	n	Δo	n	Δt
d^1	Ti^{3+}	1	0.4	1	0.4	1	0.6
d^2	V^{3+}	2	0.8	2	0.8	2	1.2
d^3	Cr^{3+},V^{2+}	3	1.2	3	1.2	3	0.8
d^4	Cr^{2},Mn^{3+}	2	1.6	4	0.6	4	0.4
d^5	Mn^{2+},Fe^{3+}	1	2.0	5	0	5	0
d^6	Fe^{2+},Co^{3+}	0	2.4	4	0.4	4	0.6
d^7	Co^{2+}	1	1.8	3	0.8	3	1.2
d^8	Ni^{2+}	2	1.2	2	1.2	2	0.8
d^9	Cu^{2+}	1	0.6	1	0.6	1	0.4
d^{10}	Cu^{1}	0	0	0	0	0	0

Jahn-Teller effect

When orbitals of a highly symmetrical nonlinear polyatomic molecule are degenerate, the degeneracy is resolved by distorting the molecular framework to attain lower symmetry and thus lower energy. This is the **Jahn-Teller effect** and a typical example is seen in the tetragonal distortion of an octahedral coordination structure of hexacoordinate Cu^{2+} complexes.

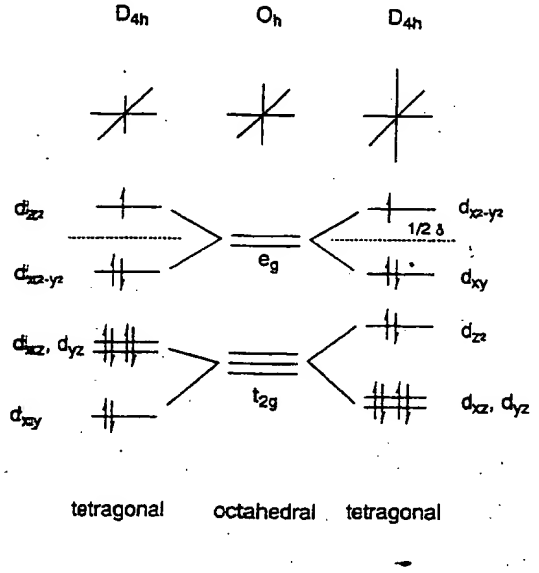

Fig. 6.8 Jahn-Teller splitting in a Cu^{2+} ion.

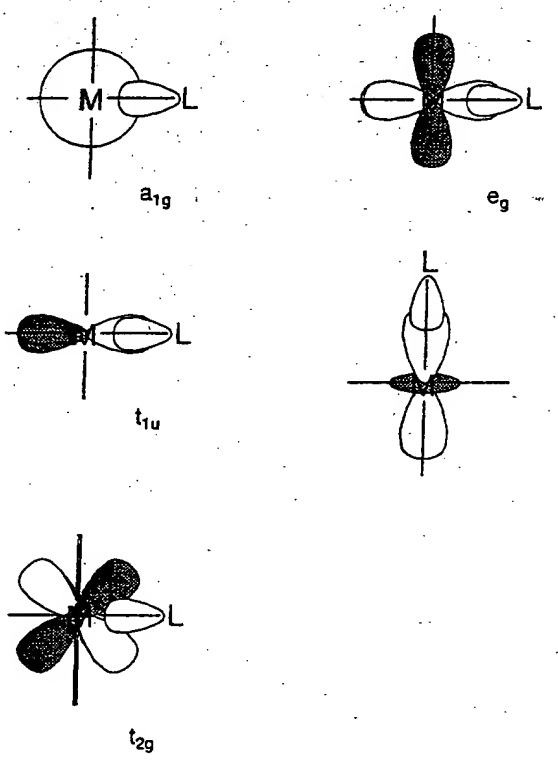

Fig. 6.9 The relation between the metal and ligand orbitals during formation of σ bonds.

They have a d^9 configurations and the e_g orbitals in the octahedral structure are occupied by three electrons. If the e_g orbitals split and two electrons occupy the lower orbital and one electron the upper orbital, the system gains energy of a half of the energy difference, δ, of two split orbitals. Therefore a tetragonal distortion in the z axis becomes favorable.

Molecular orbital theory of transition metal complexes

The characteristics of transition metal-ligand bonds become clear by an analysis of the molecular orbitals of a 3*d* metal coordinated by six identical ligands in octahedral complexes [ML_6]. As the result of the interaction between the metal *d* and ligand orbitals, bonding, non-bonding and anti-bonding complex molecular orbitals are formed.

Generally, the energy levels of the ligand orbitals are lower than those of the metal orbitals, bonding orbitals have more ligand character and non-bonding and anti-bonding orbitals have more metal character. The processes of formation of the σ and π molecular orbitals are described step by step below.

σ bond

Firstly, consider the M-L σ bond among interactions of the metal *s*, *p*, *d* and ligand orbitals by assuming the position of a metal at the origin of the Cartesian coordinate system and locating ligands on the coordinate axes. As the σ bond is a nodeless bond along the bonding axes, the metal *s* orbital (a_{1g}, non-degenerate), p_x, p_y, p_z orbitals (t_{1u}, triply-degenerate), and d_{x2-y2}, d_{z2} orbitals (e_g, doubly-degenerate) fit symmetry (+, - signs) and orbital shapes with the ligands' σ orbitals (Fig. 6.9).

When the ligand orbitals are σ_1 and σ_2 along the x-axis, σ_3 and σ_4 along the y-axis, and σ_5 and σ_6 along the z-axis in Fig. 6.5, six ligand atomic orbitals are grouped by making linear combinations according to the symmetry of the metal orbitals. Then the orbital to fit with the metal a_{1g} orbital is a_{1g} ($\sigma_1+\sigma_2+\sigma_3+\sigma_4+\sigma_5+\sigma_6$), the one to fit with the metal t_{1u} orbitals is t_{1u} ($\sigma_1-\sigma_2$, $\sigma_3-\sigma_4$, $\sigma_5-\sigma_6$) and the one to fit with the metal e_g orbitals is e_g ($\sigma_1+\sigma_2-\sigma_3-\sigma_4$, $2\sigma_5+2\sigma_6-\sigma_1-\sigma_2-\sigma_3-\sigma_4$). There is a bonding interaction between the metal e_g orbitals and the ligand group orbitals and bonding and anti-bonding molecular orbitals are formed. The relation is shown in Fig. 6.10.

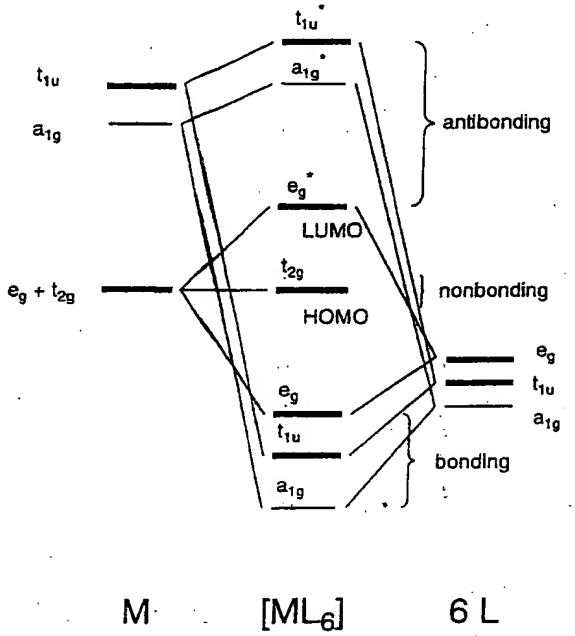

Fig. 6.10 Bonding and anti-bonding M(metal)-L(ligand) molecular orbitals.

The levels of the molecular orbitals from the lowest energy are bonding ($a_{1g}<t_{1u}<e_g$) < non-bonding (t_{2g}) < anti-bonding ($e_g^*<a_{1g}^*<t_{1u}^*$). For example, in a complex like $[Co(NH_3)_6]^{3+}$, 18 valence electrons, 6 from cobalt and 12 from ammonia, occupy 9

orbitals from the bottom up, and t_{2g} is the HOMO and e_g^* the LUMO. The energy difference between the two levels corresponds to the ligand field splitting. Namely, the e_g set (d_{x2-y2}, d_{z2}) and the ligands on the corner of the octahedron form the bonding σ orbitals but the t_{2g} set (d_{xy}, d_{yz}, d_{xz}) remain non-bonding because the orbitals are not directed to the ligand σ orbitals.

π bond

When the ligand atomic orbitals have π symmetry (i.e. with nodes) through the bond axis, the e_g orbitals (d_{x2-y2}) are non-bonding and the t_{2g} orbitals (d_{xy}, d_{yz}, d_{xz}) have bonding interactions with them (Fig. 6.11). In halide ions, X^-, or aqua ligands, H_2O, the π

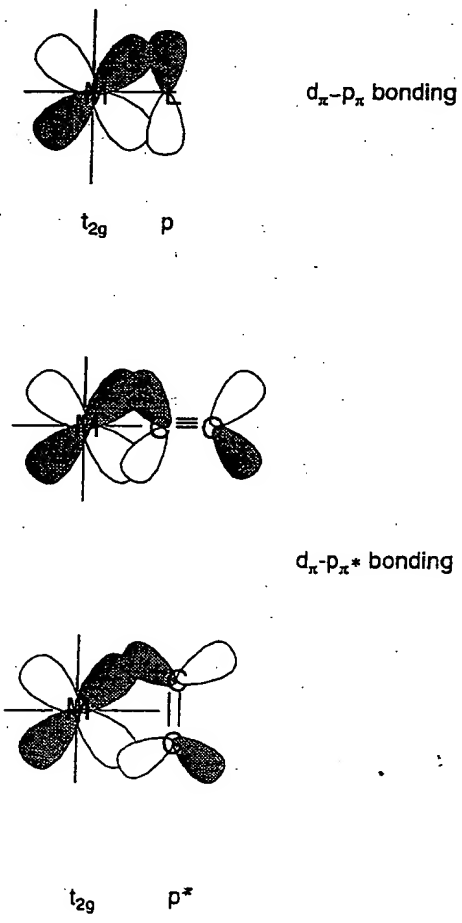

Fig. 6.11 The relation between the metal and ligand orbitals in formation of a π bond.

symmetrical *p* orbitals have lower energy than the metal t_{2g} orbitals and a bonding molecular orbital, which is lower than the t_{2g} orbital, and an anti-bonding molecular

orbital, which is higher than the t_{2g} orbitals, form. Consequently, the energy difference Δ_o between e_g and the anti-bonding orbitals becomes smaller. On the other hand, for the ligands having anti-bonding π orbitals within the molecule, such as carbon monoxide or ethylene, the π^* orbitals match the shape and symmetry of the t_{2g} orbitals and the molecular orbitals shown in Fig 6.12 (b) form. As a result, the energy level of the bonding orbitals decreases and Δ_o becomes larger.

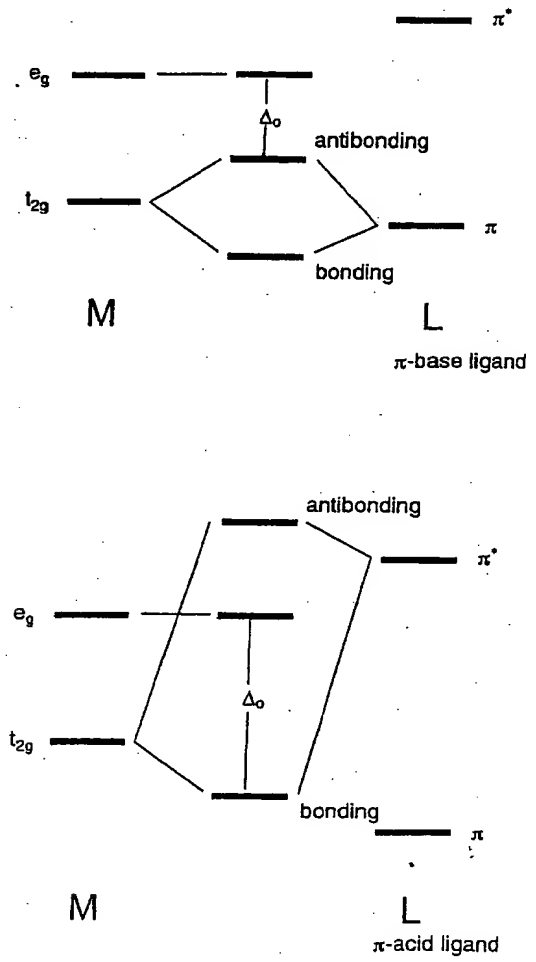

Fig. 6.12 The energy change upon formation of M-L$_\pi$ bonds.

Using these simple molecular orbital considerations, the effects of σ and π orbital interactions between the metal and ligands upon the molecular orbitals are qualitatively understandable.

(c) Spectra

Many transition metal complexes have characteristic colors. This means that there is absorption in the visible part of the spectrum resulting from an electron being excited by visible light from a level occupied by an electron in a molecular orbital of the complex to an empty level. If the energy difference between the orbitals capable of transition is set to ΔE, the absorption frequency ν is given by $\Delta E = h\nu$. Electronic transitions by optical pumping are broadly classified into two groups. When both of the molecular orbitals between which a transition is possible have mainly metal *d* character, the transition is called a ***d-d* transition** or **ligand-field transition**, and absorption wavelength depends strongly on the ligand-field splitting. When one of the two orbitals has mainly metal character and the other has a large degree of ligand character, the transition is called a **charge-transfer transition**. Charge transfer transitions are classified into metal (M) to ligand (L) charge-transfers (MLCT) and ligand to metal charge-transfers (LMCT).

Since the analysis of the spectra of octahedral complexes is comparatively easy, they have been studied in detail for many years. When a complex has only one *d* electron, the analysis is simple. For example, Ti in $[Ti(OH_2)_6]^{3+}$ is a d^1 ion, and an electron occupies the t_{2g} orbital produced by the octahedral ligand field splitting. The complex is purple as the result of having an absorption at 492 nm (20300 cm^{-1}) (Fig. 6.13) corresponding to the optical pumping of a *d* electron to the e_g orbital. However, in a complex with more than one *d* electrons, there are repellent interactions between the electrons, and the *d-d* transition spectrum has more than one absorptions. For example, a d^3 complex $[Cr(NH_3)_6]^{3+}$ shows two *d-d* absorptions in the 400 nm (25000 cm^{-1}) region, suggesting that the complex has two groups of molecular orbitals between which an electronic transition is possible with a high degree of transition probability. This means that, when three electrons in the t_{2g} orbital are excited to the e_g orbital, there are two energy differences due to repellent interactions between the electrons.

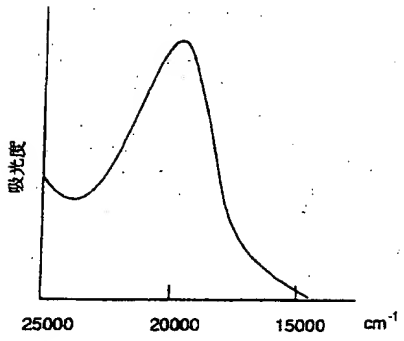

Fig. 6.13 A visible absorption spectrum of $[Ti(OH_2)_6]^{3+}$.

Tanabe-Sugano diagrams are constructed from calculations based on ligand field theory and have been widely used in the analysis of absorption spectra of d^1 to d^9 ions. The analysis becomes increasingly difficult for ions with many electrons. In any case, the existence of a *d-d* spectrum requires that the energy difference of an occupied orbital and an empty orbital is equivalent to the energy of the UV-visible spectrum, the transition is allowed by the selection rule, and the transition probability is high enough. Generally, a charge-transfer absorption is stronger than a ligand field absorption. An LMCT emerges when ligands have a non-bonding electron pair of comparatively high energy or the metal has empty low energy orbitals. On the other hand, an MLCT tends to appear when the ligands have low energy π^* orbitals, and bipyridine complexes are good examples of this. Since the lifetime of the excited state of a ruthenium complex $[Ru(bipy)_3]^{2+}$ is extraordinarily long, many studies have been performed on its photoredox reactions.

Spectrochemical series

The magnitude of the ligand field splitting parameter Δo is determined mainly by the identity of the ligands. An empirical rule called the **spectrochemical series** was proposed by a Japanese scientist Ryutaro Tsuchida. The rule was constructed from empirical data collected when spectra of complexes that have the same central metal, oxidation state, coordination number, *etc.* were measured. It is noteworthy that ligands with π acceptor properties are in a higher position in the series.

$I^- < Br^- < S^{2-} < SCN^- < Cl^- < NO_3^- < F^- < OH^- < H_2O < NH_3 < NO_2^- < PPh_3 < CN^- < CO$

Although Δ_0 does become larger in this order, it is also dependent on the identity of the central metal and its oxidation state. Namely, Δo is larger for 4*d* and 5*d* metals than for 3*d* metals and becomes larger as the oxidation number increases. The magnitude of Δ_0 is closely related to its absorption position in the electromagnetic spectrum, and is a key factor in determining the position of a ligand in the spectrochemical series. A π donor ligand (halogen, aqua, *etc.*) makes the absorption wavelength longer, and a π acceptor ligand (carbonyl, olefin, *etc.*) shorter by contribution from the π bond.

(d) Magnetism

Magnetization, M, (magnetic dipole moment per unit volume) of a sample in a magnetic field, *H*, is proportional to magnitude of *H*, and the proportionality constant, χ, depends on the sample.

$$M = \chi H$$

χ is the **volume susceptibility** and the product of χ and the molar volume V_m of a sample is the **molar susceptibility** χ_m. Namely,

$$\chi_m = \chi V_m$$

All substances have diamagnetism, and in addition to this, substances with unpaired electrons exhibit paramagnetism, the magnitude of which is about 100 times larger than that of diamagnetism. **Curie's law** shows that paramagnetism is inversely proportional to temperature.

$$\chi_m = \mathrm{A} + \frac{\mathrm{C}}{T}$$

where *T* is the absolute temperature and A and C are constants . In the Gouy or Faraday methods, magnetic moments are calculated from the change of weight of a sample suspended between magnets when a magnetic field is applied. In addition to these methods, the highly sensitive SQUID (superconducting quantum interference device) has been used recently to carry out such measurements.

Paramagnetism is induced by the permanent magnetic moment of an unpaired electron in a molecule and the molar susceptibility is proportional to the electron spin angular momentum. Paramagnetic complexes of *d*-block transition metals have unpaired

electrons of spin quantum number 1/2, and a half of the number of unpaired electrons is the total spin quantum number S.

Therefore, the magnetic moment based only on spins can be derived theoretically.

$$\mu = 2\sqrt{S(S+1)}\mu_B = \sqrt{n(n+2)}\mu_B$$

Here $\mu_B = 9.274 \times 10^{-24}$ JT^{-1} is a unit called the Bohr magneton.

Many 3*d* metal complexes show good agreement between the magnetic moments of paramagnetic complexes measured by a magnetic balance with the values calculated by the above formula. The relationship between the number of unpaired electrons and magnetic susceptibility of a complex is shown in Table 6.3. Because of this agreement with theory, it is possible to determine the number of unpaired electrons from experimental values of magnetic measurements. For example, it can be assumed that a Fe^{3+} d^5 complex with a magnetic moment of about 1.7 μ_B is a low-spin complex with an unpaired spin but a Fe^{3+} d^5 complex with a moment of about 5.9 μ_B is a high-spin complex with 5 unpaired electrons.

Table 6.3 Unpaired electrons and magnetic moments

Metal ion	Unpaired electron n	Spin-only magnetic moment (μ/μ_B) Calculated	Measured
Ti^{3+}	1	1.73	1.7~1.8
V^{3+}	2	2.83	2.7~2.9
Cr^{3+}	3	3.87	3.8
Mn^{3+}	4	4.90	4.8~4.9
Fe^{3+}	5	5.92	5.9

However, the measured magnetic moment no longer agrees with the calculated spin-only value when the orbital angular momentum contribution to the magnetic moment becomes large.. Especially in 5*d* metal complexes, this discrepancy between the measured and calculated values increases.

Exercise 6.3 Calculate the spin-only magnetic moments of high spin and low spin Fe^{3+} complexes.

"Answer" Since they are d^6 complexes, a high spin complex has four unpaired electrons with the magnetic moment is 4.90μ_B and a low spin complex has no unpaired electron and is diamagnetic.

Some paramagnetic solid materials become **ferromagnetic** at low temperatures by forming **magnetic domains** in which thousands of electron spins are aligned parallel to each other. The temperature at which the paramagnetic-ferromagnetic phase transition occurs is called the **Curie temperature**. When spins are aligned antiparallel to each other, the material changes to an **antiferromagnetic substance**, and this transition temperature is called the **Néel temperature**. The material becomes ferrimagnetic when the spins are incompletely canceled. Recently, attempts have been made to synthesize polynuclear multi-spin complexes with special ligands that make paramagnetic metal ions align to induce ferromagnetic interactions between the spins. This effect is impossible in mononuclear complexes.

6.3 Organometallic Chemistry of d Block Metals

The organometallic chemistry of transition metals is comparatively new. Although an ethylene complex of platinum called **Zeise's salt**, $K[PtCl_3(C_2H_4)]$, tetracarbonylnickel, $Ni(CO)_4$, and pentacarbonyliron, $Fe(CO)_5$, which today are classified as organometallic compounds, were prepared in the 19th century, their bonding and structures were unknown. The research of W. Hieber and others on metal carbonyl compounds was important in the 1930s, but the results of these studies were limited because of the underdeveloped techniques of structural analyses available at the time.

The discovery of ferrocene, $Fe(C_5H_5)_2$, in 1951 was epoch-making for the chemistry of this field. The very unique bonding mode of this complex became clear by means of single crystal X-ray structural analysis, NMR spectra, infrared spectra, *etc.*, and served as a starting point for subsequent developments in the field. It was a major discovery that ferrocene exhibited very high thermal stability in spite of the general view that the transition metal-carbon bonds were very unstable. It was also clearly demonstrated that the compound had a sandwich structure in which the five carbon atoms of the cyclopentadienyl groups bonded simultaneously to the central metal iron. While the various coordination modes of hydrocarbon ligands were determined one after another, the industrial importance of organometallic compounds of transition metals increased with the discoveries of olefin polymerization catalysts (Ziegler catalyst), homogeneous hydrogenation catalysts (Wilkinson catalyst), and development of catalysts for asymmetric synthesis, *etc.* The Nobel prize awarded to K. Ziegler, G. Natta (1963), E. O. Fischer, and G. Wilkinson (1973) was in recognition of this importance.

According to the definition of an organometallic compound, at least one direct bond between a metal and a carbon atom should exist, but CN complexes *etc.* with no organometallic character are usually excluded from organometallic compounds. Metal

carbonyl compounds are organometallic in various aspects of their bonding, structure and reactions, and they are a good model system for understanding of the essence of transition metal organometallic chemistry.

(a) Metal carbonyl compounds

Binary metal carbonyl compounds that consist only of a metal and CO ligands are usually prepared by the direct reaction of the powder of a highly reactive metal and carbon monoxide, or by the reduction of a metal salt to zero valance followed by reaction with high-pressure carbon monoxide. However, tetracarbonylnickel, first discovered at the end of the 19th century, forms by the reaction of nickel metal and carbon monoxide under atmospheric pressure and at room temperature. The preparation of other metal carbonyl compounds, on the other hand, requires high temperatures and high pressures.

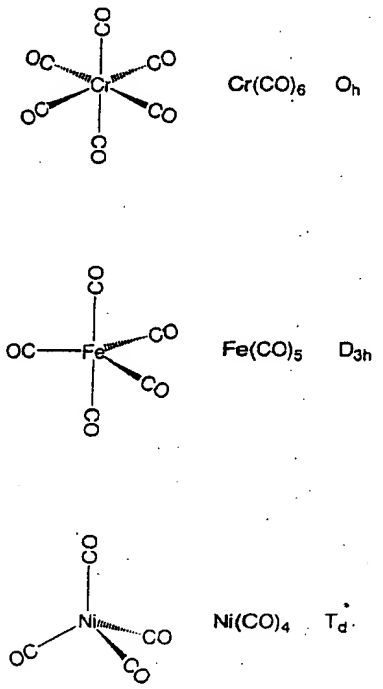

Fig. 6.14 Structures of metal carbonyl compounds.

Mononuclear metal carbonyl compounds take highly symmetric polyhedral coordination structures. Hexa-coordinate chromium, molybdenum, and tungsten hexacarbonyl, $M(CO)_6$, assume a regular octahedral, penta-coordinate pentacarbonyliron,

$Fe(CO)_5$, a triangular bipyramid, and tetracarbonylnickel, $Ni(CO)_4$, a regular tetrahedron coordination structure (Fig. 6.14). The carbon atoms of carbonyl ligands coordinate to the metal, and the CO moieties are oriented along the direction of the metal-carbon axis. Binuclear metal carbonyl $Mn_2(CO)_{10}$ has an Mn-Mn bond joining two square pyramidal $Mn(CO)_5$ parts. In $Fe_2(CO)_9$, two $Fe(CO)_3$ sub-units are bridged by three CO ligands, and in $Co_2(CO)_8$, two $Co(CO)_3$ sub-units are connected by both three CO bridges and a Co-Co bond.

There are a number of cluster metal carbonyl compounds with metal-metal bonds joining three or more metals, and terminal CO, μ-CO (a bridge between two metals), and μ_3-CO (a bridge capping three metals) are coordinated to the metal frames (refer to Section 6.3 (f)). Many cluster carbonyls are formed by a pyrolysis reaction of mononuclear or binuclear carbonyl compounds. Typical metal carbonyl compounds and their properties are shown in Table 6.4.

Table 6.4 Stable metal carbonyl compounds

	5	6	7	8	9	10
4	$V(CO)_6$ Black solid d.70	$Cr(CO)_6$ White solid d.130	$Mn_2(CO)_{10}$ Yellow solid mp 154	$Fe(CO)_5$ Yellow liquid bp 103	$Co_2(CO)_8$ Red solid mp 51	$Ni(CO)_4$ Colorless liquid bp 42.1
5		$Mo(CO)_6$ White solid sublime	$Tc_2(CO)_{10}$ White solid mp 160	$Ru_3(CO)_{12}$ Orange solid d.150	$Rh_6(CO)_{16}$ Black solid d.220	
6		$W(CO)_6$ White solid sublime	$Re_2(CO)_{10}$ White solid mp 177	$Os_3(CO)_{12}$ Orange solid mp 224	$Ir_4(CO)_{12}$ Yellow solid d.220	

Back donation

A metal carbonyl compound consists of carbon monoxide coordinated to a zero valent metal. For a long time, it had been unclear why such bonding was possible, let alone stable at all. The belief that normal coordination bonds were formed by the donation of electrons from highly basic ligands to a metal formed the basis of the coordination theory of A. Werner. Because the basicity of carbon monoxide is very low, and transition metal-carbon bonds are generally not very stable, a suitable explanation for the stability of metal carbonyl compounds was sought. If the shape and symmetry of the metal *d* orbital and of the CO π (antibonding) orbital for the carbon-oxygen bond are

suitable for overlap, a bonding interaction between the metal and carbon is expected. The bonding scheme shown in Fig. 6.15 was proposed from this point of view. The mechanism by which electrons are donated to the vacant carbon monoxide π^* orbital from the filled metal *d* orbital is called **back donation**. Since accumulation of superfluous electrons on a low oxidation state metal atom is prevented, back-donation leads to the stabilization of the M-C bond.

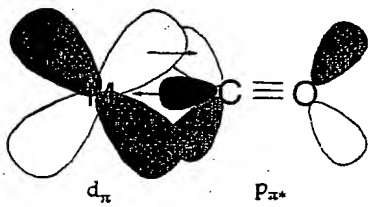

Fig 6.15 Back donation in metal carbonyls.

A rise in the order of the metal - carbon bond is reflected in the increase of the M-C, and decrease of the C-O, stretching frequencies in vibrational spectra. Infrared spectra are useful because carbonyl frequencies are easily detectable. The lowering of the oxidation state of a metal by the flow of negative charge from its coordinated ligands is reflected in the reduction of the C-O stretching frequencies.

(b) Hydrocarbon complexes

An organometallic compound is one which has metal-carbon bonds, and between one and eight carbon atoms in a hydrocarbon ligand bond to a metal. **Hapticity** describes the number of atoms in a ligand that have direct coordinative interaction with the metal and the number is added to η. An example is η^5 (pentahapto)-cyclopentadienyl (Table 6.5).

A ligand that donates an odd number of electrons to a metal is formally a radical and it is stabilized by bonding to the metal. A ligand that donates an even number of electrons to a metal is generally a neutral molecule and it is stable even if it is not bonded to the metal. Carbene or carbyne ligands are exceptions to this rule. The chemical formula of an organometallic compound is expressed in many cases without using the square brackets [ ] usual for such a complex, and we shall follow this convention in this book.

Table 6.5 Hapticity and number of donating electrons of hydrocarbon ligands

Name	Hapticity	Number of electrons	Example
Alkyl	η^1	1	$W(CH_3)_6$
Alkylidene	η^1	2	$Cr(CO)_5\{C(OCH_3)C_6H_5\}$
Alkene	η^2	2	$K[PtCl_3(C_2H_4)]$
π-allyl	η^3	3	$Ni(\eta^3\text{-}C_3H_5)_2$
Diene	η^4	4	$Fe(CO)_3(\eta^4\text{-}C_4H_6)$
Cyclopentadienyl	η^5	5	$Fe(\eta^5\text{-}C_5H_5)_2$
Arene	η^6	6	$Cr(\eta^6\text{-}C_6H_6)_2$
Tropylium	η^7	7	$V(CO)_3(\eta^7\text{-}C_7H_7)$
Cyclooctatetraene	η^8	8	$U(\eta^8\text{-}C_8H_8)_2$

Exercise 6.4 Describe the difference between cyclopentadiene and cyclopentadienyl ligands.

"Answer" The chemical formula of cyclopentadiene is C_5H_6 and it is bonded to a metal as a η^2 or η^4 ligand. The chemical formula of cyclopentadienyl is C_5H_5 and it is bonded to a metal as a η^1, η^3, or η^5 ligand.

Alkyl ligands

Alkyl or aryl transition metal compounds have M-C single bonds. In spite of many attempts over most of the course of chemical history, their isolation was unsuccessful and it was long considered that all M-C bonds were essentially unstable. Stable alkyl complexes began to be prepared gradually only from the 1950s. $Cp_2ZrCl(Pr)$, WMe_6, $CpFeMe(CO)_2$, $CoMe(py)(dmg)_2$, (dmg = dimethylglyoximato), $IrCl(X)(Et)(CO)(PPh_3)_2$, $NiEt_2(bipy)$, $PtCl(Et)(PEt_3)_2$ are some representative compounds. Among various synthetic processes so far developed, the reactions of compounds containing M-halogen bonds with main-group metal-alkyl compounds, such as a Grignard reagent or an organolithium compound, are common synthetic routes. Especially vitamin B_{12}, of which D. Hodgkin (1964 Nobel Prize) determined the structure, is known to have a very stable Co-C bond. Metal alkyl compounds which have only alkyl ligand, such as WMe_6, are called **homoleptic alkyls**.

It is gradually accepted that a major cause of the instability of alkyl complexes is the low activation energy of their decomposition rather than a low M-C bond energy. The most general decomposition path is β **elimination**. Namely, the bonding interaction of a hydrocarbon ligand with the central transition metal tends to result in the formation of a metal hydride and an olefin. Such an interaction is called an **agostic interaction**.

Although an alkyl and an aryl ligand are 1-electron ligands, they are regarded as anions when the oxidation number of the metal is counted. The hydride ligand, H, resembles the alkyl ligand in this aspect.

π allyl complexes

If an allyl group, CH_2=CH-CH_2-, is bonded to a metal via a carbon atom, it is a 1-electron ligand like an alkyl group. If the double bond delocalizes, three carbon atoms bond to the metal simultaneously as a 3-electron ligand. This is also an odd electron and formally anionic ligand and is stabilized by being coordinated to the metal. $Pd(C_3H_5)(Ac)(PPh_3)$, $Co(C_3H_5)_3$, *etc.* are well-known examples. Since η^1, η^2, and η^3 coordination modes are possible in the catalytic reactions of unsaturated hydrocarbons, various reactions occur.

π cyclopentadienyl complexes

The cyclopentadienyl ligand, C_5H_5, is abbreviated as Cp. C_5Me_5, in which the hydrogen atoms of Cp are replaced with methyl groups, is a useful ligand called **Cp star** and is denoted by Cp*. Ferrocene, Cp_2Fe, is a very stable orange-colored iron compound in which two cyclopentadienyl groups are bonded to iron. It was discovered independently in two laboratories, but the discoverers proposed incorrect structures. The correct structure was clarified by the group of G. Wilkinson, who won a Nobel Prize (1973). The preparation of ferrocene is usually carried out according to the following reaction path:

$$2\ C_5H_6 + 2\ Na \longrightarrow 2\ Na(C_5H_5) + H_2$$

$$FeCl_2 + 2\ Na(C_5H_5) \longrightarrow Fe(C_5H_5)_2 + 2\ NaCl$$

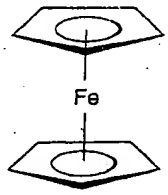

Fig. 6.16 Structure of ferrocene.

Single crystal X-ray structure analysis showed that the structure of ferrocene is an iron

atom sandwiched between two C_5H_5 rings (Fig. 6.16). Five carbon atoms bond to the iron simultaneously in ferrocene, and unsaturated C-C bonds are delocalized in the five-membered rings. Since this kind of bond was not known before, it aroused interest, many derivative compounds were prepared, and a wide range of chemistry has since been studied (Table 6.6).

Table 6.6 Typical sandwich compounds ($Cp = \eta^5$-C_5H_5)

	4	5	6	7	8	9	10
4	Cp_2TiCl_2 Red mp 230	Cp_2V Black mp 167	Cp_2Cr Scarlet mp 173	Cp_2Mn Brown mp 193	Cp_2Fe Orange mp 174	Cp_2Co Black mp 173	Cp_2Ni Green d.173
5	Cp_2ZrCl_2 White mp 248	Cp_2NbCl_2 Brown	Cp_2MoCl_2 Green d.270	Cp_2TcH Yellow mp 150	Cp_2Ru Yellow mp 200		
6	Cp_2HfCl_2 White mp 234	Cp_2TaCl_2 Brown	Cp_2WCl_2 Green d.250	Cp_2ReH Yellow mp 161	Cp_2Os White mp 229		

The cyclopentadienyl ligand is a 5-electron and formally anionic ligand. If only one of the five carbon atoms is bonded to a metal, it is a 1-electron ligand like an alkyl group. It becomes a 3-electron ligand in rare cases and coordinates to a metal as a π-allyl system that extends over 3 carbon atoms. The Cp group of ferrocene has reactivity analogous to that of aromatic compounds. Since the Cp group has played a significant role as a stabilizing ligand to realize the preparation of new compounds with new metal-ligand bonding modes, it can reasonably be claimed that this ligand has made the greatest contribution to organometallic chemistry of any other ligand. Although two Cp rings are bonded to the metal in parallel in ferrocene, Cp_2TiCl_2 and Cp_2MoH_2 have bent Cp ligands and they are called bent-sandwich compounds.

Olefin complexes

Zeise's salt, $K[PtCl_3(C_2H_4)]$, is the oldest known organometallic compound and was synthesized and analyzed in *ca.* 1825 by Zeise, although its coordination structure was assumed only in 1954 and confirmed by the neutron diffraction in 1975. The mode of coordination of an olefin to a transition metal is described by the Dewar-Chatt-Duncanson model and the bond between the metal and olefin is stabilized by the contribution of d_π-p_{π^*} back donation. An olefin is a 2-electron ligand and there are many olefin complexes in which the central metal is in a relatively low oxidation state.

Dienes or trienes with two or more double bonds coordinate to a metal as 4-electron or 6-electron ligands. $Fe(CO)_3(C_4H_6)$ and $Ni(cod)_2$, in which a butadiene or

cyclooctadienes (cod) are coordinated to the metal, are well known examples. Since cyclooctadienes are easily eliminated from $Ni(cod)_2$, it is conveniently used for generating atomic, zero valent nickel. This complex is sometimes called **naked nickel**.

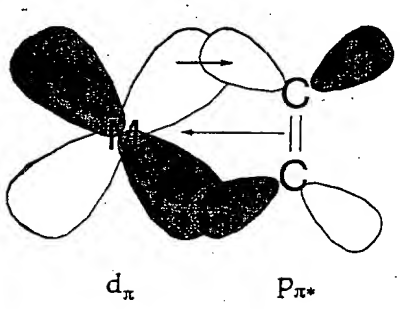

Fig. 6.17 Back-donation in olefin complexes.

Arene complexes

Aromatic compounds are 6-electron donors that coordinate to transition metals in the η^6 coordination mode with six carbon atoms. Bisbenzenechromium, $Cr(C_6H_6)_2$, is a typical example of such a compound. The compound is prepared by reducing chromium chloride in benzene and it has a sandwich structure in which a chromium atom is inserted between two benzene rings. When a benzene ligand is replaced by three carbonyls, $Cr(CO)_3(C_6H_6)$ is obtained.

18 electron rule

Counting valence electrons is of utmost importance in chemistry. Changes in the number of valence electrons has a profound influence on the bonding, structure, and reactions of a compound. Since both the metal and organic moieties are involved in organometallic compounds, counting the number of electrons becomes complicated. Hydrocarbyl ligands are classified as either neutral molecules coordinating to the metal or radicals bonding to the metal, and the radicals, such as alkyls and cyclopentadienyl, are generally called anionic ligands. Transfer of one electron from the metal to the radical ligand makes the ligand formally anionic. However, it is less confusing to consider that both the metal and the ligands are neutral when counting the number of valence electrons. The numbers of donor electrons in typical carbon ligands from this viewpoint are listed in Table 6.5. It is important to note that even in the same ligand, the number of donor

electrons supplied by the ligand differs depending upon the number of ligating atoms that have coordinative interactions with the metal. For example, 1, 3 or 5 electrons can be donated from a cyclopentadienyl ligand, depending on the type of coordinative interactions with the metal.

When the total number of valence electrons of the metal and ligands is 18, a transition metal organometallic compound usually has high thermal stability. For example, $Cr(CO)_6$, $Fe(CO)_5$, $Ni(CO)_4$, $Fe(C_5H_5)_2$, $Mo(C_6H_6)(CO)_3$ *etc.* satisfy the **18 electron rule**, but the monomeric parts of $Mn_2(CO)_{10}$, $Co_2(CO)_8$ or $[Fe(C_5H_5)(CO)_2]_2$ have only 17 electrons and the extra electron comes from the partner metal by forming a metal-metal bond. Unlike the 8 electron rule in main group compounds, applicability of the 18 electron rule is limited. That is to say, it is a sufficient condition but compounds with high thermal stability are not necessarily 18 electron compounds.

Although there are many Group 6 (chromium group) through Group 9 (cobalt group) organometallic compounds with carbonyl or cyclopentadienyl ligands that satisfy the 18 electron rule, many compounds of the early transition metals (Group 3 - 5) and Group 10 (nickel group) fail to conform to this rule. For example, $W(CH_3)_6$ (12e), $TiCl_2(C_5H_5)_2$ (16e), and $IrCl_2(CO)(PPh_3)_2$ (16e), $V(CO)_6$ (17e), $Co(C_5H_5)_2$ (19e), $Ni(C_5H_5)_2$ (20e), *etc.* do not satisfy the 18 electron rule. However, the 18 electron rule provides useful clues as to the bonding modes present in a given complex. For example, $Fe(C_5H_5)_2(CO)_2$ with two pentahapto cyclopentadienyl ligands formally has 22 electrons but if one of the ligands is monohapto, the compound has 18 electrons. Structural analysis has shown that this is the actual coordination of this complex.

Exercise 6.5 Calculate the valence electron number of $CpMn(CO)_3$.
"Answer" They are a total of 18 electrons from Mn (7), Cp(5) and three CO(6).

(c) Phosphine complexes

Tertiary phosphines, PX_3, are very useful as stabilization ligands in transition metal complexes and they coordinate to the metals in relatively high to low oxidation states. Phosphines are frequently used as carbonyl or cyclopentadienyl ligands in the chemistry of organometallic complexes. PX_3 are Lewis bases and coordinate to the metal using the lone pair on phosphorus and show π-acidity when carrying substituents X including Ph, Cl, or F that have strong electron accepting properties. The electronic flexibility of PX_3 is the reason it forms so many complexes. Generally, the π-acidity becomes smaller in the order $PF_3>PCl_3>PPh_3>PR_3$. Triphenylphosphine and triethylphosphine are typical substituted phosphines. The tertiaryphosphine complexes mainly of metal halides are listed in Table 6.7. Manganese, Mn, and the early transition metals form very few

phosphine complexes.

Table 6.7 Typical tertiary phosphine complexes (dmpe = 1,2-bisdimethylphosphino-ethane; dppe = 1,2-bisdiphenylphosphinoethane)

	4	5	6	7
4	$[TiCl_4(PPh_3)_2]$	$[VCl_3(PMePh_2)_2]$	$[CrCl_2(dmpe)_2]$	$[Mn(CO)_4(PPh_3)]$
5	$[ZrCl_4(dppe)]$	$[NbCl_4(PEtPh_2)_2]$	$[MoCl_3(PMePh_2)_3]$	$[TcCl_3(PMe_2Ph)_3]$
6	$[HfCl_4(dppe)]$	$[TaCl_4(PEt_3)_2]$	$[WCl_4(PPh_3)_2]$	$[ReCl_3(PMe_2Ph)_3]$

	8	9	10	11
4	$[FeCl_2(PPh_3)_2]$	$[CoCl_2(PPh_3)_2]$	$[NiCl_2(PEt_3)_2]$	$[CuBr(PEt_3)]_4$
5	$[RuCl_2(PPh_3)_3]$	$[RhCl(PPh_3)_3]$	$[PdCl_2(PPh_3)_2]$	$[AgCl(PPh_3)]$
6	$[OsCl_3(PPh_3)_3]$	$[IrCl_3(PPh_3)_3]$	$[PtCl_2(PPh_3)_2]$	$[AuCl(PPh_3)]$

Many derivatives can be prepared by substituting the halogens of the phosphine complexes. A number of the complexes of polydentate phosphines with more than two coordination sites, as well as those of monodentate phosphines, have been prepared, and they are used also as stabilization ligands in hydride, alkyl, dinitrogen, and dihydrogen complexes. The complexes of rhodium or ruthenium, in which optically active phosphines are coordinated, are excellent catalysts for asymmetric synthesis.

(d) Small molecule complexes

Two or three atomic molecules, such as H_2, N_2, CO, NO, CO_2, NO_2, and H_2O, SO_2, *etc.*, are called **small molecules** and the chemistry of their complexes is very important not only for basic inorganic chemistry but also for catalyst chemistry, bioinorganic chemistry, industrial chemistry, and environmental chemistry. The complexes of small molecules other than water and carbon monoxide were synthesized comparatively recently. Dihydrogen complexes in particular were reported only in 1984.

Dihydrogen complexes

The oxidative addition reaction of a hydrogen molecule, H_2, is one of the methods used to generate the M-H bond of a hydride complex. Schematically, the above reaction is written as

$$M + H_2 \longrightarrow H\text{-}M\text{-}H$$

but it was believed that there must be an intermediate complex containing a coordinated

dihydrogen. The first example of a stable complex of this sort, $[W(CO)_3(H_2)(P^iPr_3)_2]$, was reported by G. Kubas in 1984 (Fig. 6.18). It was proved by the neutron diffraction that the H_2 is coordinated as an η^2 ligand by maintaining the bond between hydrogen atoms with an interatomic distance of 84 pm.

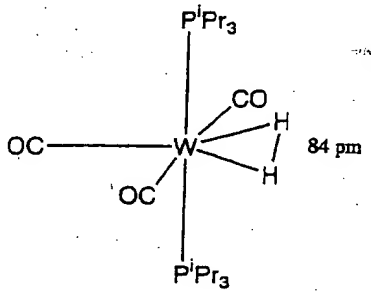

Fig. 6.18 Structure of $[W(CO)_3(H_2)(P^iPr_3)_2]$.

Once this new coordination mode was established, new dihydrogen complexes have been prepared one after another, and dozens of dihydrogen complexes are now known. Dihydrogen complexes are interesting not only from the viewpoint of bond theory but they have also greatly contributed to the study of the activation process of the hydrogen molecule.

Dinitrogen complexes

Since N_2 is isoelectronic with CO, the possible stability of dinitrogen complexes analogous in structure to carbonyl complexes was the subject of speculation for many years. These compounds generated great interest because of the parallels with the interaction and activation of nitrogen molecules on the iron catalyst used in ammonia synthesis and the nitrogen fixing enzyme nitrogenase. However, the first dinitrogen complex, $[Ru(N_2)(NH_3)_5]X_2$, was prepared by A. D. Allen (1965) unexpectedly from the reaction of a ruthenium complex and hydrazine. Subsequently, it was discovered by chance that nitrogen gas coordinates to cobalt, and $[CoH(N_2)(PPh_3)_3]$ was prepared in 1967 (Fig. 6.19). Many dinitrogen complexes have been prepared since these early beginnings.

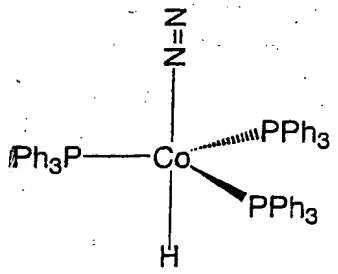

Fig. 6.19 Structure of $[CoH(N_2)(PPh_3)_3]$.

In most dinitrogen complexes, N_2 is coordinated to the metal by one nitrogen atom. That is to say, the M-N≡N bond is common and there are few complexes in which both nitrogen atoms bond to the metal in the η^2 coordination mode. In 1975, the coordinated dinitrogen in a molybdenum complex was discovered to be protonated by mineral acids to form ammonia, as decribed in the following reaction. The electrons required for the reduction are supplied by the molybdenum in a low oxidation state as this reaction shows.

$$[Mo(PMe_2Ph)_4(N_2)_2] + 6\,H^+ \longrightarrow 2\,NH_3 + N_2 + Mo(V) + ...$$

In spite of attempts to prepare ammonia and organic nitrogen compounds from various dinitrogen complexes, no nitrogen fixation system which is equal to biological systems has yet been discovered. Ammonia synthesis is a long-established industrial process, and its parameters have been extensively studied and little room for improvement remains. However, elucidating the mechanism of the biological nitrogen fixation reaction at ordinary temperatures and pressures remains one of the major challenges of bio-inorganic chemistry.

Dioxygen complexes

Although it has long been recognized that schiff base complexes of cobalt absorb oxygen, the discovery that **Vaska's complex,** $[IrCl(CO)(PPh_3)_2]$, coordinates dioxygen reversibly to form $[IrCl(CO)(PPh_3)_2(O_2)]$ was very significant. In this complex, two oxygen atoms bond to iridium (side-on), and dioxygen has a peroxide character (O_2^{2-}). However, many superoxide (O_2^-) complexes in which only one oxygen atom is bonded to the metal are known. There are also binuclear dioxygen complexes in which O_2 bridges two metals. The relation between reversible coordination of dioxygen and its reactivity is important in relation to the behavior of dioxygen in living systems (refer to Section 8.2 (a)).

(e) Metal-metal bonds

The concept of the formation of a coordinate bond between ligands and a central metal proposed by A. Werner was the basis for the development of the chemistry of complexes. The bonding mode and structures of known complexes have become the guidepost of the preparation of a much larger number of new complexes. For most of the dinuclear or polynuclear complexes that contain two or more metals in a complex, it was sufficient to take into consideration only the bonds between the metal and ligands.

The concept of direct bonds between metals was born of the necessity of explaining the structural chemistry of the dinuclear metal carbonyls that have a partial structure with an odd number of electrons. Two $Mn(CO)_5$ units in $Mn_2(CO)_{10}$ are connected by a direct Mn-Mn bond (Fig. 6.20) without the help of bridge ligands. According to X-ray structural analysis (1963), the Mn-Mn distance of 292 pm was significantly longer than twice that of the metal radius of 127 pm but a Mn-Mn direct bond was envisaged in the absence of a bridge carbonyl ligand. This compound's diamagnetism indicates a structure with an even number of electrons (18 electrons) by sharing electrons between two d^7-Mn (17 electrons) moieties, each with five carbonyl ligands.

Similarly, it can be concluded that $Co_2(CO)_8$, with two bridging carbonyl ligands, should have a direct Co-Co bond to be compatible with its diamagnetism.

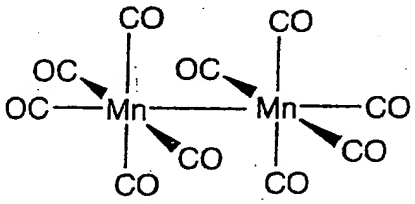

Fig. 6.20 Structure of $Mn_2(CO)_{10}$.

The concept of the single bond between metals introduced for dinuclear metal carbonyl compounds is also very useful in explaining the structure of cluster carbonyl compounds containing two or more metals. The metal-metal bond has been established today as one of the common bonding modes, together with the metal-ligand bond, present in coordination complexes. However, it is not always clear to what extent the interaction between metals exists in the polynuclear complexes which have bridging ligands. As a criterion, the bond order can be evaluated from the bond distance in standard metals (for example, in bulk metals). However, even if the bond distance between metals analyzed by

X-ray is sufficiently short, this does not prove the existence of a bond between metals unless the orbital conditions to account for such bonds are also fulfilled.

M-M multiple bonds

There are many dinuclear compounds in which the metal atoms are bound by multiple bonds with bond orders of 2 to 4. The M-M quadrupole bond was proposed first for $Re_2Cl_8^{2-}$, and this remains the best-known example (Fig. 6.21). The Re-Re distance in this compound is only 224 pm, which is unusually short compared with the Re-Re distance of 275 pm in rhenium metal. Another unusual feature is that the $ReCl_4$ units assume an **eclipsed** configuration (chlorine atoms overlap along the direction of the Re-Re bond) even though the **staggard** configuration (in which chlorine atoms do not overlap along the Re-Re bond direction) should be more stable because the distance between $ReCl_4$ units is very short, resulting in the distances between the chlorine atoms being very short (experimental value of 332 pm). As a result, the repulsive interaction between the chlorine atoms becomes strong.

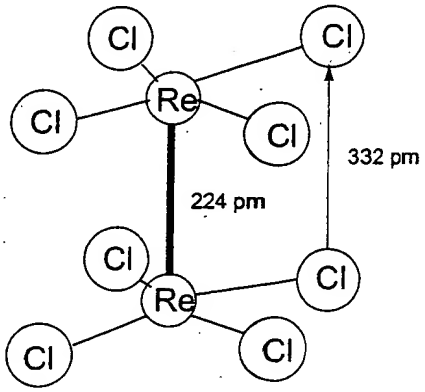

Fig. 6.21 Structure of $Re_2Cl_8^{2-}$.

F. A. Cotton explained this anomaly by introducing the concept of the delta bond between metals in 1964. Namely, if one takes the z-axis in the direction of the Re-Re bond, a σ bond is formed between the d_{z2}, the π bonds between d_{yz} and d_{xz} orbitals and the δ bond between d_{xy} orbitals among the five d orbitals. d_{x2-y2} is mainly used for the Re-Cl bond. The delta bond is formed by a weak sideway overlap of d_{xy} orbitals, when they are located perpendicular to the direction of the metal-metal bond axis and become eclipsed (Fig. 6.22). Therefore, although the δ bond is relatively weak among bonding interactions, it is sufficient to maintain the chlorine ligands in their eclipsed positions.

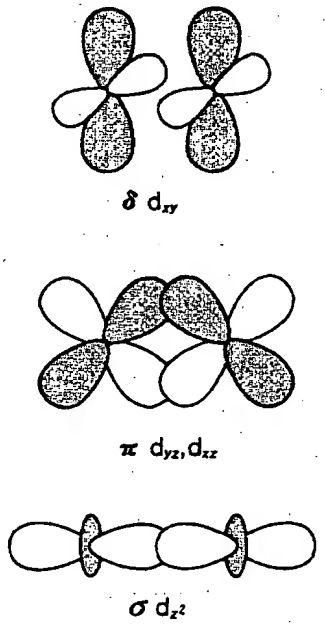

Fig. 6.22 Overlap of *d* orbitals in Re≡Re quadrupole bond.

The energy levels of the molecular orbitals of σ, π, and δ bonds decrease in this order, and the energy difference between the bonding and antibonding delta orbitals is small. Therefore, even if one electron is removed (oxidation) from $Re_2Cl_8^{2-}$, which has a quadruple bond, or one electron is added (reduction) to it, the Re-Re distance should hardly change.

The Mo(II) compound $[Mo_2(CH_3COO)_4]$ which is isoelectronic with Re (III) has a Mo-Mo quadruple bond. $[W_2Cl_9]^{3-}$ and $[W_2(NMe_2)_6]$ are examples of compounds which have the metal-metal triple bonds. Although the issue of whether such metal-metal multiple bonds really exist has been argued many times, the concept has now been established and hundreds of dinuclear compounds with metal-metal multiple bonds are known at present. Metal-metal distances determined by X-ray analysis are most useful in determining whether a metal-metal bond is a multiple one, but as in the case of metal-metal single bonds, the bond distance alone cannot be the absolute determiner and it is necessary to draw conclusions from molecular orbital calculations.

(f) Metal cluster compounds

Analysis of the structures of newly prepared polynuclear complexes that contain

two or more metals was, until recently, very difficult. However, with the progress of single crystal X-ray structural analysis, our understanding of the chemistry of polynuclear complexes is progressing quickly. Metal-cluster complexes are polynuclear complexes built by three or more transition-metal atoms with bonds between the metals coordinated by ligands to form polyhedral frames, such as a triangle, a regular tetrahedron, a regular octahedron, and an icosahedron. Even if there is no strong bond between metals, as long as there is some bonding interaction, they may be included as cluster compounds.

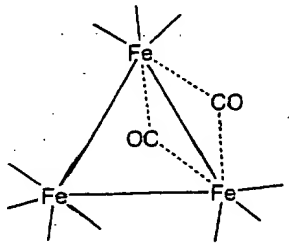

$Fe_3(CO)_{12}$

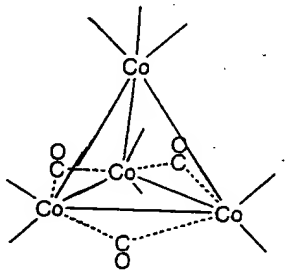

$Co_4(CO)_{12}$

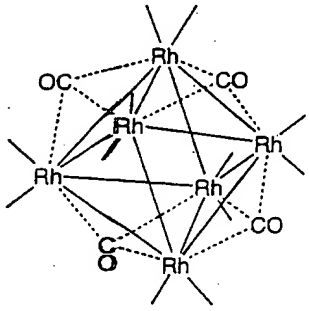

$Rh_6(CO)_{16}$

Fig. 6.23 Examples of metal cluster carbonyls (terminal carbonyl ligands are omitted for clarity.

Metal cluster complexes may be broadly classified into groups according to the general character of the associated ligands. They are low oxidation state metal clusters

with π-acceptor ligands like carbonyls (CO), isonitriles (RNC) or phosphines (PR_3) and with π-donor ligands like oxygen (O), sulfur (S), chlorine (Cl) or alkoxides (OR). Many carbonyl cluster and sulfur cluster compounds have been synthesized. Carbonyl cluster compounds are obtained by heating or irradiating mononuclear carbonyl compounds. The chemical properties of cluster compounds such as $Fe_3(CO)_{12}$, $Ru_3(CO)_{12}$, $Os_3(CO)_{12}$, $Co_4(CO)_{12}$, $Ir_4(CO)_{12}$ or $Rh_6(CO)_{16}$ have been studied in detail (Fig. 6.23).

Since $Os_3(CO)_{12}$ forms many kinds of cluster compounds by pyrolysis, it has been used to study the skeletal structures of osmium cluster compounds and their relationship to skeletal electron numbers. A M-M bond is satisfactorily described by the 2 center 2 electron bond and the 18 electron rule is also applicable to each metal for small clusters such as a triangle and a regular tetrahedron. When clusters become large, the Wade rule that describes the relation between the structures of boranes and skeletal electron numbers, or the Lauher rule that draws the number of the bonding metal-metal orbitals for various metal polyhedral structures from the molecular orbital calculations of bare rhodium clusters without ligands, are more applicable. The relationship between the number of cluster valence electrons and the cluster's polyhedral shape as shown in Table 6.8 has contributed much to the theory of cluster chemistry.

Table 6.8 Metal frameworks and cluster valence electrons in metal cluster carbonyl compounds

Metal framework	Cluster valence electron	Example
Triangle	48	$Fe_3(CO)_{12}$
Tetrahedron	60	$Co_4(CO)_{12}$
Butterfly	62	$[Fe_4(CO)_{12}C]^{2-}$
Trigonal bipyramid	72	$Os_5(CO)_{16}$
Square pyramid	74	$Fe_5C(CO)_{15}$
Octahedron	86	$Rh_6(CO)_{16}$
Trigonal prism	90	$[Rh_6C(CO)_{15}]^{2-}$

Monovalent anions such as halogens, alkoxides, carboxylate ions, and divalent anions such as oxygen and sulfur stabilize the cluster frameworks by helping metals assume oxidation states suitable for cluster formation and connect metal fragments by bridging. Since neutral ligands such as phosphines, carbonyl, or amines can also be coordinated to metals, a variety of cluster complexes have been prepared.

The halide clusters of molybdenum, Mo_6X_{12}, tungsten, W_6X_{12}, niobium, Nb_6X_{14}, and tantalum, Ta_6X_{14}, are solid cluster compounds that have been known for many years. The octahedral metal frameworks were shown by X-ray structure analysis more than 50 years ago. The molecular cluster complexes were prepared in the 1960s from solid-state

halide clusters by the reaction of ligands such as amines and phosphines, and these cluster compounds generated considerable interest for some time. New halide cluster compounds with octahedral structures have again been prepared recently and they are being studied from new perspectives. The molecular cluster complex $[Mo_6S_8L_6]$ (where L is PEt_3, py, *etc.*), which has similar Mo_6 frameworks with those of the superconducting Chevrel phase compounds $MxMo_6S_6$ and their tungsten and chromium analogs have been prepared and the relationships between their structures and physical properties attract great interest (Fig. 6.24).

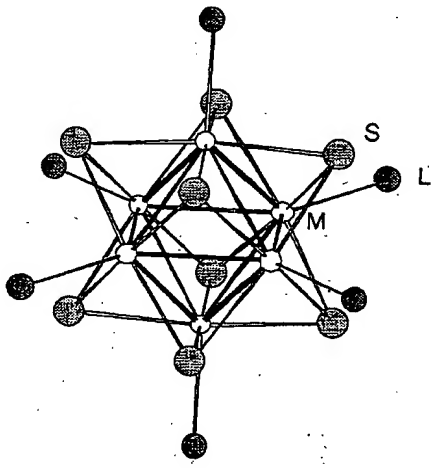

Fig. 6.24 Structure of $[Mo_6S_8L_6]$.

As will be described in the Chapter on bioinorganic chemistry, clusters such as Fe_4S_4 are contained in nitrogenase, the nitrogen-fixing enzyme, and also in the active center of ferredoxins, and they play important roles in the activation of dinitrogen or multi-electron transfer reactions. Since R. H. Holm synthesized the $Fe_4S_4(SR)_4$ cluster (Fig. 6.25), our understanding of the chemistry of the iron-sulfur cluster has developed considerably.

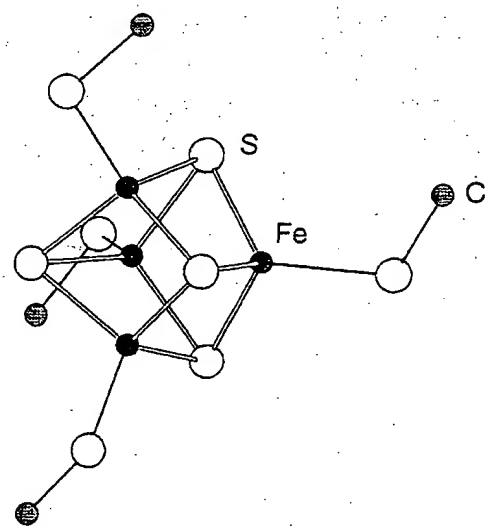

Fig. 6.25 Structure of $[Fe_4S_4(SR)_4]^{2-}$.

As the metal species of metal cluster carbonyls are in near-zero valence oxidation states, they had been expected to play a role in specific catalysis Although many organic syntheses using metal cluster compounds as catalysts have been attempted and some interesting reactions were discovered, in most cases the clusters decomposed during the reactions and they turned out to be false cluster catalysts. Despite this, there have been some examples of reactions that pass through several elementary reaction stages on the metal of the cluster. Hence, it is likely that catalytic reactions that employ the **multi-center coordination** and **multi-electron transfer** abilities of cluster compounds will be developed in the future.

Metal clusters have been helpful as models of the surfaces of bulk metals, metal oxides, or metal sulfides, and they have been useful in the study of chemisorption and successive reactions on solid surfaces. The fine metal grains which maintain the basic cluster frameworks are deposited by the pyrolysis of metal carbonyl cluster compounds chemically bonded to carriers such as silica and alumina. If used in solid catalysis, it is expected that analysis of the catalytic reaction on a metal cluster framework will be possible.

6.4 Reactions of complexes

The reactions of complexes are classified into the substitution reaction of ligands, the conversion reaction of ligands, and the redox reaction of the central metal. The

substitution and redox reactions in particular have been studied in detail.

(a) Ligand substitution reaction

Ligand substitution reactions of complexes

$$L_nMX + Y \longrightarrow L_nMY + X$$

are very important for the preparation of various kinds of derivatives. The detailed conditions which complexes and ligands fulfill have been studied in order to understand their stereochemistry and attain practical rates of substitution reactions. As with other types of chemical reactions, we require an understanding of both equilibrium and reaction rates.

Formation constant

The equilibrium constant of a ligand substitution reaction is called a **formation or stability constant**. The concept and the method of computing successive formation constants were proposed by N. Bjerrum (1941). Equilibrium constants for the replacement of a hydrated ion M by other ligands L in an aqueous solution are

$$M + L \rightarrow ML \qquad K_1 = \frac{[ML]}{[M][L]}$$

$$ML + L \rightarrow ML_2 \qquad K_2 = \frac{[ML_2]}{[ML][L]}$$

$$ML_2 + L \rightarrow ML_3 \qquad K_3 = \frac{[ML_3]}{[ML_2][L]}$$

.....

$$ML_{n-1} + L \rightarrow ML_n \qquad K_n = \frac{[ML_n]}{[ML_{n-1}][L]}$$

and the overall formation constant β_n is

$$\beta_n = \frac{[ML_n]}{[M][L]^n} = K_1K_2K_3 \cdots K_n$$

The thermodynamic stability of a substitution product becomes larger as the formation constant increases.

On the other hand, an understanding of the effect of the leaving ligand, X, and the entering ligand, Y, on the substitution rate and on the intermediate species formed are essential to elucidate the reaction chemistry of metal complexes. It is especially useful to summarize the electronic structure of the central metals, the stereochemistry of complexes, and the correlation between the parameters representing their steric properties and the reaction rate. Generally, reaction mechanisms can be classified into associative, interchange, and dissociative mechanisms according to the differences in the intermediate state (Fig. 6.26).

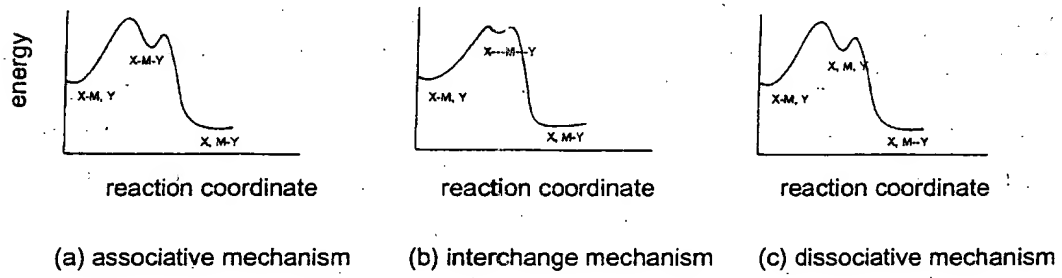

Fig. 6.26 The stability of the intermediate of ligand substitution.

Associative mechanism If the substitution rate of a ligand substitution of a complex is dependant upon the entering ligand, Y, coordinating to the central metal and is insensitive to the leaving ligand, X, it is presumed to take the associative mechanism which increases the coordination number. Such a substitution reaction is often seen in planar tetra-coordinate Pt(II) complexes, and the intermediate species are triangular bipyramidal penta-coordinate complexes. The reaction is first-order with respect to both the tetra-coordinate complex and Y, and is second-order as a whole. Since it is accompanied by a reduction of molecular species in the intermediate stage, thermodynamic measurements of the reaction indicate the activation entropy, ΔS, to be negative. The intermediate species in the case of the associative mechanism in hexa-coordinate complexes are hepta-coordinate complexes.

Interchange mechanism When the life of an intermediate state is very short, the reaction proceeds by the interchange mechanism, as the coordination of Y and

elimination of X are considered to occur simultaneously.

Dissociative mechanism A substitution reaction that is highly sensitive to the identity of the leaving ligand, X, and practically insensitive to the identity of the entering ligand, Y, assumes the dissociative mechanism in which the coordination number decreases in the intermediate state. This is often observed in octahedral hexa-coordinate complexes, and the intermediate states are penta-coordinate complexes that form by the elimination of X. As the elimination is accompanied by an increase of molecular species in the intermediate stage, the entropy of activation, ΔS, becomes positive.

Exercise 6.6 The order of the rate of ligand substitution of Pt(II) complexes is $H_2O<Cl^-<I^-<PR_3<CN^-$ for entering ligands. Which mechanism, associative or dissosiative, do the substitutions take?

"Answer" Since they are dependent on the entering ligands, the associative mechanism is more likely.

Trans effect In square-planar tetra-coordinate complexes typically of Pt(II), the ligand trans to the leaving ligand X governs the substitution rate. This is called the **trans effect**. The substitution rate increases as the σ donor or π acceptor ability of the trans ligand becomes larger in the order of $NH_3 < Cl^- < Br^- < I^- < NCS^- < PR_3 < CN^- < CO$.
An analogous effect may also be seen in octahedral hexa-coordinate complexes, although the effect is usually relatively small.

The H_2O exchange rate in aqua ions Inert, intermediate, and labile are classification of the exchange rate proposed by H. Taube (1952). The exchange rate of aqua ions (ions coordinated by water molecules) of main-group and transition metals differ greatly depending upon the identity of the metal species. Since the rate of water ligand exchange is well correlated with the exchange rates of other ligands, it is useful for general comparison of the exchange rates in the complexes of different metal ions. For alkali and alkaline earth metals, the exchange rates are very high (10^5-10^9 s^{-1}), and the complexes of these metals are classified as labile. As the dissociative mechanism is generally found in these cases, ions with smaller ionicity and of larger size attract water ligands less and their exchange rates becomes higher. In Group 12 metal ions Zn^{2+}, Cd^{2+}, Hg^{2+}, Group 13 metal ions Al^{3+}, Ga^{3+}, $In3^+$ and Group 3 metal ions Sc^{3+}, Y^{3+}, rapid water ligand exchange takes place by a dissociative mechanism.

On the other hand, the exchange rates of M (II) ions in *d* block transition metal ions is medium (10-10^4 s^{-1}), and that of M (III) ions are lower still. The rates of d^3 Cr^{3+} and d^6 Co^{3+} are notably slow (10^{-1}-10^{-9} s^{-1}), and their complexes are termed inert. There has been

a great deal of study of ligand-exchange reactions. The exchange rates are smaller the larger the ligand field stabilization energy. Therefore, the ligand-exchange rates of 4*d* and 5*d* transition metall complexes are generally slow.

****

Test tube experiments

Easy chemical or biological reactions performed in test tubes are sometimes called test tube experiments. Solutions in test tubes are mixed at room temperature in air and the mixture is shaken to observe a color change or formation of precipitates and the results of the reactions are speculated on. University professors occasionally attempt these sorts of experiments. Although easy, these simple experiments show only the effects of visible light absorption and solubility. However, since even great discoveries can be born from such experiments, they should not be dismissed.

H. Taube wrote that he found a hint of the inner-sphere electron transfer mechanism from test tube experiments. He mixed $Cr^{2+}(aq)$ and I_2 in a test tube in order to clarify the oxidation of $Cr^{2+}(aq)$ and observed the change of color to the one characteristic of $[Cr(H_2O)_6]^{3+}$ via green. The green color is due to $[(H_2O)_5CrI]^{2+}$ which is unstable and changes to $[Cr(H_2O)_6]^{3+} + I^-$. He assumed that this was due to the formation of a Cr-I bond before Cr(II) was oxidized by I_2. Subsequently, he performed another test tube experiment using $[(NH_3)_5CoCl]^{2+}$ as an oxidant and found that $Cr^{2+}(aq)$ was converted into $[Cr(H_2O)_6]^{3+}$ via green $[(H_2O)_5CrCl]^{2+}$. This reaction established the inner-sphere electron transfer mechanism in which a Co-Cl-Cr bridge forms between Co^{3+} and Cr^{2+} and led to the Nobel Prize in a later year.

****

(b) Redox reactions

The oxidation number of the central metal in a transition-metal compound can vary in a few steps from low to high. Namely, the oxidation state of a compound is changeable by redox reactions. As a consequence of this, the bond distance and the bond angle between the metal and coordinating elements, or between metals, change, and at times the whole structure of a complex can be distorted remarkably or the compound may even decompose.

The reactions of a metal compound with various reducing or oxidizing agents are also very important from the viewpoint of synthetic chemistry. Especially, reduction reactions are used in the preparation of organometallic compounds, such as metal carbonyls or cluster compounds.

Meanwhile, the study of electron transfer between complexes, especially the redox reactions of transition metal complexes, has developed. Taube won the Nobel Prize (1983) for the study of electron transfer reactions in transition metal complexes, classifying such reactions into two mechanisms. The mechanism of electron transfer in which a bridging ligand is shared between two metals is called the **inner-sphere mechanism**, and the one involving a direct transfer of electrons between two metals without a bridging ligand is called the **outer-sphere mechanism**.

Inner-sphere mechanism When $[CoCl(NH_3)_5]^{2+}$ is reduced by $[Cr(OH_2)_6]^{2+}$, an intermediate complex, $[(NH_3)_5Co\text{-}Cl\text{-}Cr(OH_2)_5]^{4+}$, is formed in which the chlorine atom forms a bridge between cobalt and chromium. As a result of an electron transfer from chromium to cobalt through chlorine, $[Co(NH_3)_5Cl]^{+}$, in which cobalt is reduced from a trivalent to a divalent oxidation state and $[Cr(OH_2)_6]^{3+}$, in which chromium is oxidized from a divalent to a trivalent oxidation state, are formed. This kind of reaction is a redox reaction via the inner-sphere mechanism. The anions other than halogens suitable for such bridge formation are SCN^-, N_3^-, CN^-, *etc.*.

Outer-sphere mechanism When $[Fe(phen)_3]^{3+}$ (phen is orthophenanthroline) is reduced by $[Fe(CN)_6]^{4-}$, no ligand bridge forms between the metals and an electron moves from the HOMO of Fe(II) to the LUMO of Fe(III) in a very short and direct contact between the two complexes. As the result of the electron transfer, $[Fe(phen)_3]^{2+}$ and $[Fe(CN)_6]^{3-}$ form. This kind of reaction is a redox one via the outer-sphere mechanism, and is characteristic of a complex system that has a very slow ligand substitution rate compared with the speed of electron transfer, especially in systems that have the same ligands but different oxidation-numbers, for example, $[Fe(CN)_6]^{3-}$ - $[Fe(CN)_6]^{4-}$ has a high rate of electron transfer. R. A. Marcus won the Nobel Prize (1992) for his study of this outer-sphere electron transfer mechanism.

Problem

6.1 Which cavity, either the octahedral or tetrahedral one, in an array of oxygen atoms do Fe^{2+} ions tend to occupy in iron oxide Fe_3O_4 containing both Fe^{2+} and Fe^{3+} ions?

6.2 Describe a method of preparing *trans*-$[PtCl(Et)(PEt_3)_2]$.

6.3 Propose mononuclear and dinuclear metal complexes containing cyclopentadienyl and carbonyl ligands that satisfy the 18-electron rule.

6.4 Devise a method of selective syntheses of *cis*-$[PtCl_2(NH_3)_2]$ and *trans*-$[PtCl_2(NH_3)_2]$ using the trans effect.

6.5 How can it be proven that the reduction reaction of $[CoCl(NH_3)_5]^{2+}$ by $[Cr(OH_2)_6]^{2+}$ proceeds by the inner-sphere electron transfer mechanism?

UNIVERSITY of WINDSOR

Chemistry & Biochemistry

Back To Faculty List

Chemistry and Biochemistry
University of Windsor
Essex Hall
401 Sunset Avenue Windsor,
Ontario Canada N9B 3P4
Phone: (519) 253-3000 ext:3521
FAX:(519)-973-7098
Email:chembio@uwindsor.ca

Samuel A. Johnson
Inorganic Transition Metal and Materials
Ph.D. (University of British Columbia)
sjohnson@uwindsor.ca
Assistant Professor
253-3000 Ext: 3769
373-2 Essex Hall
http://137.207.10.226/johnson/

Research Interests:

The research projects outlined below involve organic, inorganic and organometallic synthesis, as well as materials evaluation. Students can expect to develop skills in handling highly air-and moisture-sensitive compounds. Characterization techniques include NMR, IR, EPR and UV-vis spectroscopy and X-ray crystallography.

Dinitrogen Activation by Transition Metals: Towards the Catalytic Functionalization of N_2 Under Ambient Conditions

Dinitrogen surrounds us... N_2 comprises ~80% of the air we breathe.

Despite the importance of nitrogen containing compounds, it is very difficult to utilize this abundant feedstock without resorting to very harsh conditions (>500 ^{o}C, 100 atm). The goal of this project is to use transition metal complexes to develop new reactivities of dinitrogen, such as simple insertion reactions. The ultimate goal is the design of a catalytic process that utilizes dinitrogen under ambient conditions.

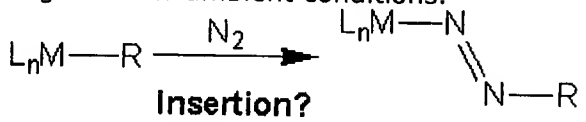

The Synthesis of Reactive Trimetallic Complexes and Clusters

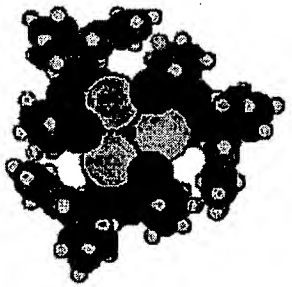

The goal of this project is to design ligands that can bind multiple metal centers and hold them in close proximity. The ideal ligand design will retain reactive sites on the metal centers so that the reactivity of these complexes can be studied. The desired reactivity will be a cross between the behaviour of metal surfaces and complexes bearing a single metal centre. This unique reactivity should result in the development of new catalytic reactions.

Low Oxidation State Early Transition Metals as Electron Donors in Nonlinear-Optical Materials

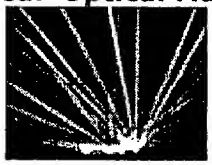

The intense recent interest in nonlinear-optical (NLO) materials is primarily due to their application in the area of photonics, where photons are used to acquire, store, process and transmit information in lieu of electrons. Nonlinear-optical materials can manipulate light propagation by the application of an electric field or a laser pulse, and can therefore serve as the circuitry of a photonic device.

Transition metal complexes have been applied in a variety of roles in optoelectronic materials, which include NLO applications. Researchers have taken advantage of the unique properties of transition metal complexes, such as their large polarizabilities, to design molecules with NLO responses competitive with strictly organic molecules. Although this approach to NLO materials has been extended to include complexes that contain metal-

metal multiple bonds, the use of the early-transition metals has been entirely avoided. There are a number of reasons for this, the most notable of which is that the early transition metals in low oxidation states are more air and moisture sensitive than the late transition metals; the use of low-valent early transition metal (LVETM) complexes as electron donors in NLO active molecules is a significant synthetic challenge.

Regardless of the difficulty associated with handling LVETM complexes, they could prove to be excellent electron donors in NLO-active molecules. Compared to the complexes of the late transition metals, the lower effective nuclear charge experienced by the *d* electrons in low-valent complexes of the early transition metals should render them more polarizable and strongly reducing. We are currently synthesizing simple model complexes to test for NLO response, and will then address issues concerning stability by designing complexes that provide enough coordinative saturation and steric protection to the metal centre to render these complexes kinetically stable.

For more detailed information (e.g., target molecules) please contact me at sjohnson@uwindsor.ca

Selected Publications:

Johnson, S. A.; Liu, F.-Q.; Suh, M. C.; Zürcher, S.; Haufe, M.; Tilley, T. D. "Regioselective Coupling of Pentafluorophenyl Substituted Alkynes: Mechanistic Insight into the Zirconocene Coupling of Alkynes and a Facile Route to Conjugated Polymers Bearing Electron-Withdrawing Pentafluorophenyl Substituents" J. Am. Chem. Soc. **2003**, *125*, 4199-4211.

Fryzuk, M. D.; Johnson, S. A.; Patrick, B. O.; Albinati, A.; Mason, S. A.; Koetzle, T. F. "New Mode of Coordination for the Dinitrogen Ligand: Formation, Bonding, and Reactivity of a Tantalum Complex with a Bridging N2 Unit That Is Both Side-on and End-on" *J. Am. Chem. Soc.* **2001**, *123*, 3960-3973.

Fryzuk, M. D.; Johnson, S. A. "The Continuing Story of Dinitrogen Activation" *Coord. Chem. Rev.* **2000**, *200-202*, 379-409.

Fryzuk, M. D.; Johnson, S. A.; Rettig, S. J. "Synthesis of [P2N2]Ta(C2H4)

Et, a Neutral Species with a -Agostic Ethyl Group in Equilibrium with an -Agostic Ethyl Group in Solution ([P2N2] = PhP(CH2SiMe2NSiMe2CH2)2PPh)" *J. Am. Chem. Soc.* **2001**, *123*, 1602-1612.

4. Crystal Field Theory

This theory largely replaced VB theory for interpreting the chemistry of coordination compounds. It was proposed by the physicist Hans Bethe in 1929.

Subsequent modifications were proposed by J. H. Van Vleck in 1935 to allow for some covalency in the interactions. These modifications are often referred to as **The Ligand Field Theory**.

Ref. For a review on the evolution of bonding models see C. J. Ballhausen, *J. Chem. Ed.* **1979** *56* 194-197, 215-218, 357-361.

Pure crystal field theory assumes that the interactions between the metal ion and the ligands are purely electrostatic (ionic). The ligands are regarded as point charges. Although somewhat unrealistic, it uses symmetry considerations which are valid for Ligand Field Theory as well as MO Theory.

It is of outmost importance to draw the d orbitals correctly in order to get an idea of which of these orbitals will interact with the ligands (point charges).

The 5d orbitals in an isolated gaseous metal are **degenerate**. If a spherically symmetric field of negative charges is placed around the metal, these orbitals remain degenerate, but all of them are raised in energy as a result of the repulsion between the negative charges on the ligands and in the d orbitals. If rather than a spherical field, discrete point charges are allowed to interact with the metal, the **degeneracy of the d orbitals is removed** (or, better said, lifted).

The splitting of d orbital energies and its consequences are at the heart of crystal field theory.

Octahedral Geometry

On going from a spherical to an octahedral symmetry, all d orbitals are raised in energy, relative to the free ion. However, not all d orbitals will interact to the same extent with the six point charges located on the +x, -x, +y, -y, +z and -z axes respectively. The orbitals which lie along these axes (i.e. x^2-y^2, z^2) will be destabilized more that the orbitals which lie in-between the axes (i.e. xy, xz, yz).

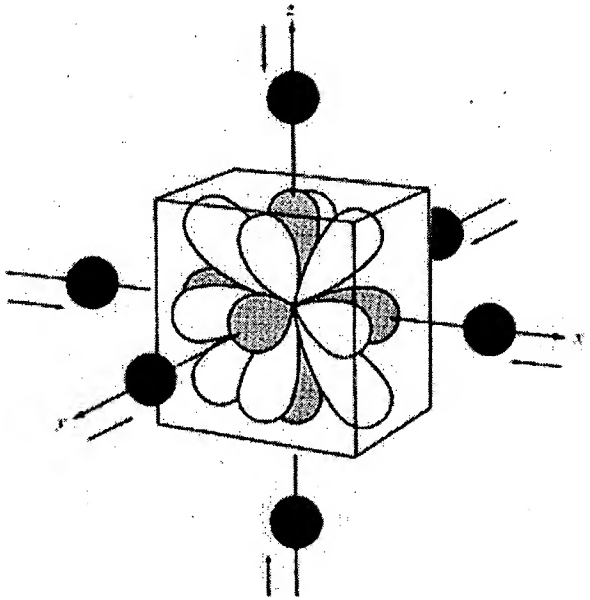

Fig. 11.6 Complete set of *d* orbitals in an octahedral field produced by six ligands. The e_g orbitals are shaded and the t_{2g} orbitals are unshaded. The torus of the d_{z^2} orbital has been omitted for clarity.

Referring to the character table for the Oh point group reveals that the x^2-y^2, z^2 orbitals belong to the E_g irreducible representation and xy, xz, yz belong to the T_{2g} irreducible representation.

The extent to which these two sets of orbitals are split (the e_g and the t_{2g} use lower case for orbitals) is denoted by Δ_0 or

alternatively 10Dq. As the barycenter must be conserved on going from a spherical field to an octahedral field, the t_{2g} set must be stabilized as much as the e_g set is destabilized.

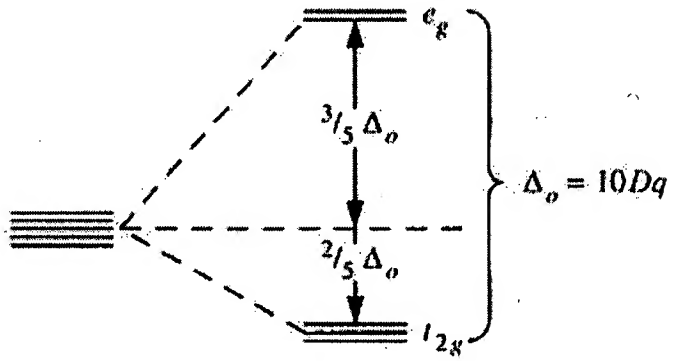

Illustration

$[Ti(H_2O)_6]^{3+}$.

This is a d1 complex and the electron occupies the lowest energy orbital available, i.e. one of the three degenerate t2g orbitals. The purple colour is the result of the absorption of light which results in the promotion of this t2g electron into the eg level.

$$t_{2g}^{1}e_g^{0} \rightarrow t_{2g}^{0}e_g^{1}$$

The UV-Vis absorption spectrum reveals that this transition occurs with a maximum at 20300 cm^{-1} which corresponds to Δ_0 243 kJ/mol.

(Remember that 1000 cm^{-1} = 11.96 kJ/mol or 2.86 kcal/mol or 0.124 eV.)

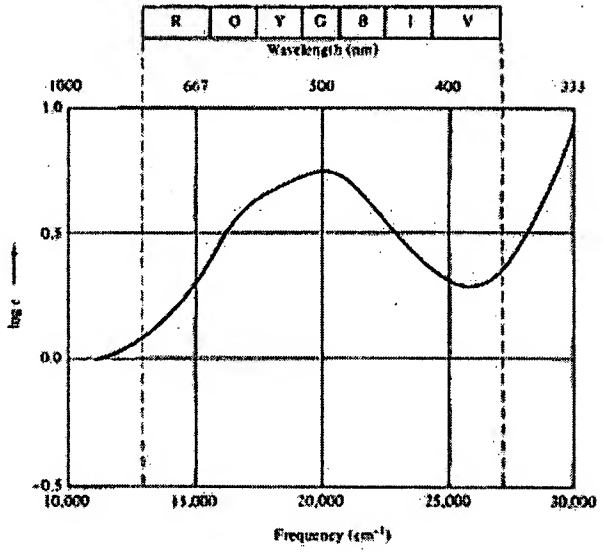

Typical Δ_0 values are of the same order of magnitude as the energy of a chemical bond.

What happens when more than 1 electron in d orbitals?

For d^2-d^9 systems the electron-electron interactions must be taken into account (vide supra).

For d^1-d^3 systems, Hund's rule predicts that the electrons will not pair and occupy the t_{2g} set.

For d^4-d^7 systems, there are two possibilities:

Either put the electrons in the t_{2g} set and therefore pair the electrons. This is the so called **low spin case** or **strong field situation**.

Or put the electrons in the eg set, which lies higher in energy, but the electrons do not pair. this is the so called **high spin case** or **weak field situation**.

Therefore, there are two important parameters to consider

The Pairing energy (P)

and

the e_g - t_{2g} Splitting (referred to as Δ_0, 10Dq)

For both the high spin (hs) and low spin (ls) situations, it is possible to compute the **Crystal Field Stabilization Energy** as a function of electron count and field strength.

The electron pairing energy P is composed of two terms

a) **The Coulombic repulsion**

This repulsion must be overcome when forcing electrons to occupy the same orbital. As 5d orbitals are more diffuse than 4d orbitals which are more diffuse than 3 d orbitals, the pairing energy becomes smaller as one goes down a period.

As a rule, 4d and 5d transition metals are always low spin

b) **The loss of exchange energy**

The exchange energy which is konwn as Hund's rule is proportional to the number of electrons having parallel spins. The greater this number, the more difficult it is to pair electrons. Therefore

The d^5 (Fe^{3+}, Mn^{2+}) configuration is the most enclined to form high spin complexes

Tetrahedral Geometry

The tetrahedral symmetry can be derived from a cubic symmetry where only four of the eight corners are occupied by point charges. In such a situation, it is the xy, yz, xz orbitals which are destabilized as they point towards the incoming point charges. the x^2-y^2 and z^2 are stabilized so that the barycenter is preserved.

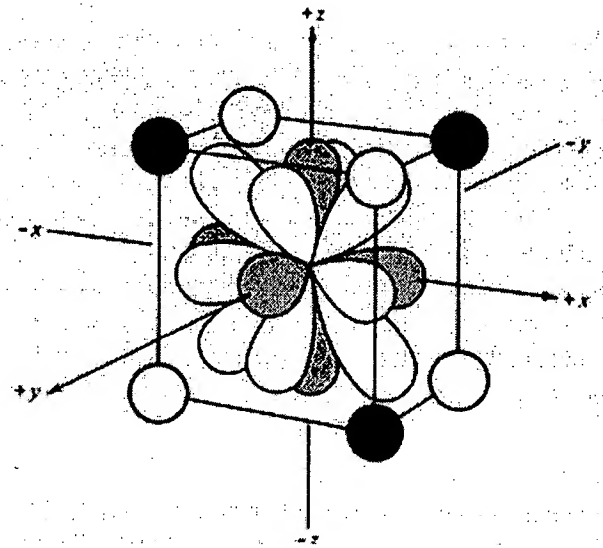

Fig. 11.10 Complete set of *d* orbitals in a cubic field. Either set of tetrahedral ligands (● or ○) produces a field one-half as strong as the cubic field.

Please note that the irreducible representations are t_2 and e in the Td point group.

The crystal field splitting in a tetrahedral symmetry is intrinsically smaller than in the octahedral symmetry as there are only four ligands (instead of six ligands in the octahedral symmetry) interacting with the transition metal ion. The point charge model predicts that

$$\Delta_t = 4/9\ \Delta_o$$

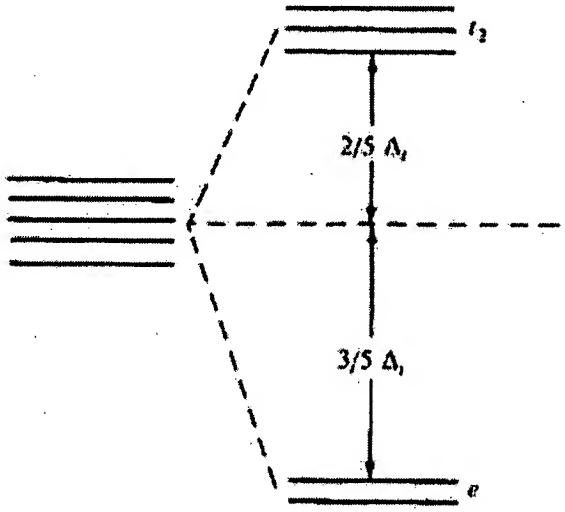

As a result, low spin configurations are rarely observed. Usually, if a strong field ligand is present, the square planar geometry will be favoured.

Square Planar Geometry

In order to derive the square planar geometry, let us consider a tetragonal distortion.

Removing both point charges from the z axis, stabilizes the z^2 orbital of the e_g set. As the bonding of the remaining four point charges increases the x^2-y^2 orbitals rises in energy.

Again here, as the symmetry is lowered, the degeneracy is lifted and the orbitals have different irreducible representations.

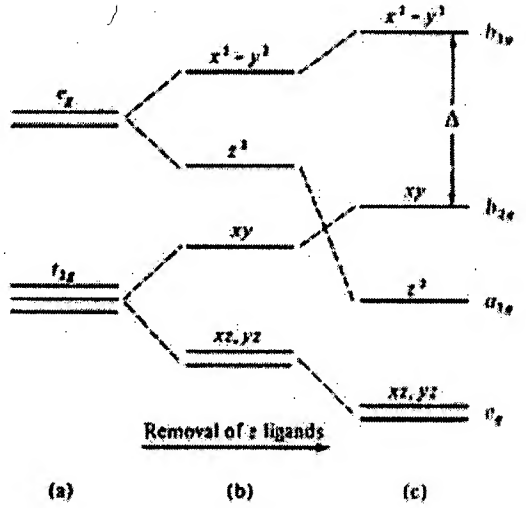

Fig. 11.12 An octahedral complex (a) undergoing z axis elongation such that it becomes tetragonally distorted (b) and finally reaches the square planar limit (c). The a_{1g} (d_{z^2}) orbital may lie below the e_g (d_{xz} and d_{yz}) orbitals in the square planar complex.

Other Geometries

orbital splitting patterns for various relevant geometries can be derived with the crystal field theory

---

Factors which influence the magnitude of Δ

a) **Oxidation state of the metal**

The higher the charge of the metal, the greater Δ. As a rule of thumb Δ increases by ca. 50% when the oxidation state increase by one unit.

b) **Nature of the metal ion**

Δ increases on going from 3d < 4d < 5d

(ca. 50% going from Co to Rh. ca. 25% going from Rh to Ir.)

c) **Number and geometry of the ligands**

Δ_0 is ca. 50% larger that Δ_t.

d) **Nature of the ligands**

Based on similar data for a wide variety of complexes, it is possible to list ligands in order of increasing field strength in the so-called *spectrochemical series*

$I^- < Br^- < S^{2-} < SCN^- < Cl^- < N_3^-, F^- <$ urea, $OH^- <$ ox, $O^{2-} <$ H2O < $NCS^- <$ py, $NH_3 <$ en < bpy, phen < $NO_2^- <$ $CH_3^-, C_6H_5^- < CN^- <$ CO.

It is possible to arrange the metals according to a spectrochemical series as well. The approximate order is

$$Mn^{2+} < Ni^{2+} < Co^{2+} < Fe^{2+} < V^{2+} < Fe^{3+} < Co^{3+} < Mn^{3+} < Mo^{3+} < Rh^{3+} < Ru^{3+} < Pd^{4+} < Ir^{3+} < Pt^{4+}$$

Jorgensen has proposed a formula which allows to estimate the Δ

$$\Delta = f \cdot g$$

where f is a function of the ligand and g is a function of the metal

Applications of Crystal- and Ligand Field Theory

Ionic Radii. For a given oxidation state, the ionic radius decreases steadily on going from left to right in a transition series. Populating antiboding orbitals (i.e. filling the e_g levels in an octahedron) leads to an increase in ionic radius. Therefore, the ionic radius depends on the spin state of the metal (i.e. high spin or low spin).

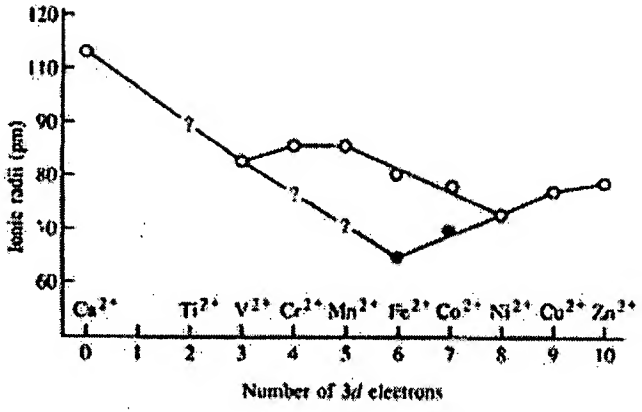

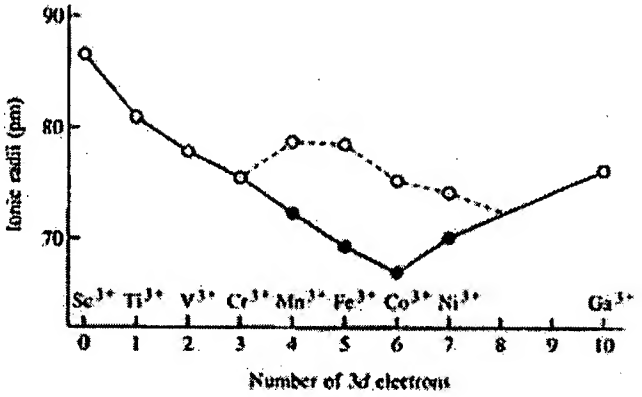

Hydration Enthalpy. Let us look at the variation of enthalpy of M^{2+} ions (NB. Since water is a weak field ligand, the complexes are high spin).

$$M^{2+}_{(g)} + 6\ H_2O_{(l)} = [M(O_2H)_6]^{2+}_{(aq)}$$

Plotting the enthalpy across the first transition series

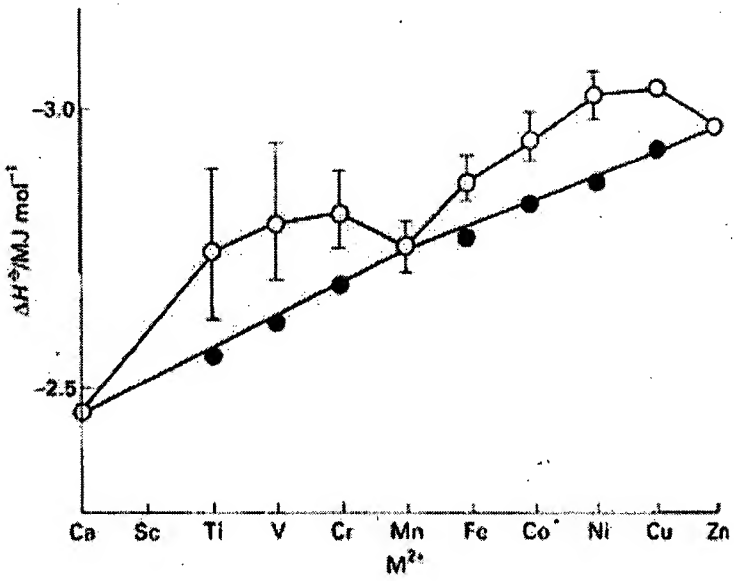

6.11 The hydration enthalpy of M^{2+} ions of the first row of the *d* block. The straight lines show the trend when the ligand field stabilization energy has been subtracted from the observed values. Note the general trend to greater hydration enthalpy (more exothermic hydration) on crossing the period from left to right.

This **double-humped** pattern is very frequent when properties are plotted for transition metals acrsoss a transition series.

The straight line (full black circles) is obtained by substracting the CFSE for the given electron count. The linear increase in stability on going through a transition series is caused primarily by the increasing acidity (largely due to a decreasing size of the metal cation and electrostatic effects). This forms the basis of the Irving-Williams series.

The **Irving-Williams** series states that for a given ligand, the stability of the complexes increases from Ba to Cu (and then drops for Zn). It should be noted however that as one moves towards the right, the late transition metals prefer softer ligands. (see the HARD-SOFT ACID-BASE Theory).

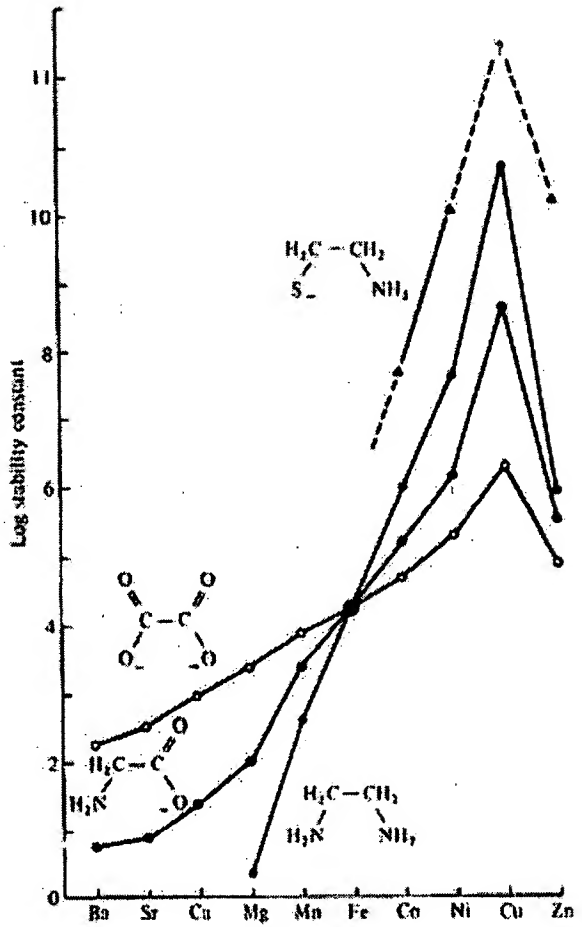

Fig. 9.5 The Irving-Williams effect: The stability increases in the series Ba–Cu, decreases with Zn. [From Sigel, H.; McCormick, D. B. *Acc. Chem. Res.* 1970, *3*, 201. Reproduced with permission.]

Geometry Preference as a Function of Electron Count. If one keeps in mind that the Δ_t is about half that of Δ_o, it is possible to predict qualitatively which electron counts should favour which geometry.

on to Chapter 5

back to the Table of Content

Alternative Low-Symmetry Structure for 13-Atom Metal Clusters

C. M. Chang[1,*] and M. Y. Chou[2]

[1]*Department of Physics, National Dong Hwa University, Hualien 974, Taiwan, R.O.C.*

[2]*School of Physics, Georgia Institute of Technology, Atlanta, Georgia 30332-0430*

(Dated: March 13, 2004)

Abstract

The atomic geometry, electronic structure, and magnetic moment of $4d$ transition-metal clusters with 13 atoms are studied by pseudopotential density-functional calculations. We find a new buckled biplanar structure with a C_{2v} symmetry, stabilized by enhanced s-d hybridization. It has a lower energy than the close-packed icosahedral or cuboctahedral structure for elements with more than half filled d-shells. The magnetic moments of this buckled biplanar structure are found to be smaller than those of the icosahedral structure and closer to available experimental results.

PACS numbers: 36.40.Cg, 36.40.Mr, 61.46.+w, 73.22.-f

Small atomic clusters are known to exhibit novel electronic, magnetic, optical, and chemical properties [1], and have stimulated intensive research efforts in recent years. Enhanced stability against dissociation or fragmentation has been found in clusters of particular size. These clusters are termed as "magic" clusters [2–7]. Two major factors have been identified for the origin of these magic clusters: electronic shell closure [3] in alkali- and noble-metal clusters; and atomic or geometric closed shells [2, 5] in rare-gas clusters and others. In the latter case, the 13-atom cluster is the most studied aggregate, for it corresponds to the first geometric shell closing for both the icosahedral and cuboctahedral structures. Recently, it has been demonstrated by laser-vaporization and time-of-flight mass spectrometry [6] that 13 is a common magic number for many transition-metal clusters including Fe, Ti, Zr, Nb, and Ta. However, it is still difficult to directly determine the atomic arrangements of such small clusters experimentally.

Accurate first-principles calculations can in turn provide reliable information about the geometrical structures of small clusters. The ground-state structure for most 13-atom metal clusters studied previously was predicted to be either an icosahedron (Ni_{13} [8], Rh_{13} [9], Pd_{13} [10], Al_{13} [11], and Nb_{13} [12]) or a cuboctahedron (Pt_{13} [13], and Au_{13} [14]). However, none of the calculations have searched the entire phase space. High-symmetry compact structures are not necessarily the ground state, since the bonding in small metal clusters can be different from that in the bulk. A recent calculation for Cu_{13}, Ag_{13}, and Au_{13} clusters has found many isomers with energies lower than that of an icosahedron [15], while in another calculation the neutral Au_{13} and anionic Au_{13}^- clusters are found to prefer a 2D planar structure due to strong relativistic effects [16]. Therefore, the question worth asking is whether this is a more general phenomenon than for noble metals only, and whether one can identify a trend or understand the mechanism behind it.

In this Letter, we describe the results of an extensive study of the structure and energetics of 13-atom clusters for the whole series of $4d$ transition metals by first-principles total energy calculations and molecular dynamics (MD) simulations. To our surprise, a new buckled biplanar structure for this magic cluster size is found to be a competitive alternative to more compact arrangements such as the icosahedral structure. For late transition-metal clusters this low-symmetry structure is even more favorable than an icosahedron. This result would not come from any pairwise potential and is a direct consequence of the electronic properties.

The first-principles calculations based on density functional theory (DFT) [17] were per-

formed using the Vienna *Ab-initio* Simulation Package (VASP) [18] with a plane-wave basis and Vanderbilt-type ultrasoft pseudopotentials [19]. The kinetic energy cutoffs used were the maximal default values recommended by the pseudopotential database, which ranged from 120 to 205 eV for the 4d transition metals considered here. For the exchange-correlation functional we used the spin-polarized generalized gradient approximation (GGA) [20]. A cubic supercell with a side dimension of 20 Å was employed in the calculation. The Brillouin zone integration was approximated by a 3×3×3 Monkhorst-Pack k-point mesh [21] in the total-energy calculations where all the atoms are allowed to relax following the Hellmann-Feynman forces. The cluster geometry is optimized without symmetry constraints until the total energy is converged to 10^{-5} eV in the self-consistent loop and the force on each atom is less than 0.02 eV/Å. We have also carried out finite-temperature MD simulations for selected clusters in order to search for possible structures. Only the Γ-point is used in these MD simulations, and the atomic motion is described by using the Nosé dynamics [22] for a canonical ensemble. The time step used for integrating the atomic equations of motion is one femtosecond.

We first studied the well-known high-symmetry arrangements such as the icosahedral [Fig. 1(a)], cuboctahedral, and decahedral structures. For Pd_{13}, the icosahedron, which has the highest compactness for 13-atom clusters, is most stable among these three geometries. The decahedral structure, which can be obtained from an icosahedron by rotating the top pentagonal cap by 36° (thus transforming the ten triangular faces between the top and bottom pentagonal caps into 5 square faces) is 0.30 eV higher in energy than the icosahedral structure. The cuboctahedron, which maintains the face-centered-cubic (fcc) geometry, has the highest energy among the three structures, 1.01 eV above that of the icosahedron. These results are consistent with that of a recent first-principles calculation [10] in which an icosahedron was found to be more stable than a cuboctahedron for Pd_{13}. We next performed first-principles MD simulations at 300 K for Pd_{13}. With an initial geometry of a cuboctahedron, the simulation generated a surprising structure that has never been reported previously. Instead of transforming into an icosahedron, the atoms rearranged themselves to yield a new buckled biplanar (BBP) structure with a C_{2v} symmetry, as shown in Fig. 1(b). Its total energy evaluated at 0 K is 0.02 (0.52) eV lower than that of an icosahedron based on a spin-polarized (non-spin-polarized) calculation. As can be seen in Fig. 1(b), this BBP structure has seven atoms in the top layer forming a hexagonal array, and six atoms in the

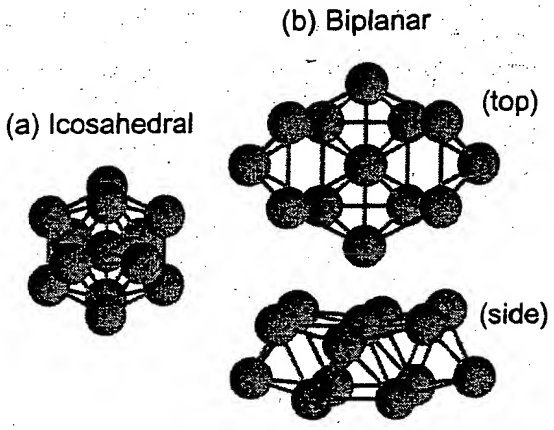

FIG. 1: (color online) Atomic arrangements of (a) the icosahedral and (b) the new buckled biplanar (BBP) structures for 13-atom clusters.

TABLE I: Relative total energy per cluster of the buckled biplanar structure (BBP) with respect to the icosahedral structure (ICO). The spin magnetic moment per atom (μ_B/atom), and the average nearest-neighbor distance (a_{avg}) for both structures are also shown.

	Y_{13}		Zr_{13}		Nb_{13}		Mo_{13}		Tc_{13}	
	ICO	BBP	ICO	BBP	ICO	BBP	ICO	BBP	ICO	BBP
Energy (eV)		1.59		1.89		4.00		0.67		-1.66
μ_B/atom	1.00	0.38	0.46	0.15	0.23	0.08	0.62	0.31	1.00	0.69
a_{avg} (Å)	3.39	3.32	2.90	2.90	2.93	2.69	2.70	2.58	2.58	2.53
	Ru_{13}		Rh_{13}		Pd_{13}		Ag_{13}		Cd_{13}	
	ICO	BBP	ICO	BBP	ICO	BBP	ICO	BBP	ICO	BBP
Energy (eV)		-0.78		-0.13		-0.02		-0.84		-0.18
μ_B/atom	0.92	0.46	1.62	1.31	0.62	0.31	0.38	0.08	0.00	0.00
a_{avg} (Å)	2.59	2.53	2.67	2.60	2.75	2.69	2.89	2.85	3.42	3.32

bottom layer consisting of a central square of four atoms plus two side atoms. It is a much more open and extended structure than an icosahedron. The layers are slightly bent and the atoms of either layer are not exactly on the same plane. From the MD simulations at 300 K, this BBP structure seems to be thermally stable and the shape is well kept in the simulation.

In order to determine if this is a common low-energy structure for 13-atom metal clusters, we have systematically compared the energy of this BBP structure with that of an icosahedron for the $4d$ transition-metal series. In each total-energy calculation, the atomic positions are fully relaxed. The calculated total energy with respect to that of an icosahedron is summarized in Table I. We can see clearly that the 13-atom clusters of early transition metals (Y_{13}, Zr_{13}, Nb_{13}, Mo_{13}) prefer the icosahedral structure, while those of late transition metals (Tc_{13}, Ru_{13}, Rh_{13}, Pd_{13}, Ag_{13}, and Cd_{13}) may prefer the BBP structure. Therefore, the BBP structure seems to be favored only when the d shell is more than half filled.

In the total-energy calculation for the icosahedral structure, atoms are relaxed without symmetry constraints. Except for Nb_{13} and Mo_{13}, most clusters exhibit little deviation from the ideal icosahedral symmetry. In the bulk, Nb and Mo do not favor close-packed structures and choose the body-centered cubic structure instead. Therefore, it is not surprising that icosahedral Nb_{13} and Mo_{13} show significant distortions after being allowed to relax. The results listed in Table I for icosahedral Nb_{13} and Mo_{13} are those of fully relaxed (distorted) geometries. Without distortions, the ideal icosahedral structure for Nb_{13} (Mo_{13}) is 0.49 (1.16) eV higher in energy than the fully-relaxed BBP structure, and has a magnetic moment of 0.54 (0.79) μ_B/atom and an average nearest-neighbor (NN) distance of 2.74 (2.65) Å.

The competition between the icosahedral and BBP structures reflects a delicate balance among various energy terms. Being a more extended and open structure, the BBP arrangement has a lower electrostatic energy associated with the electron-electron and ion-ion repulsion, as well as a lower kinetic energy. On the other hand, the more compact icosahedral structure is designed to maximize the interaction between the electrons and the ionic cores. The number of NN pairs is 42 in an icosahedron, compared with 36 in the BBP structure. Without paying a high penalty in the Hartree energy, the latter can take a slightly smaller NN distance than the former in order to optimize the electron-ion interaction. The average NN distance in the BBP structure is therefore consistently smaller than that of the icosahedral structure (see Table I), although the difference is not substantial. Fig. 2 shows these average NN distances for the whole series compared with the bulk values. Except for Cd_{13}, the average NN distance in the cluster is smaller than that in the bulk, indicating a stronger d interaction in the finite system. Cd is an exception because it basically has two s electrons as the valence electrons that can screen better in the Cd_{13} cluster, giving rise to

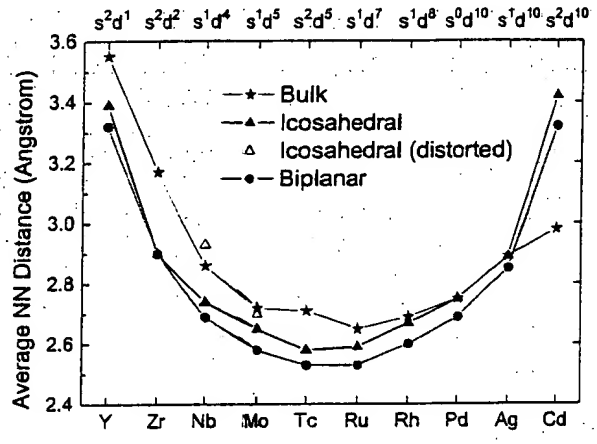

FIG. 2: (color online) Average nearest-neighbor (NN) distance for the icosahedral (filled triangles) and buckled bi-planar (filled circles) structures for 4*d* 13-atom clusters compared with the bulk values (stars). The values for the low-energy distorted icosahedral structure of Nb_{13} and Mo_{13} are also shown (open triangles). The atomic valence electron configuration for each element is given at the top of the figure.

a larger atom-atom separation than in the bulk.

The shape of the average NN distance curve as a function of the number of valence electrons in Fig. 2 also reflects the bonding characteristics in the transition-metal series. Since the *d* orbitals are only slightly screened by the outer *s* electrons, increasing the nuclear charge and adding more *d* electrons in the beginning of the series will cause stronger electron-ion interaction, increase cohesion, and decrease the NN distance. At certain point near half-filled in the series, the electron-electron repulsion starts to outweigh the electron-ion interaction, the cohesive energy decreases and the NN distance increases as the *d* shell gets filled. In clusters one has much more degrees of freedom in arranging the atoms. Therefore, for late transition metal clusters, it is expected that a structure with reduced electron-electron interactions may be favored, such as the BBP structure found in this work.

This phenomenon can also be understood by considering electronic orbitals. In chemistry terms, once half of the *d* orbitals are filled, the anti-bonding orbitals are occupied and the cohesion is weakened. Hence a cluster structure with enhanced *s*-*d* hybridization may become favorable for elements with more than half filled *d* shells. These structures are often of lower dimensions. It has been reported in a recent study of Au_N^- ($N \leq 13$) [16] that planar structures are favored due to strong hybridization of the atomic 5*d* and 6*s* orbitals resulting

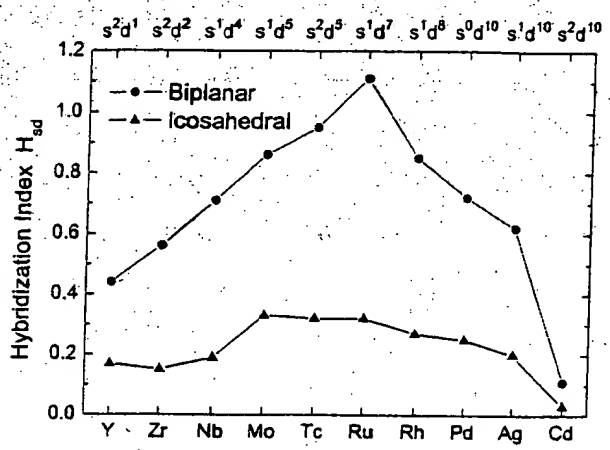

FIG. 3: (color online) The s-d hybridization index (see text) for the icosahedral (filled triangles) and buckled bi-planar (filled circles) structures for $4d$ transition metal 13-atom clusters. The values for icosahedral Nb_{13} and Mo_{13} are from the undistorted geometry. The atomic valence electron configuration for each element is given at the top of the figure.

from relativistic effects . Here we can compare the s-d hybridization indices [16] for the icosahedral and BBP structures defined by

$$H_{sd} = \sum_{I=1}^{13} \sum_{i=1}^{occ.} w_{i,s}^{(I)} w_{i,d}^{(I)} , \qquad (1)$$

where $w_{i,s}^{(I)}$ ($w_{i,d}^{(I)}$) is the square of the projection of the ith Kohn-Sham orbital onto the s (d) spherical harmonics centered at atom I, integrated over a sphere of radius equal to half of the shortest NN distance in each cluster. The spin index is implicit in the sum of orbitals i in Eq. (1). The results for these two structures are plotted in Fig. 3. In order to examine the generic features, the values for the undistorted icosahedral Nb_{13} and Mo_{13} are shown. It is clear that the BBP structure has consistently higher vales of H_{sd} than the icosahedron. For late transition metals, s-d hybridization is energetically favorable, thus the lower-symmetry BBP structure can be stabilized.

The other interesting issue for small metal clusters is the magnetic properties. It is known that small metal clusters made of nonmagnetic elements in the bulk can actually become magnetic, the Rh clusters [23] being an example. Therefore, we have also calculated the spin magnetic moments for the $4d$ transition-metal clusters of 13 atoms in the two structures, and the results are summarized in Table I. Our values for icosahedral clusters Ru_{13} (1.54 μ_B/atom), Rh_{13} (1.62 μ_B/atom), and Pd_{13} (0.62 μ_B/atom) are consistent with those of

previous studies [10, 24]. When compared with the experimental results of Ru_{13} (< 0.29 μ_B/atom [25]), Rh_{13} (0.88 [23] or 0.48 [25] μ_B/atom), and Pd_{13} (< 0.40 μ_B/atom [25]), we find the calculated values for icosahedrons are generally too high. However, as shown in Table I the spin magnetic moments of the BBP structure are consistently lower than those of the icosahedral structure, and the values for Ru_{13} (0.62 μ_B/atom), Rh_{13} (1.31 μ_B/atom), and Pd_{13} (0.31 μ_B/atom) are closer to the experimental results, especially for Pd_{13}. The giant magnetic moments found in previous calculations [10, 24] may not correspond to the correct ground state of the cluster.

We have also checked the energies of these two structures for selected transition-metal clusters in the 3*d* and 5*d* series. Ti_{13} and Hf_{13} (early 3*d* transition metals with the *d*-shell less than half filled) prefer the icosahedral structure with an energy difference of 1.84 and 2.03 eV, respectively. For the late transition metal clusters in the 3*d* and 5*d* series, such as Co_{13}, Cu_{13}, Ir_{13}, Pt_{13}, and Au_{13}, the BBP structure is preferred and the energies are 0.91, 0.53, 2.49, 1.56 and 1.78 eV lower than that of an icosahedron, respectively [26]. From these results, it is expected that the trend also holds for 3*d* and 5*d* metal clusters.

The situation with *sp*-metal clusters would be different, since the aforementioned factors stabilizing the BBP structure do not apply. We have performed first-principles MD simulations at 300 K for Al_{13} with either the cuboctahedron or the BBP structure as the initial structure and found that Al_{13} indeed transforms to an icosahedron very quickly in both cases. The total energies for the decahedron, cuboctahedron, and the BBP structure are 0.11 eV, 0.75 eV, and 1.56 eV higher than that of an the icosahedron, respectively. Even though the BBP structure is not favorable for Al_{13}, it can be a useful building block for larger clusters. For example, the low-energy bicapped decahedron structure found for Al_{15} [11] can also be obtained by adding two more atoms on top of BBP Al_{13}.

In summary, we have performed first-principles molecular dynamics simulations and total energy calculations to study the structures and energetics for the whole series of 4*d* transition metal clusters with 13 atoms. Instead of the high-symmetry icosahedral, cuboctahedral, and decahedral structures, we find another low-lying structure with a buckled biplanar arrangement that has a C_{2v} symmetry. This novel buckled biplanar structure for 13-atom clusters has a shorter average nearest-neighbor distance than the icosahedron and is commonly favored by late transition metals with more than half filled *d* shells. The spin magnetic moments of the buckled biplanar structure are generally smaller than those of the

icosahedral structure, and are in better agreement with existing experimental values.

We would like to thank Professor C. Cheng and Dr. C. M. Wei for many helpful discussions. This work is supported by the National Science Council (Grant No. NSC-92-2112-M-259-010, CMC) and the National Center for Theoretical Science of Taiwan, R.O.C., the National Science Foundation (Grants No. DMR-02-05328, MYC), and the Department of Energy (Grant No. DE-FG02-97ER45632, MYC). Computer time was made available on IBM-SP2-SMP by the National Center for High-performance Computing of R.O.C.

---

* Electronic address: cmc@mail.ndhu.edu.tw

[1] *Quantum phenomena in clusters and nanostructures*, edited by S. N. Khanna and A. W. Castleman (Springer-Verlag, Heidelberg, 2003).

[2] O. Echt *et al.*, Phys. Rev. Lett. **47**, 1121 (1981).

[3] W. D. Knight *et al.*, Phys. Rev. Lett. **52**, 2141 (1984).

[4] K. E. Schriver *et al.*, Phys. Rev. Lett. **64**, 2539 (1990).

[5] T. P. Martin *et al.*, Chem. Phys. Lett. **172**, 209 (1990).

[6] M. Sakurai *et al.*, J. Chem. Phys. **111**, 235 (1999).

[7] O. C. Thomas *et al.*, J. Chem. Phys. **114**, 5514 (2001).

[8] M. Calleja *et al.*, Phys. Rev. B **60**, 2020 (1999).

[9] B. V. Reddy *et al.*, Phys. Rev. B **59**, 5214 (1999).

[10] M. Moseler *et al.*, Phys. Rev. Lett. **86**, 2545 (2001).

[11] J. Akola *et al.*, Phys. Rev. B **58**, 3601 (1998); B. K. Rao *et al.*, Phys. Rev. B **62**, 4666 (2000).

[12] V. Kumar *et al.*, Phys. Rev. B **65**, 125403 (2002).

[13] N. Watari *et al.*, J. Chem. Phys **106**, 7531 (1997).

[14] O. D. Häberlen *et al.*, J. Chem. Phys. **106**, 5189 (1997).

[15] J. Oviedo and R. E. Palmer, J. Chem. Phys. **117**, 9548 (2002).

[16] H. Häkkinen *et al.*, Phys. Rev. Lett. **89**, 033401 (2002); H. Häkkinen *et al.*, J. Phys. Chem. A **107**, 6168 (2003).

[17] P. Hohenberg and W. Kohn, Phys. Rev. **136**, B864 (1964); W. Kohn and L. J. Sham, Phys. Rev. **140**, A1133 (1965).

[18] G. Kresse and J. Hafner, Phys. Rev. B **49**, 14251 (1994); G. Kresse and J. Furthmüller,

Comput. Mater. Sci. **6**, 15 (1996).

[19] D. Vanderbilt, Phys. Rev. B **41**, 7892 (1990); G. Kresse and J. Hafner, J. Phys.: Condens. Matter **6**, 8245 (1994).

[20] J. P. Perdew, *Electronic Structure of Solids '91*, edited by P. Ziesche and H. Eschrig (Akademie Verlag, Berlin, 1991); J. P. Perdew *et al.*, Phys. Rev. B **46**, 6671 (1992).

[21] H. J. Monkhorst and J. D. Pack, Phys. Rev. B **13**, 5188 (1976).

[22] S. Nosé, J. Chem. Phys **81**, 511 (1984).

[23] A. J. Cox, J. G. Louderback, and L. A. Bloomfield, Phys. Rev. Lett. **71**, 923 (1993).

[24] B. V. Reddy, S. N. Khanna, and B. I. Dunlap, Phys. Rev. Lett. **70**, 3323 (1993).

[25] A. J. Cox, J. G. Louderback, S. E. Apsel, and L. A. Bloomfield, Phys. Rev. B **49**, 12295 (1994).

[26] Similar to Au_{13}^- (Ref. 16), we also find that Au_{13} prefers planar structures due to relativistic effects. A C_s triangular structure and a D_{6h} six-capped hexagonal "star" have energies 0.74 eV and 0.03 eV lower than that of the biplanar structure, respectively. These 2D planar structures are not favored by other 13-atom transition-metal clusters.

Groups 1B to 8B The Transition Elements

Overall Relationships of Structures to Activities

These Elements represent the filling of the (3d), (4d) and (5d) orbitals, with 0 to 10 electrons but the filling of the $(3p)^6$ configuration at Argon actually completes the third Period of the Table. The first row of this Transition Block occurs apparently "out of sequence", *after* the filling of the $(4s)^2$configuration. This because the (3d) orbitals penetrate the core so poorly, that the (4s) orbital can fill first. Thus, all Transition Elements have "delayed configurations", [Rare Gas]$([n+1]s)^2nd^m$, with n ranging from 3 to 6 and m ranging for 0 to 10, as shown in Table (1).

Table (1) Electronic Configurations of Transition Elements

3B	4B	5B	6B	7B	8B			1B	2B
Sc	Ti	V	Cr	Mn	Fe	Co	Ni	Cu	Zn
$(3d)^1$	$(3d)^2$	$(3d)^3$	$(3d)^4$	$(3d)^5$	$(3d)^6$	$(3d)^7$	$(3d)^8$	$(3d)^9$	$(3d)^{10}$

Spatial and Electronic Structures

The poor penetration of the core by these (nd) orbitals is caused by the presence of *two angular Nodes* in their probability distributions, as shown in figure (1)

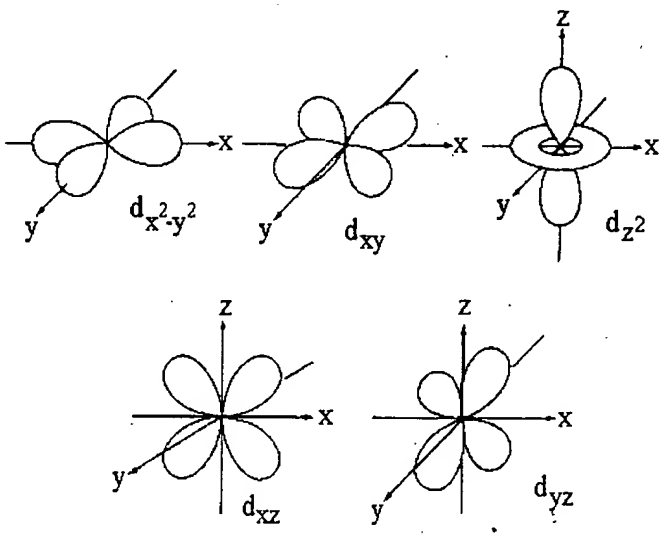

Figure (1) The Shapes of the (nd) Orbitals.

These Nodes force the (nd) electron density to be zero in two directions and only allow the (nd) electrons to penetrate the core in very narrow, solid angle regions. This puts the (nd) orbitals at a strong disadvantage against the ($[n+1]^2$) electrons which are allowed to penetrate from all angles, as shown in Figure (2). However, as the Atomic Number of the elements increase along each Period, each added (nd) electron has *no shielding effect* against any other (nd) electron, since they are all at the same distance from the nucleus.

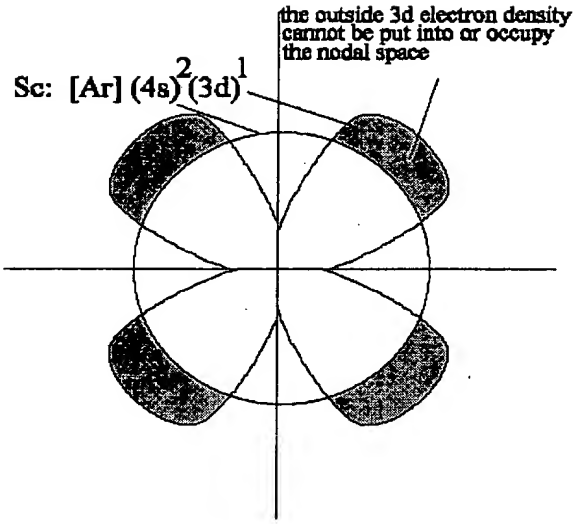

Figure (2) Shielding of $(nd)_{xy}$ by ([n+1]s)

This absence of new shielding means that as positive protons are added to the nucleus along the Period, the (nd) orbitals can become more stable, so that at the end of each Transition Period, the (nd) orbital is *more stable* than the ($[n+1]^2$) electrons and, as the ([n+1]p) begins to fill to form the next Period in the Main Block, these (nd) orbitals become part of the Core. The overall effects on the available Stable Oxidation Numbers for Transition Elements are shown in Figure (3).

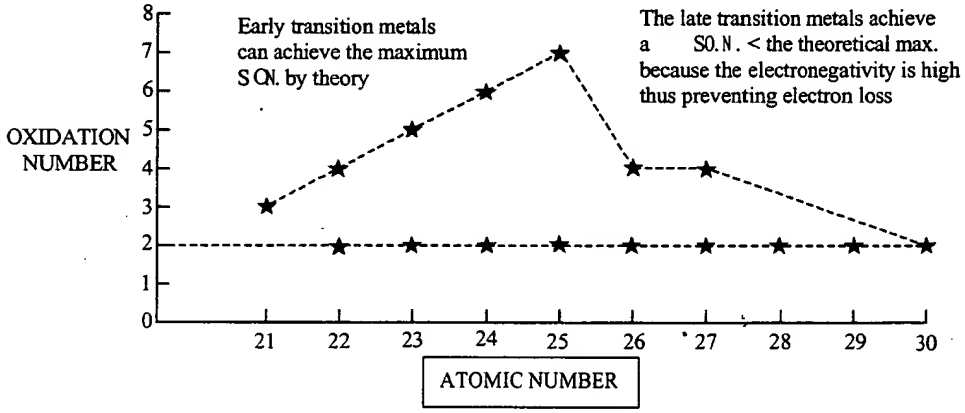

Figure 3 The trends in Max and Min SON values of Transition Elements with Atomic Number

Again, as was seen in the Main Block, the addition of layers of ([n+1]d) orbitals increases the atomic radius and should decrease both the Hardness and the Electronegativity of the transition elements down each Group. The actual values of the Hardnesses of these Elements are shown in Table (2) and the corresponding Electronegativities are shown in table (3).

Table (2) Hardnesses of the Transition Elements

3B	4B	5B	6B	7B	8B			1B	2B
310	325	300	295	360	370	350	310	315	360
290	310	290	305	325	305	305	375	300	470
245	335	365	345	370	365	360	330	330	525

Table (3) Electronegativities of the Transition Elements

3B	4B	5B	6B	7B	8B			1B	2B
325	330	350	360	360	390	410	425	410	425
320	350	375	380	375	405	415	430	430	400
295	335	395	425	385	475	515	535	555	480

Forms of Transition Elements

The Transition Elements are all metals and most of them are crystalline solids at room temperature. In most cases, these solids have either cubic or hexagonal close-packed Structures. Their characteristic Activities include high melting and boiling points, high mechanical strength and ductility, high conductivity of both heat and electricity and reflective surfaces.

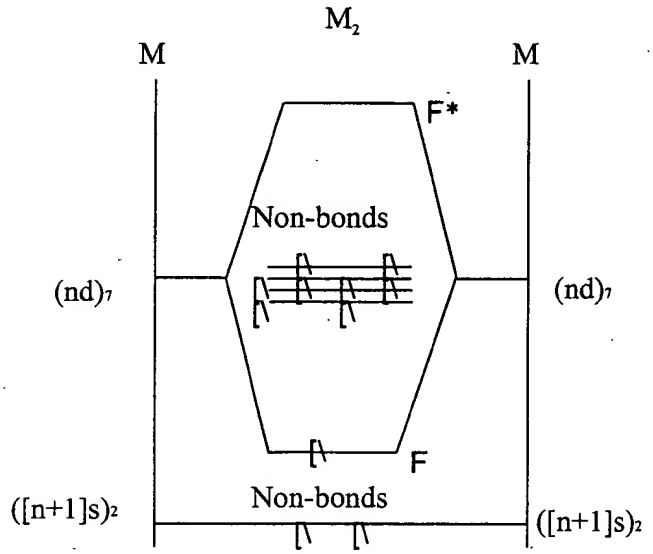

Figure 4 MOs of Group 7B Diatomics

The metallic bonding in these solids is similar in some ways to the bonding in the covalent bonding in the diatomic molecules of the second Period Main Group Elements with the addition of unrestricted, non-bonding (nd) orbitals. As shown in Figure (4), the description of a diatomic molecule of an Element of Group 7B is initially the same as that of the diatomic of the corresponding Element in Group 7a, except the σ bond is formed by the overlap of (nd z^2) orbitals instead of (p z) orbitals. All of the other (nd) orbitals are defined by symmetry as potential π bonding orbitals. However, like the potentially (pπ) bonding orbitals of the heavy Main Block Elements, when the Pauli and Aufbau Principles are applied, they remain non-bonding because the metal atoms are too large to allow significant (dπ) overlap along the bond axis. Then, like the heavy Main Block Elements, these Transition Block Elements compensate for their inability to form strong (dπ) bonds by forming a (dσ) bonded solid. The difference between the nonmetallic Structures of the Main Block

Elements and the metallic Structures of the Transition Block Elements is the difference in local stabilities of the non-bonding ($p\pi$) orbitals in the Main Block and of the non-bonding ($d\pi$) orbitals of the Transition Block.

The ($p\pi$) orbitals in the Main Block are very stable and not available to interact with radiant energy. In contrast, the poorly penetrating ($d\pi$) orbitals of the Transition Block have low stabilities and large radii, their resulting weak overlaps form a "band" of weakly bonding and antibonding "Lattice Orbitals". The available electrons would all be placed into the ($d\pi$) bonding orbitals, localized on the "parental" atoms by the Pauli and Aufbau Principles. However, they are easily dislodged into ($d\pi$) antibonding orbitals, which are delocalized over the whole lattice, by radiant energy. Thus, at room temperatures and above, there is enough energy to "excite" these electrons into the conductive "electron gas" within the lattice, which is the defining characteristic of all metals.

Identifying SONs of Transition Elements

As with the Elements in the other Blocks of the Periodic Table, the Transition Elements are often bound by donor covalent bonds within complicated chemical Structures and their electrical charge cannot be measured experimentally. The consequent theoretical assignment of their SONs generally follows the same Octet Rule used for the other Elements but the similarity of the ([n+1]s) and (nd) orbital energies complicates the procedure.

For most Transition Elements, the HOAO is the ([n+1]s) orbital and the removal of its two electrons defines a +II SON. The higher SONs are then generated by successive removal of any available (nd) electrons, as shown in Figure (3). The SON_{Max}, representing the loss of *all available* (nd) electrons, can be reached in all Transition Element Groups from 3B to 7B. Since this includes all Transition Elements up to the "half-filled" (nd) shell, they are classified together as the "Early Transition Elements". In contrast, in the "late Transition Elements, from Group 8B to 2B which represent the filling of the (nd) shell, the improving penetration of the core by the (nd) electrons causes a rapid decrease in available SON_{Max} values with increasing Atomic Number.

Between these SON limiting values of + II and SON_{Max} , several intermediate SON values may be possible. In the Early Transition Elements, the poor penetration of the core by the (nd) electrons means that these SONs represent thermodynamically *unstable* oxidizing agents. These Structures can only be captured chemically if they are made kinetically *inert* by Pauli pair formation, thus the only SONs of practical importance are found in compounds with all of the (nd) electrons paired into MOs.

In contrast,, the improved penetration by the (nd) electrons through the core in the Late Transition Elements means that intermediate SONs are thermodynamically stable and do not require the kinetic inertia provided by Pauli pairing. Indeed, these SONs are so stable that many (nd) configurations of odd-electrons or unpaired even-electrons exist in air-stable compounds, in spite of formally being Free Radicals.

Reduction to Minimum SONs

In reactions of these Elements and those with lower Electronegativities, Pauling's Electroneutrality Rule predicts that to minimize the total Free Energy of the whole

system, these atoms would at least retain or possible gain electrons into their partly filled (nd) orbitals.
This either leaves the Transition Element in a "zero-valent" condition or reduces it to a negative SON in the product of the reaction. Since these reduced species are usually thermodynamically unstable the only SONs of chemical importance are those representing (nd) configurations of Pauli paired bonding orbitals. An example of a zero-valent condition is given by the reaction of metallic Nickel with the gas carbon monoxide to form nickel tetracarbonyl;

$$Ni + 4CO \Rightarrow Ni(CO)_4(1)$$

in which the product is a *covalently bonded liquid* at room temperature. The bonding, shown in Figure (5), is described as "back donation" from the filled, Lewis Base (3d) non-bonding orbitals on a Nickel atom to the empty, Lewis Acid (π^*) antibonding orbitals on the carbon end of the carbon monoxide molecules.With cobalt, the analogous anion $[Co(CO)_4]^-$ forms and is stable enough to support its acid.

Oxidation of the Elements

The Intermediate SONs

The SON of +II, representing loss of the $([n+1]\ s)^2$ pair, provides a large proportion of the thermodynamically stable compounds of the Transition Elements. The electronic properties of the First Transition Row (the fourth Period in the Table) ions are shown in Table (3). Compounds of all of these ions are known, except for Sc +II.

Table (3) Electronic Structures Of First Transition Row Elements

+II Ion	Configuration $(3d)^m$	r nm	η kJ/M	$(10^6)\alpha$ (nm^3) M/kJ	χ kJ/M	$\Pi\ (10^4)$ kJ/M
Ca	0	0.10	1880	0.05	3025	3.03
Sc	1	0.090	575	1.27	1810	2.01
Ti	2	0.086	670	0.95	1980	2.35
V	3	0.079	710	0.69	2120	2.68
Cr	4	0.074	745	0.54	2240	3.03
Mn	5	0.082	870	0.63	2375	2.95
Fe	6	0.078	700	0.68	2250	2.88
Co	7	0.074	790	0.51	2435	3.29
Ni	8	0.073	820	0.42	2570	3.67
Cu	9	0.073	800	0.49	2750	3.77
Zn	10	0.075	1050	0.45	2780	3.71

The simplest of these compounds are the "binary salts" in which these cations unite with the common monovalent, divalent or trivalent anions, in stoichiometric formulas; MX_3, MX and M_3X_2.In these salts, the high Polarizing Power Π of the Lewis Acid cations forces these Lewis Base anions to form donor-covalent bonds. Even so, the lattice Structures are usually consistent with the geometry predicted by Pauling's radius Ratio Rule.

When these +II ions dissolve, their large radii indicate that they do not hydrolyse like the smaller, more Polarizing Main Block cations, but their Polarizing Power is high enough to attract polar solvent molecules or polar dissolved Lewis Bases as "ligands", or species which are "tied to" the cation. A wide range of neutral and negatively charged species, including those shown in Table (4) are commonly found as ligands in these complexes. In this Table, the substituents on the donor atoms can be any other atom or group, including the H atom, halogens, or organic groups.

Table (4) Typical Lewis Base Ligands in Transition Element Complexes

Donor Atom		Neutral Ligands		Anionic Ligands	
Group	Atom	Name	Formula	Name	Formula
5A	N	Amine	R_3N	Amide	R_2N^-
	P	Phosphine	R_3P	Phosphide	R_2P^-
	As	Arsine	R_3As	Arsenide	R_2As^-
6A	O	Ether	R_2O	Oxide	RO^-
	S	Thioether	R_2S	Sulfide	RS^-
7A	F	-	-	Fluoride	F^-
	Cl	-	-	Chloride	Cl^-
	Br	-	-	Bromide	Br^-
	I	-	-	Iodide	I^-

In the resulting "complexes" the "coordination number", cn, defines the number of bound ligands, which can vary from 2 to 12. The value of cn in stable complexes is almost always determined by the Polarizing Power of the cation. For any given value of Π from Table (3), the charge requirement can be satisfied in the two limiting cases of either a small number of highly polarizable ligands or a large number of weakly polarizable ligands. This ligand polarizability is often called its "Donicity". Thus, the coordination number is predictable from the ratio of these cation and ligand properties ;

$$cn = \Pi (M +II) / \alpha (L) \quad (2)$$

In a minority of cases, this purely electronic prediction can be altered by "steric Interference" in the "coordination Sphere" of directly bound ligands. A 6-coordinate complex is shown in Figure (5). If some or all of these ligands are large enough to come

into direct contact with each other before they get close enough to the metal ion to form a stable bond, some of these "oversized" ligands are rejected from the coordination sphere, reducing the cn from the value predicted electronically down to the value predicted by the Pauling Radius Ratio for these ligands in this complex

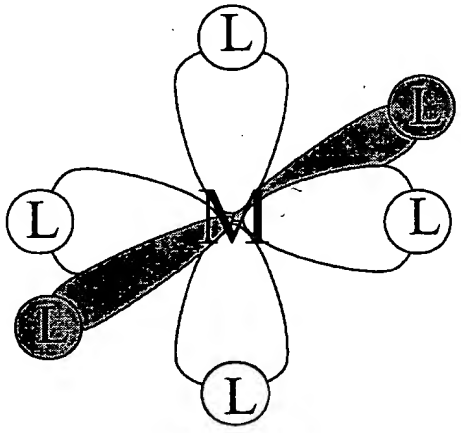

Figure 5.5 A 6-coordinate complex

Complex Structure and Bonding

Once this combination of electronic and steric factors has determined the cn of a complex, the donor covalent bonding of ligands to Transition Element cations can be described with the LCAO MO model. As usual, the first step is to define the GOs formed from the participating AOs.

In the simplest case, the AOs of the cations are the cation HOAO, $(nd)^m$ and LUAOs, ([n+1]s) and ([n+1]p), while typical Lewis Base ligands use HOAO $(np)^6$ or equivalent HOMOs in "polyatomic ligands" like amines and ethers. To form the corresponding GOs, the full symmetry of the complex must then be determined. The most typical of these is a complex with a cn of 6 in an octahedral Structure, in which the six identical ligands occupy the identical positions at each end of the three Cartesian axes, ± (x, y, z). In this Structure, the (np z) HOAOs of the ligands are directly in line with the (nd x^2-y^2,z^2) and the ([n+1]p xyz) LUMOs of the Transition element cation. This is electronically optimal because it maximizes the GO overlaps and sterically favourable because it minimizes ligand-ligand contact.

To describe the energy of this *purely σ bonding* condition, the Energy Level Diagram is constructed, as shown in figure (7). Following the model developed by C. J Ballhausen and H. B. Gray in 1964, the most stable MO in the complex is the (a_{1g}) formed by *large overlap* of the (a_{1g}) GO of the ligands with the ([n+1]s a_{1g}) of the cation. Then comes the MO formed by the *smaller overlap* of the (t_{1u}) GO of the ligands with the ([n+1]p t_{1u}) LUAO of the cation. Finally, the least stable MO forms from the *poorly overlapped* ligand (e_g) GO and the (nd e_g) HOAO of the cation. The remaining ligand GOs, (t_{1g} , t_{2g} , t_{1u} , t_{2u}), and cation HOAO (nd t_{2g}) *have π symmetry* and, in most complexes, theses types of ligand and cation orbitals are too far apart in space to have any overlap. Thus, they usually remain *non-bonding* in these complexes.

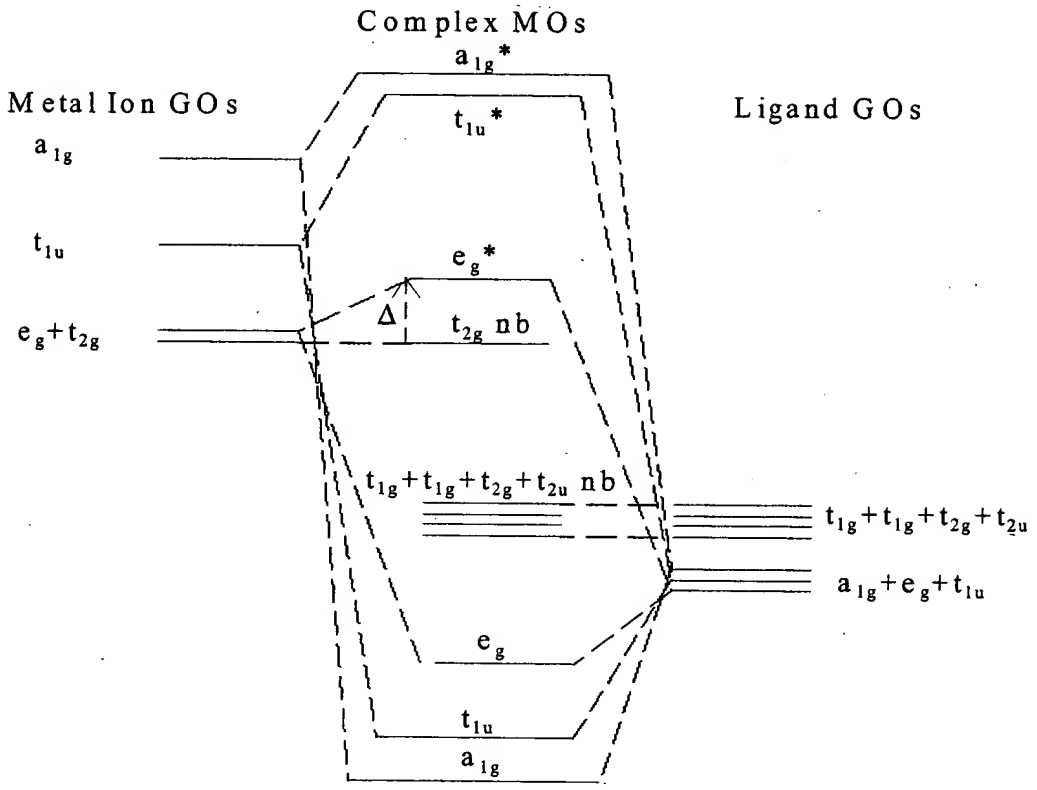

Figure (6) The σ MOs of Octahedral Complexes

When the Pauli and Aufbau Principles are applied to these Diagrams, the three σ bonding and the four ligand-centred π-non-bonding MOs are fully occupied. Above these HOMOs, the remaining electrons distribute themselves into the cation-centred MOs ($ndt_{2g}\pi nb$) and ($nde_g\sigma$)* MOs. The difference in energy between these two MOs is usually very small and any electrons in the ($ndt_{2g}\pi nb$) can be excited into the ($nde_g\sigma$)* MO with the small amount of energy available in visible light. Since this gives the complex a very obvious bright colour, this energy gap has been studied in all Transition Element complexes for more than 100 years. In the LCAO model it is called the "Ligand Field Splitting Energy" and is identified quantitatively as Δ in figure (7).

In the purely ionic Crystal Field model developed by H. Bethe in 1929, this energy gap was defined as 10Dq. In this model the gap originates from the Coulombic repulsion forces acting on the electrons in the (nd) HOAOs of the cation from anionic, point charge ligands. Since the (nde_g) HOAOs point at the ligands they are destabilized by this repulsion. However, the (ndt_{2g}) HOAOs point between the ligands and Bethe assigned this geometry as a "stabilization" condition. This allowed him to describe the total effect on the (nd) HOAOs as a "barycentric" perturbation, that is, an equally weighted energy splitting of these HOAOs *above and below the original HOAO energy,* This *oversimplified* but convenient "Crystal Field" mconcept is shown in Figure (7).

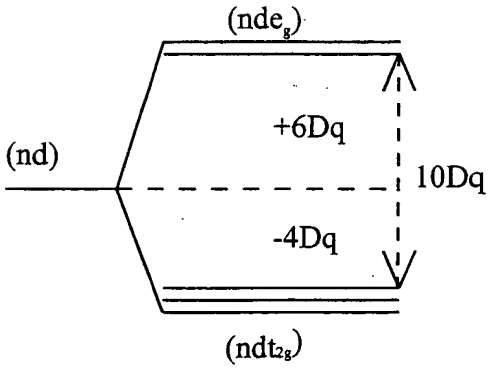

Figurre 7 The Crystal Field Model

When the Pauli and Aufbau Principles are applied for each of the Transition Element cations, the different possible ways in which the electrons may be distributed can be studied in detail. Since the (ndt_{2g}) HOAOs are all degenerate, up to 6 electrons can be placed at the same energy. If there are between 4 and 6 electrons in this HOMO, some must form Pauli pairs. However, the resulting Pauli spin pairing destabilization energy, which comes from putting two electrons close together in a single orbital "lobe", can be so strong that it is larger than the 10Dq destabilization energy needed to promote a (ndt_{2g}) electron to the (nde_g) orbital.

If this promotion does not occur, the $(ndt_{2g})^m$ configuration of paired electrons is called a "Low Spin" Structure. However, if promotion of some electrons to a $(ndt_{2g})^{(m-q)}(nde_g)^q$ configuration minimizes the destabilization energy of the whole complex, the resulting electronic Structure is called "High Spin" because it maximizes the number of unpaired electrons in both the (ndt_{2g}) and (nde_g) orbitals. This unpairing formally converts the complex to a many-electron Free Radical form. In complexes of the Early Transition Elements, these High Spin configurations do indeed behave like Main Block Free Radicals because their poorly penetrating (nd) orbitals are large enough to overlap and react with reagent species. However, since the more efficiently penetrating (nd) orbitals of the Late Transition elements have much smaller radii, they do not overlap or react readily with external reagents, but instead retain this Free Radical Structure in many chemical conditions. This thermodynamic stability of High Spin electronic Structures is even more common in complexes of the Lanthanide or Actinide Elements. The unpaired electrons in their highly penetrating $(nf)^m$ configurations are almost totally unaffected by the chemical environment of their cations.

$$LFSE = \sum_{m,q} (m-q)(-4Dq) + (q)(+6Dq) \quad (3)$$

To calculate the net stabilization achieved in each of these different electronic configurations, the Ligand Field model, shown in figure (8) was used to define the "Ligand Field Stabilization Energy" LFSE of a ligand field configuration as the sum of all stabilizing electrons at (-4Dq) and destabilizing electrons at (+6Dq) ; Then the net stability of the HOMO system of $(ndt_{2g})^{(m-q)}$ and $(nde_g)^{(q)}$ orbitals becomes ;

$$\Delta G_{Sys} = (r)(SPE) - LFSE \quad (4)$$

where (r) is the number of pairs of electrons in the configuration and SPE is the Spin Pairing Energy.

The Maximum SONs

The Rare Gas maximum SONs, representing $([n+1])s)^0(nd)^0$ configurations, can all be reached chemically in the Early Transition Elements. Since they carry no (nd) electrons, both their Structures an Activities closely resemble those of their corresponding Main Block Elements with the same SONs. The only important difference is that the *empty* (nd) orbitals on the 3B to 7B Transition Elements in these maximum SONs leave the positive nucleus completely unshielded in the ($nd\pi_{xy, xz, yz}$) directions and therefore provide a new route for Nucleophyllic attack by negatively charged reagents. Thus, the *covalently bonded liquid* $TiCl_4$closely resembles CCl_4 except that it is hydrolysed instantly by the nucleophile water;

$$TiCl_4 + 2H_2O \Rightarrow TiO_2 + 4HCl \quad (5)$$

Thus, while maximum SON Main Block Elements accept π electron pairs from Lewis π Base ligands into empty ($np\pi$) orbitals, the corresponding Early Transition Elements accept the same π pairs into their empty ($nd\pi$) orbitals. The sulfate ion $(SO_4)^{2-}$ is $p\pi \Rightarrow p\pi$ bonded while the chromate ion, $(CrO_4)^{2-}$ is $p\pi \Rightarrow d\pi$ bonded. Otherwise, the two anions have identical Structures and very similar Activities in both acid and salt forms. In contrast, the Late Transition Elements are too stable to lose all of their (nd) electrons in any chemical reactions. However, the achievable maximum SONs have very high Polarizing Powers, Π, and satisfy their high charge requirements in one of two types of Structure; σ bonded complexes with the largest possible numbers of Hard ligands, giving high cn values, or π bonded complexes with the necessary numbers of Soft ligands, giving small cn values. The σ bonded complexes are typified by the trianion $[FeF_6]^{3-}$ and the π bonded complexes by the "Sandwich Compound"dication $\{[(CH_3)_5C_5]_2Fe\}^{2+}$.

All of these maximum SON compounds of the Late Transition Elements tend to be strong oxidizing agents. As well, if they occur as π bonded anions which avoid hydrolysis in water, they can also form strong Bronstead acids. As with the Early Transition Elements, both Activities depend on the availability of empty ($nd\pi$) orbitals, which can accept electron pairs from nucleophiles. However, in these Late Transition Elements, the ($nd\pi$) orbitals are partly or even completely filled, which severely limits both the π oxidizing and acidic Activities. Thus, Co^{3+} and Ni^{4+} are both cations with maximum SONs but neither is an efficient π Lewis Acid because their $(nd\pi t_{2g})^6$ configuration completely fills their π acceptor orbitals. As the result, neither cation is an efficient oxidizing agent and neither hydrolyses in water to form an oxyanion with Bronstead acidity.

This π shielding of the Co^{3+} and Ni^{4+} nuclei by the $(nd\pi t_{2g})^6$ configuration is so effective that these cations are "kinetically inert". Nucleophyllic Ligand exchange reactions, which happen instantly in Early Transition Elements, become extremely slow and follow two alternative Mechanisms. As defined by C H Langford (Carleton, 1966), the two processes at the Rate Determining Step are; an Association in which the incoming ligand *bonds first* to the Transition Metal cation, raising the cn or a Dissociation, in which the outgoing ligand *leaves first*, reducing the cn. If the two

processes occur together, the Mechanism is called an Interchange. In the Association Mechanism, the Free Energy of Activation is high because the incoming ligand must *push the π-shield out of position and sterically repel the other ligands* into a distorted geometry to bond to the Transition Metal ion. In the Dissociation Mechanism, the Free Energy of Activation is high because the outgoing ligand must *break its bond with the Transition Metal ion spontaneously*. Clearly, both types of Mechanism are difficult process and their rates often depend strongly on very specific factors in the Structures of complexes and Nucleophiles.